

AALBORG UNIVERSITY

---

# Laboratory Emulation and Control of a Sewer System with Storage

---

Control & Automation:  
Master Thesis

Group:  
CA10-1035

June 2019





**AALBORG UNIVERSITY**  
STUDENT REPORT

**Title:**

Laboratory Emulation and Control  
of a Sewer System with Storage

**Project period:**

10<sup>th</sup> Semester, Spring 2019

**Project group:**

CA10-1035

**Participants:**

Llorenc Salleras Mestre  
Pravin Karthick Murugesan

**Supervisors:**

Carsten Skovmose Kallesøe  
Tom Søndergaard Pedersen  
Jorge Val Ledesma

**Abstract:**

This project covers the development of a controller for a laboratory system that emulates a sewer network. A sewer network receives wastewater from residential areas, industries, runoff rainwater and transports them to a wastewater treatment plant (WWTP). In one particular case, at Fredericia, there are some heavy industries discharging occasionally large amounts of wastewater over a short time. Such fluctuating flow and and/or contaminant concentrations causes a stress on the WWTP. In this research project, we worked on a laboratory setup imitating a sewer network. We use a buffer tank to hold back water, a gravity sewer pipe to transport water, pumps to continuously generate a typical pattern of water flow and a overflow tank to collect water from sewer pipe outlet. Now, this led us to a problem statement: *How can a laboratory setup that mimic a real sewer network be assembled so that we can later utilize MPC, along with disturbance predictions and a storage tank that results in stable working conditions for the wastewater treatment plant.* Controlling the output flow from the buffer tank into the top of sewer pipe gives the possibility to smooth out the flow of water at the end of gravity sewer pipe. With a simplified model, prediction of flow disturbances, performance function and constraints, a Model Predictive Controller (MPC) was developed and the final results were promising.



# Preface

---

This report, created by Llorenç Salleras Mestre and Pravin Karthick Murugesan documents the work of our Master Thesis in Control and Automation at Aalborg University, 2019.

The report can be understood by anyone with a control engineering background. It is written with an intention of being a reference material for students who are going to work with the wastewater laboratory system. MATLAB/SIMULINK and CODESYS are the primary software tools used for this project. All figures were made by us with the application draw.io unless a reference is included in the figure caption.

Units are indicated in a parenthesis after the variable has been defined, for example,  $h$  is level ( $mm$ ). Non-SI units such as *litres*, *minutes* have been used in parts of the thesis. Equations are referred with an identifier in a parenthesis, for example, (4.16). The same applies to figures and tables. A nomenclature with a list of symbols and abbreviations can be found after the table of contents.

References of books, articles, project reports can be found in the bibliography section. Additional information regarding the project work is included in the appendix section.

Two different flow data (measured at the inlet to the wastewater treatment plant) has been used in this thesis. Both of them have been received from the project management group at Fredericia Spildevand og Energi A/S. The time of flow measurements taken and their respective use in this work is given below.

- 1 October 2017: For evaluating kalman filter performance in Chapter (4)
- 2 February-March 2019: Creation of a disturbance model in Chapter (4) and simulation studies in Chapter (6) are based on this data



# Acknowledgement

---

We want to thank our supervisors Carsten Skovmose Kallesøe, Tom Søndergaard Pedersen and Jorge Val Ledesma for their timely feedback, guidance and support. Their guidance and encouragement made it possible for us to complete our Master Thesis.

Kirsten Mølgaard and Palle Andersen, even though not part of the official supervision group, gave us their opinions and ideas for improving the project work. Their presence in the meetings turned out to be really helpful in many ways. We appreciate and thank their assistance.

Special mention to Palle Andersen for his idea of modeling flow in a tube as a delay. We thank him for showing us how it can be done.

We received all the help one can get with running experiments in the laboratory from Jorge Val Ledesma and Carsten Skovmose Kallesøe. We sincerely and wholeheartedly thank them for this.

# Contents

---

<b>List of Symbols</b>	<b>xi</b>
<b>1 Introduction</b>	<b>1</b>
1.1 Sewer construction . . . . .	2
1.2 Sewer as a chemical and biological reactor . . . . .	2
1.3 Working of a wastewater treatment plant . . . . .	3
1.4 Challenges of wastewater treatment . . . . .	6
1.5 Problem statement . . . . .	7
<b>2 Description of Laboratory Setup</b>	<b>9</b>
2.1 Sewer network . . . . .	9
2.2 Instrumentation . . . . .	11
2.3 Automation . . . . .	13
2.3.1 Hardware . . . . .	13
2.3.1.1 Data acquisition . . . . .	13
2.3.1.2 Raspberry Pi . . . . .	15
2.3.2 Software: CODESYS . . . . .	15
2.3.3 Communication protocol: Modbus TCP/IP . . . . .	17
<b>3 Modeling by First Principles</b>	<b>19</b>
3.1 Tank volume . . . . .	19
3.2 Flow in pipe . . . . .	20
3.2.1 Modeling of sewer system in Fredericia . . . . .	21
3.2.2 Modeling of laboratory setup . . . . .	24
<b>4 Control</b>	<b>25</b>
4.1 Time-series analysis in the frequency domain . . . . .	25
4.2 State-space model . . . . .	27
4.3 Kalman filter . . . . .	29
4.4 Delay in the sewer network . . . . .	32
4.4.1 In Fredericia . . . . .	32
4.4.2 Cross correlation analysis in laboratory . . . . .	34
4.5 Model predictive control . . . . .	35
4.6 System to control . . . . .	35
4.6.1 Control objective . . . . .	37
4.6.2 Model . . . . .	37
4.6.3 Performance function . . . . .	38
4.6.4 Constraints . . . . .	39
4.7 Disturbances . . . . .	42
4.8 Summary . . . . .	43
<b>5 Implementation</b>	<b>45</b>
5.0.1 YALMIP . . . . .	45
5.0.2 SIMULINK . . . . .	45
5.1 Flowchart . . . . .	47

---

<b>6</b>	<b>Tests and Results</b>	<b>49</b>
6.1	Simulation results . . . . .	50
6.1.1	Simulation with tank constraint . . . . .	51
6.2	Experimental results . . . . .	54
6.2.1	Pump control . . . . .	55
6.2.2	Valve control . . . . .	55
6.2.3	Manning equation . . . . .	57
6.2.4	Kalman filter . . . . .	59
6.2.5	Model predictive control . . . . .	61
6.2.5.1	Without tank constraint . . . . .	61
6.2.5.2	With tank constraint . . . . .	63
6.2.5.3	Soft tank constraint . . . . .	65
<b>7</b>	<b>Discussion</b>	<b>69</b>
<b>8</b>	<b>Conclusion</b>	<b>73</b>
<b>9</b>	<b>Future work</b>	<b>75</b>
	<b>Bibliography</b>	<b>77</b>
<b>A</b>	<b>Appendix</b>	<b>79</b>
A.1	Data from fredericia . . . . .	79
<b>B</b>	<b>Appendix</b>	<b>81</b>
B.1	Other figures and simulation results . . . . .	81
<b>C</b>	<b>Appendix</b>	<b>85</b>
C.1	Wetted area calculation . . . . .	85



# List of Symbols

Symbol	Description	Unit
$Q$	Sewage flow	$m^3/hr$
$A$	Cross-sectional area of the sewage flow	$m^2$
$x$	Spatial variable	$m$
$t$	Time	$s$
$g$	Acceleration due to gravity	$m/s^2$
$h$	Sewage level inside the sewer	$m$
$S_b$	Slope of sewer	.
$S_f$	Friction coefficient	.
$v$	Sewage velocity	$m/s$
$n$	Gauckler–Manning coefficient	.
$R_h$	Hydrological radius	$m$
$P$	Wetted perimeter	$m$
$M$	Total mass	$kg$
$m$	Mass flow rate	$kg/s$
$V$	Sewage volume in tank	$m^3$
$T_s$	Sampling time	$s$
$F$	Force	$N$
$P$	Pressure	$bar$
$a$	Area	$m^2$
$\rho$	Sewage density	$\frac{Kg}{m^3}$
$Y$	Flow at WWTP inlet	$m^3/hr$
$U$	Controlled pump flow into sewer line	$m^3/hr$
$Q_i$	Flow from industries	$m^3/hr$
$Q_h$	Flow from households	$m^3/hr$
$\tau$	Transport delay in sewer line	$s$
$\mathcal{J}$	Performance function	.
$\mu$	Mean flow at WWTP inlet	$m^3/hr$
$H_p$	Prediction horizon	.
$H_u$	Control horizon	.

Abbreviation	Description
<i>WWTP</i>	Wastewater Treatment Plant
<i>MPC</i>	Model Predictive Control
<i>PLC</i>	Programmable Logic Controllers
<i>HMI</i>	Human Machine Interface
<i>DAQ</i>	Data Acquisition
<i>SWMM</i>	Storm Water Management Model



---

A sewer system collects all the wastewater arising from our homes, neighbouring industries, rainwater from the streets and transports to a wastewater treatment plant. Once the wastewater is processed, it is disposed to a river or sea or other water bodies depending on the treatment plant's location. In some scenarios, such as an event of heavy rainfall, the surplus wastewater bypasses the later stages of the treatment plant and is discharged into the nearest water body. By definition, a sewer system is a network of manholes, pipes, pumps, tanks, valves and sensors located between the origin of wastewater and a wastewater treatment plant (WWTP).

Sewer networks were not created in recent times. They have existed since the early historic period. Mesopotamian Empire (3500–2500 BC), covering lands of Southern Europe, Northern Africa, the Middle East and West Asia, was the first known civilization to take care of sanitation problems that came up due to community living [Jones, 1967]. The Indus Valley civilization (2500–2000 BC), present day Pakistan and Northwestern India, had a wastewater management system. Two excavated sites, Harappa and Mohenjo-daro, showed evidences of having the world's first urban sanitation systems [Webster, 1962]. Historical records also show that Egyptians during the First Intermediate Period (2181-2055 BC) [Breasted, 1907] and Romans (800 BC - 476 AD) [Hodge, 2002] had their versions of a sewer network in place. In the Industrial Age, late 18<sup>th</sup> and early 19<sup>th</sup> century, many countries in Europe, such as Britain [Wolfe, 1999], realized the importance of wastewater disposal and made efforts building sewer systems to improve environmental conditions in urban areas.

However, growing population, urbanization and introduction of strict environmental laws have created a need to improve existing sewer networks and wastewater treatment plants. Now, the wastewater industry has to aim for better control, higher service, higher efficiency and low direct discharge of wastewater into the environment. To meet such demands, the wastewater industry has to examine and incorporate advanced control system(s). In this project, one particular topic of control systems, Model Predictive Control (MPC) is analyzed for its application in the sewer network.

The project is a continuation from the previous semester [Morten Vesteraa et al., 2018] which focused on modeling, simulation and control of a sewer system. We came up with a simple model describing the flow in a sewer line accounting for transport delay. MPC was used to minimize the variance of contaminants and wastewater flow entering the WWTP. In this project work, we use the developed model and additionally foresee flow disturbances acting on the sewer system. This prediction is done with a kalman filter and the control strategy is implemented on a laboratory setup. The setup is built to mimic a small scale version of a sewer network. So the idea of this project is to verify the model of the sewer emulation setup in laboratory and test the controller to see if it is suitable for both the laboratory setup and the real system.

Other notable contributions to this project by us are:

- being part of developing the software side of automation in the lab
- helping with sensor calibrations and running initial tests on the laboratory setup
- introducing soft constraints in MPC algorithm to make the controller work in a real/practical scenario

## 1.1 Sewer construction

Sewer characteristics such as its construction determine the processes taking place inside a sewer pipe. The different processes are elaborated in the next section. Sewer construction is broadly classified into two categories: Gravity sewers and pressure sewers, figure (1.1). In a gravity sewer, the sewage naturally flows by gravity due to its inclination. In general, all over the world, most of the sewers are gravity sewers. When the topography does not suit a gravity sewer, i.e. when there is no elevation differences, pumps are used to transport sewage to the treatment plant. This is called as a pressure sewer and they can be easily built with shallow trenches. There are additional expenses when pumps are involved. 1 - initial cost of buying them, 2 - electricity for operation and 3 - maintenance costs.

In cold countries, where sub zero temperatures are common, the sewers lines must be placed at a greater depth to avoid freezing of the sewage. This clogs the sewer and results in a bad situation to the local community. Other reason for clogging could be insufficient slope of gravity sewers. When slope is less, a minimum sewage velocity is not attained and results in clogging. The material chosen for sewer pipes should create less friction to sewage flow and also be able to withstand corroding effects. In comparison to pressure sewers, it is difficult to modify and expand a gravity sewer network as the community keeps growing.

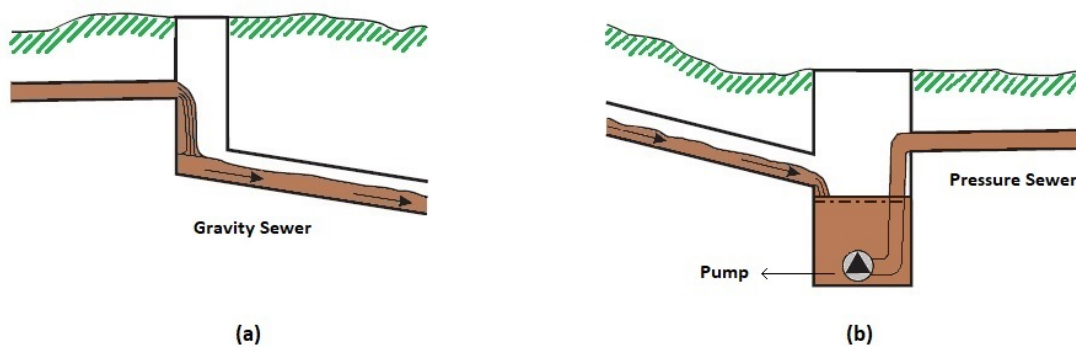


Figure 1.1: *Illustration of wastewater flow in (a) Gravity sewer and (b) Pressure sewer line.* [Morten Vesteraa et al., 2018]

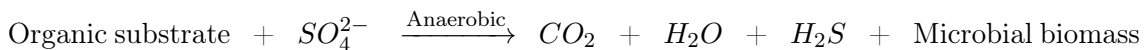
## 1.2 Sewer as a chemical and biological reactor

The wastewater leaving our homes and industries is not the same as the wastewater entering the treatment plant. As the wastewater travels long in a sewer with high residence time, changes in its quality occur as a result of microbial, chemical, and physicochemical processes [Hvitved-Jacobsen et al., 2013]. In that sense, a sewer network acts as a reactor and not just as a transport system for wastewater. So both wastewater and the products of the mentioned processes enter the treatment plant.

Inside a sewer, microorganisms (bacteria) digest on organic matter (wastewater) in presence of an electron acceptor ( $O_2/NO_3^-/SO_4^{2-}$ ) to form some low molecular organics ( $CO_2/H_2O/NH_3$ ) and new bacteria. In some literature, organic matter is alternatively referred as substrate and microorganisms as biomass. Organic matter is essential for the life of existing bacteria and also for the formation of new bacteria. In a sewer network, the heterotrophic bacteria dominate over autotrophic bacteria.



Knowing the redox conditions is very important in understanding the chemical and biological transformations in a sewer. Aerobic or anaerobic process occur depending the availability of external electron acceptors. Presence of dissolved oxygen ( $O_2$ ) and sulphate ( $SO_4^{2-}$ ) leads to an aerobic process and anaerobic process respectively. The difference between them is illustrated below.



Aerobic transformations of the wastewater may cause a reduced capacity for nitrogen and phosphorous removal at the treatment plant. The problem with too much nitrogen and phosphorus in the water causes algae to grow faster. This is catastrophic to the ecosystem. To solve this issue, preservation of readily biodegradable organic matter in sewers is important [Hvitved-Jacobsen et al., 2013]. Formation of hydrogen sulfide leads to a substantial degradation of the sewer network. It causes corrosion, toxicity of the sewer lines and the odour is bad.

Construction type of the sewer influences the reactions taking place in a sewer. Aerobic conditions exist for a partly filled gravity sewer and an aerated pressure sewer. Pressure sewer, full-flowing gravity sewer or a gravity sewer with low slope leads to anaerobic conditions [Hvitved-Jacobsen et al., 2013].

We can conclude that the biological system in a sewer is important as it affects the biochemical processes and it is essential to manage them in sewer networks [Hvitved-Jacobsen et al., 2013]. The redox conditions have an impact on the sewer system and treatment process as they determine the life of microorganisms. Processes happening in the sewer network not only affects the sewer network itself but also the treatment process at the WWTP and the surrounding environment. So one could say that the actual treatment of wastewater starts at the sewer network.

### 1.3 Working of a wastewater treatment plant

Centuries ago, when raw sewage was disposed into water bodies, there was a natural process of purification. First, the sewage got diluted due to the huge volume of clean water in the water bodies and second, bacteria and other microorganisms in the water consumed the organic matter, turning it into new bacterial cells, carbon dioxide and other products. But today's cities generate a much greater volume of wastewater which cannot be just purified by nature alone. For instance, in the year 1859, river Thames in Britain was so polluted and was called "monster soup" by the Victorians [Lofrano and Brown, 2010]. Such incidents demanded an environmental change which ultimately led to building wastewater treatment plants. As the sewer network delivers the wastewater to a plant for treatment,

the role of the treatment plant is to purify wastewater and discharge it into rivers or other receiving waters. In this way, human intervention helps speeding up the natural process of water purification.

We can broadly segregate wastewater treatment into two stages: Primary stage and Secondary stage. The primary stage of the treatment makes use of physical methods such as filters/screens to remove big solids from the sewage that might clog pipes or damage equipment. The filtered sewage is then passed into a grit chamber, where sand and gravel settle at the bottom. After going through a screen and grit chamber, the sewage still contains some organic matter, inorganic matter and other suspended solids. To remove them, the sewage is then stored in a sedimentation tank allowing the minute solids to settle down, forming a mass of solids called sludge, which is later removed by pumping. Lighter substances such as grease and oil floats at the surface and is also removed. With strict environmental standards, primary treatment alone is not sufficient to meet the water quality requirements before releasing into rivers. To meet them, a secondary treatment process was put in place to remove other contaminants. In some cases, a third level of advanced wastewater treatment was also used.

The secondary stage of the treatment uses biological processes (bacteria) to further refine wastewater. Among many principal treatment techniques, the activated sludge process will be discussed first and followed by others after figure (1.4). The sewage from the sedimentation tank is now pumped into an aeration tank, where it is mixed with air and sludge. The sludge contains a lot of bacteria and the sewage remains inside the aeration tank for several hours. During this time, the organic matter in the sewage is broken down into harmless by-products (new bacterial cells, carbon dioxide and other products) by bacteria. The effluent then moves to a settling tank where the sludge moves to the bottom. The sludge now contains additionally billions of bacteria and other tiny organisms. The sludge can be used again (pumped back into the aeration tank) to treat new sewage. So in simple terms, the activated sludge process works by bringing air and sludge into close contact with sewage.

Process	Treatment Agent(s)	Wastes Treated
Trickling filters	Packed bed (stones or synthetic) covered by microbial film	Acetaldehyde, benzene, chlorinated hydrocarbons, nylon, rocket fuel
Activated sludge	Aerobic microorganisms suspended in wastewater	Refinery, petrochemical and biodegradable organic wastewaters
Aerated lagoon	Surface impoundment plus mechanical aeration	Biodegradable organic chemicals
Waste stabilization ponds	Shallow surface impoundments plus aeration to promote growth of algae and bacterial and algal symbiosis	Biodegradable organic chemicals

Figure 1.2: *Different techniques for wastewater treatment [Cheremisnoff, 1997]*

To complete the treatment process, the sewage is usually disinfected with chlorine before being discharged into receiving water bodies [Lazarova et al., 1999]. This is practised in United States and other countries as well. Chlorine is added to kill any pathogenic bacteria that may be present and to reduce odor. If required by local environmental laws, excess chlorine is removed by a process called dechlorination.

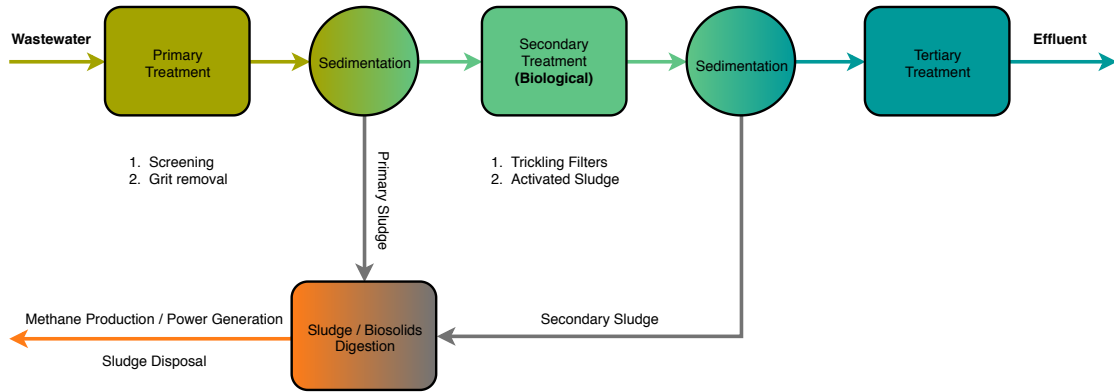


Figure 1.3: An usual order of wastewater treatment. Methane gas produced as a result of sludge digestion is burned to produce energy. This energy is used to power the wastewater treatment plant. Colours illustrate the conversion of raw wastewater to clean effluent and energy.

Other methods to treat sewage exist in the form of chemical methods and energy intensive methods. Chemical methods rely on the application of chemicals that help in the separation of contaminants from water. These chemicals sometimes instead of removing contaminants, they assist in the neutralization of harmful effects associated with contaminants. Energy intensive methods that include electrochemical techniques, are by large applied to drinking water applications [Cheremisinoff, 2001].

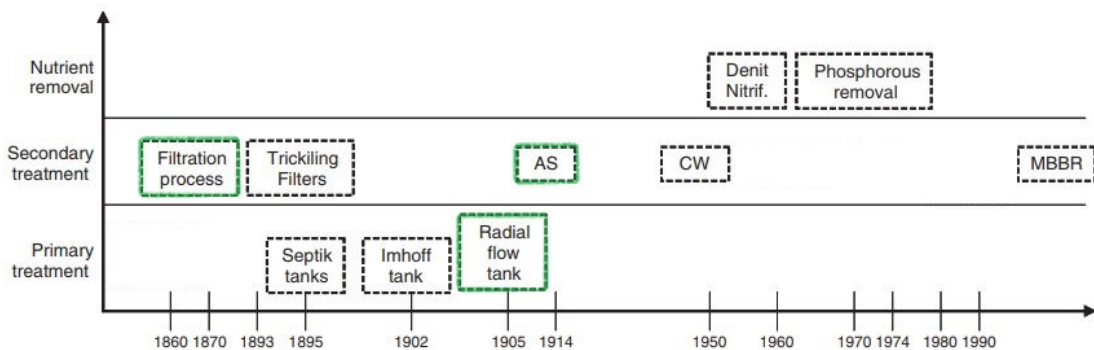


Figure 1.4: Evolution of wastewater treatment through the years [Lofrano and Brown, 2010]. These are alternative methods to filtration and activated Sludge process.

In above figure, the respective terms are: AS - Activated Sludge, CW - Constructed Wetlands, MBBR - Moving Bed Biofilm Reactors. The filtration and activated sludge process have been briefly discussed previously. Radial flow tank is a particular type of sedimentation tanks. All three of them are placed in a green box.

A trickling filter is a bed of stones about five feet deep through which wastewater flows. Microorganisms attached to these stones consume the organic matter and multiply [Cheremisinoff, 1997]. The cleaner wastewater then trickles out to undergo further treatment. A septic system is a simple and self-contained underground wastewater treatment system. They do not have high treatment efficiency and can be only used in rural areas that are not connected to a sewer system. Imhoff tank consists of a V-shaped settling chamber with a residence time of up to three hours. It is an improvement over the septic tank method as sludge can be separated from the effluent. Constructed wetland, an engineered ecosystem that mimic natural wetland, can be used to treat wastewater. They are a cheaper alternative as they do not involve any mechanical or energy consuming equipment [Vymazal, 2010]. In a moving bed biofilm reactor, the settling tank (seen in activated sludge process) is replaced with membrane filtration. This method results in better solid-liquid separation and also enables a high biomass concentration to be maintained in the bioreactor [Leyva-Díaz et al., 2017]. When level of nutrients in the water exceed a safe limit, it could cause a significant increase in the growth of blue-green algae [National-Geographic, 2013]. This decreases the oxygen, food resources and water quality that is needed by marine life to survive. To avoid such problems, denitrification and phosphor removal methods were introduced.

## 1.4 Challenges of wastewater treatment

The two main problems associated with methods using sludge for treating wastewater (such as activated sludge and moving bed biofilm reactor) are variations in flow and concentration of contaminants. These variations affect the operational efficiency of the treatment plant. A typical flow pattern from any community would look like the figure below.

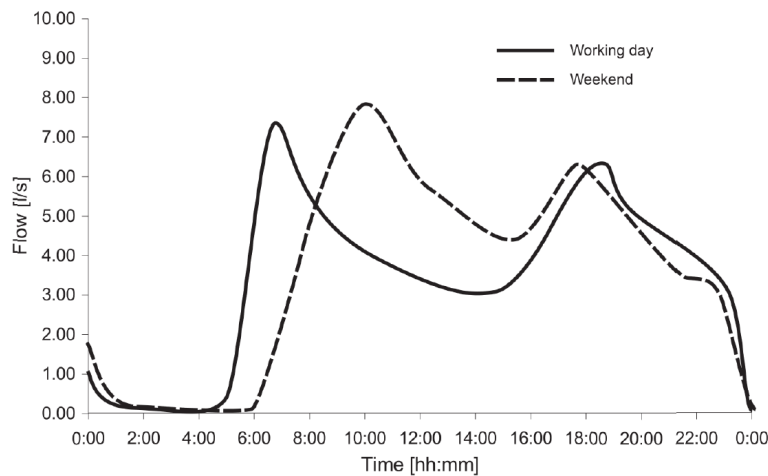


Figure 1.5: *Wastewater production from a small village Frejlev, Denmark [Schlütter, 1999].* Here, it is assumed there is no infiltration by the groundwater into the sewer system.

The flow variations observed is due to the human routine. We mostly consume household water during the day time. These variations are problematic to the treatment process down at the plant. As discussed in section (1.3), sludge is pumped into the aeration tanks to purify the wastewater. With proper living conditions in place, only a certain amount of sludge can be stored for reuse. When a sudden peak in flow occurs, around 06:00, there might not be enough sludge to completely purify the wastewater entering the plant.

The flow variations are worsened by rainwater causing a scenario in which the inlet flow to the treatment plant exceeds its capacity. When not dealt with carefully the rain water can flush out the sludge from the bio-reactors resulting in the loss of bacteria for wastewater treatment. In such cases, the wastewater only undergoes primary treatment and is then discharged to an adjacent water body. Apart from these problems, there can be some big industries releasing varying loads of wastewater into the sewer network. This particular problem is clearly seen in Fredericia where industries like Carlsberg, Shell and Arla are present. In addition, the industrial wastewater also has changing contaminant concentration levels. The bacteria in the aeration tanks need time to accommodate to a change in contaminant concentration. Sudden peaks in concentration level could again cause operational inefficiency. In Fredericia, at the moment, when there is a big increase in contaminants entering the WWTP, the management uses chemicals to coagulate them and remove the settled products from the sedimentation tank. The effluent then moves onto the secondary treatment stage. This is a temporary solution they have considered.

To summarize on the problems, living organisms used for biological treatment processes are affected by movement, chemical conditions, temperature and other factors [Cheremisinoff, 1997]. The performance of these microorganisms are best under a steady environment. If there are environmental changes, there should be enough time for the microorganisms to acclimate to such changes. A good and well maintained biomass is needed so that it can flocculate, settle and thicken in a sedimentation tank [Tandoi et al., 2017] while treating wastewater.

## 1.5 Problem statement

From the previous section, the identified problems with wastewater treatment are:

- Flow variations due to household water consumption, rainwater and large industries releasing wastewater
- Concentration variations in sewage due to natural phenomena and industries releasing highly contaminated wastewater over a short time

The flow from residential areas entering the sewer network does not exactly look as in figure (1.5). This is because groundwater present above sewer pipes could easily infiltrate into the pipes. There can also be additional surface runoff from the streets due to rainwater. Not knowing this flow profile will make it difficult when we desire to develop a control plan for the sewer system.

So, first part of the strategy we thought of to overcome mentioned issues is to predict disturbances, i.e. inflows from residential areas, with a kalman filter. The second part of the strategy is building a storage tank in the sewer network and using Model Predictive Controller to control its output flow in a way giving the best working conditions for the wastewater treatment plant. This idea together with a new laboratory setup that emulates a simplified sewer system can be used to test the controller. It is also decided to use temperature as a proxy for contaminant to emulate variations in contaminant concentration. Now, from this a problem statement can be formulated:

*How can a laboratory setup that mimic a real sewer network be assembled so that we can later utilize MPC, along with disturbance predictions and a storage tank that results in stable working conditions for the wastewater treatment plant.*

Having formulated the problem statement, we set the objectives of the project to be:

- Build a model describing the dynamics of the lab system with tubes, tank, valves and pump
- Develop a performance function and suitable constraints to form the basis for evaluation of a controller performance
- Prediction of wastewater flow from residential areas (seen as disturbance) with a kalman filter
- Use the model, disturbance prediction, performance function and constraints to develop a Model Predictive Controller

### Outline of remaining chapters

**Chapter 2** Describes the different modules and automation software used to build-up the laboratory setup.

**Chapter 3** Describes modeling of important components in a sewer system.

In **Chapter 4**, time-series analysis of flow data and kalman filter is presented. Then the proposed Model Predictive Controller is described.

In **Chapter 5**, implementation of Model Predictive Controller is elaborated upon.

In **Chapter 6**, we have the results of the different tests performed.

Finally in **Chapters 7 to 9**, we have Discussion, Conclusion and Future work.

# Description of Laboratory Setup

# 2

In this chapter, we introduce you to the laboratory setup, hardware, software and communication protocols required to emulate and control a sewer network.

## 2.1 Sewer network

To support the study of using MPC for control of a sewer system, we will build an equivalent laboratory setup of a sewer system. The objective is to reproduce the sewer system as seen in figure (2.1) and observe some physical phenomena such as wastewater transport delay in the network, wastewater flow and wastewater concentration entering the WWTP. In this section, we show how a modular setup can be used to build a sewer system. The modular setup is made up of different stations.

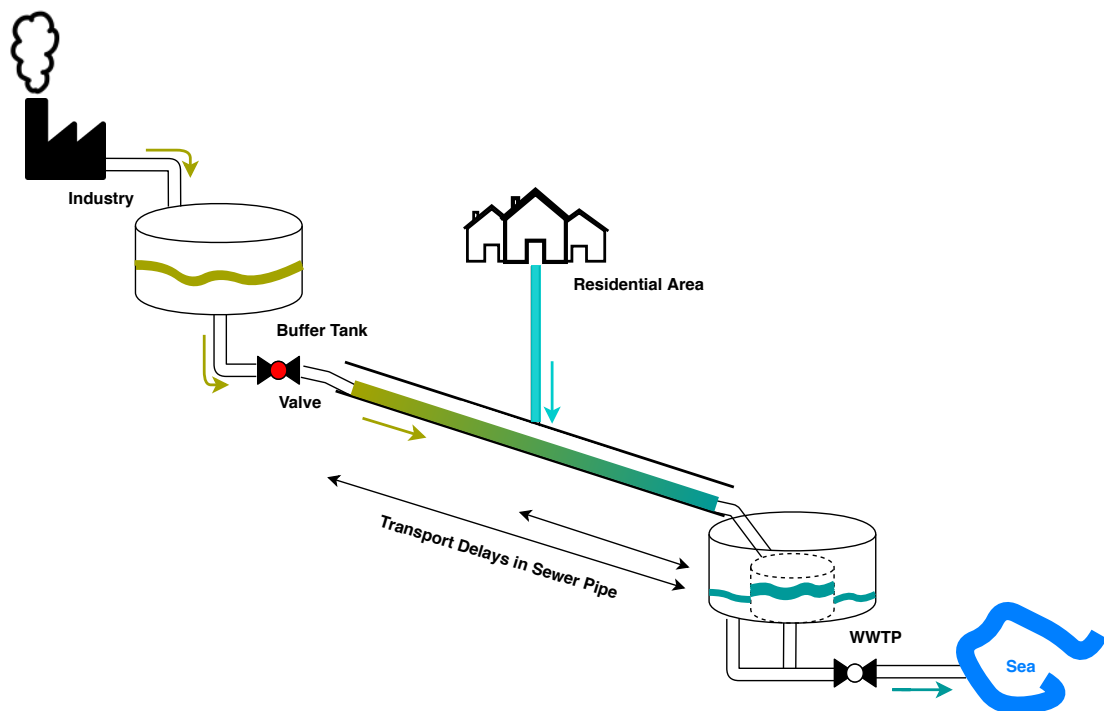


Figure 2.1: An illustration of a simple sewer network. Here, the industrial wastewater is stored in a tank before being let into the sewer network. The valve receives control signals and thus the outlet flow from the tank is controlled. The sewage then flows through long sewer pipes before reaching the WWTP.

The sewage flows in both gravity and pressure sewer pipes in a network. The transport time takes a few hours from the top to the bottom of the illustrated sewer pipe. Along the network there are many other sewage inflows from household areas but for simplicity we assume that all household flow is collected and enters the sewer network at only one point. So, a sewer system can be categorized into two storage blocks (buffer tank

and WWTP), two source blocks (household and industrial wastewater) and one transport block (sewer pipe).

In the lab setup, water will be used as the process liquid and temperature as the contaminant. Temperature is used as substitute to wastewater contaminant because the qualitative effects of mixing fluids of different temperatures and fluids with different contaminant concentrations are similar. Contaminant concentration levels are generally higher in industrial wastewater than that of household wastewater. Due to this fact, hot water in the lab experiment represents waste from industries and cold water represents waste flow from household areas.

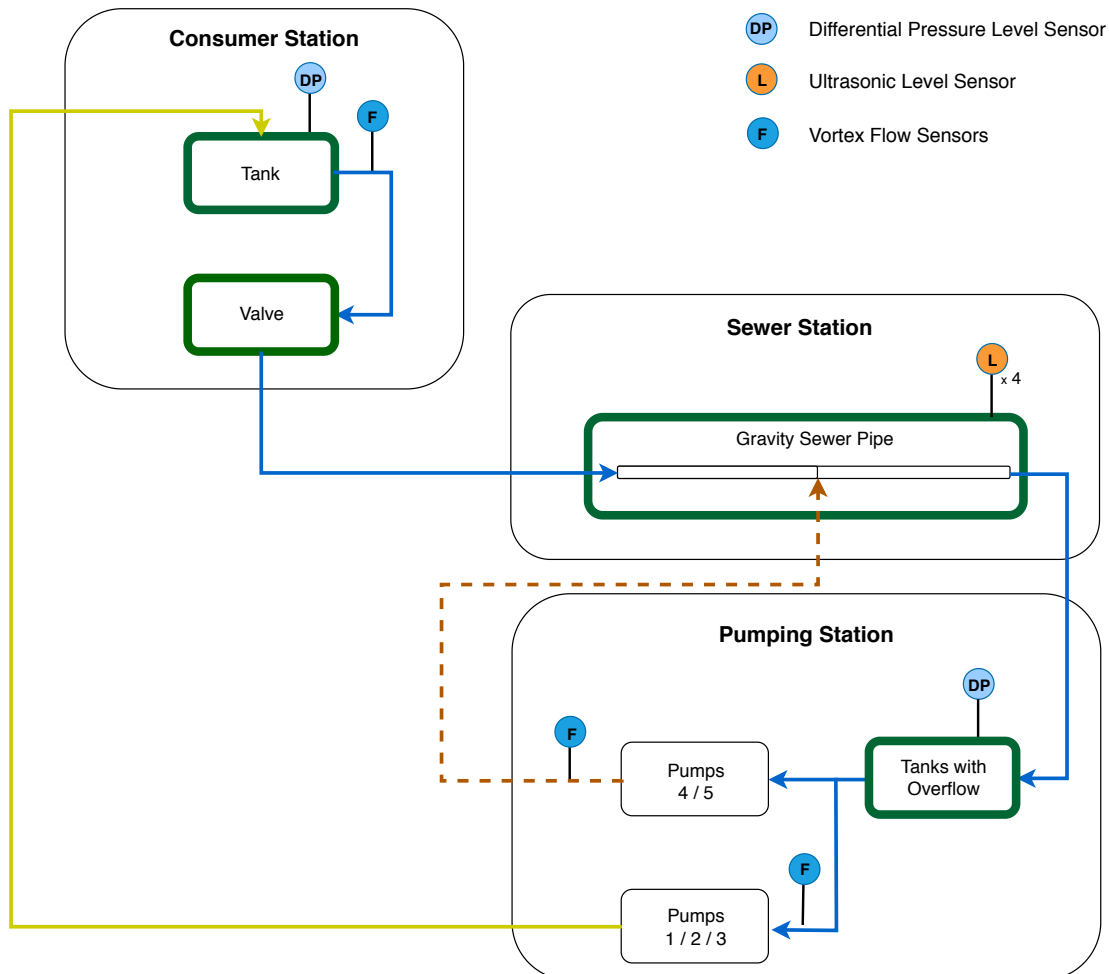


Figure 2.2: One possible arrangement of the modules to mimic a controlled sewer system. The orange dashed line indicates the typical household flow and the yellow line indicates the controlled industrial wastewater flow being added to the top of gravity pipe.

Due to time limitation and unavailability of other stations, the group was able to implement only a flow controller. More details on the system for temperature control is shown in future work section. The green boxes are the primary components of a sewer system. Here, tanks with overflow represents the WWTP receiving the wastewater.

The consumer station has a buffer tank with design capacity of 200 litres and a ball type control valve. There is a differential pressure level sensor on the tank and a vortex flow meter on the outlet line. In order to transport water from the buffer tank to the inlet of

gravity sewer pipe, using just the valve in between, its necessary to pressurize this tank with air. This represents the consumer tank being in an elevated position. We set this height to be *3.75 meters*.

The sewer station consists of a gravity sewer pipe. The pipe is made of transparent PVC and is of *20 meters* in length. The slope of the sewer pipe can be changed between 3 % to 6 %. There are four ultrasonic level sensors in the pipe. The sewer station, though a part of pumping station in practice, is chosen to be explained as a separate unit for easier comparison of a sewer system to the laboratory system.

The pumping station has five pumps and tanks with overflow. The set of pumps serve different purposes when emulating a sewer system. As seen in the previous figure, one pump set recirculates water between the pumping and consumer station and the other pump set creates a wastewater flow pattern leaving the residential areas. The tanks with overflow just means there is an interior and exterior tank. When the interior tank overflows, water goes to the exterior tank. A 3D model of the pumping station can be seen in appendix (C.3).

## 2.2 Instrumentation

For a control system to perform well, relevant parameter need to be measured on the process being monitored and automated. Sensors send these measurement readings to the control system. In our lab setup, we have sensors for finding both level and temperature and their types are briefly discussed.

### Ultrasonic level detector

The ultrasonic type level detector measures the time taken for an ultrasonic pulse to travel to the liquid surface and back. The two advantages are the absence of any moving parts and the capability to measure level without making physical contact with the process liquid. In the lab, these sensors are located in the pipe sewer. Level measurements are converted into flow measurements using hydraulic equations. They are described further in the next chapter. The speed of sound through air is *343 meters per second* in an ambient air temperature of  $20^{\circ}\text{C}$ .

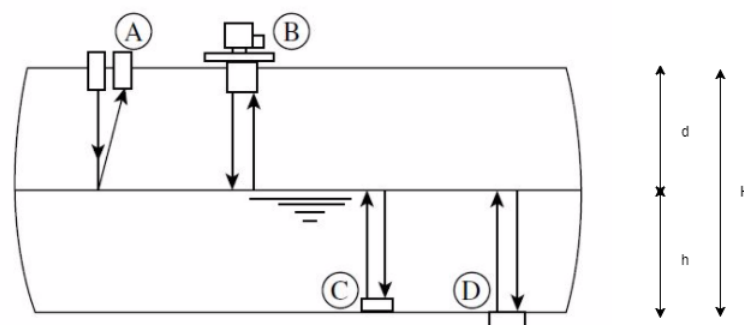


Figure 2.3: *Possible types of the sensor. In the lab setup, the sensor used is the one seen at location B [Lipták Béla G, 2003].*

$$d = \frac{\text{Speed of Sound} \times \text{Time}}{2}$$

$$h = H - d$$

where  $d$  is distance measured by sensor,  $H$  is known height of container and  $h$  is the calculated level of fluid.

### Differential pressure measurement in tank

A differential pressure instrument is used to measure level. Pressure at a certain point inside a tank depends upon the force exerted by the weight of the fluid above that point. The deeper you go, the greater the pressure force is going to be. The instrument has two sides: low-pressure and high-pressure side. For unpressurized tanks, the low-pressure side (LP) is vented to atmosphere and high side (HP) is connected to the tank bottom. This method, also known as Hydrostatic Tank Gauging, makes use of pressure difference to calculate level of fluid. Only difference when we measure level in a pressurized tank is that the low-pressure side is exposed to air pressure instead.

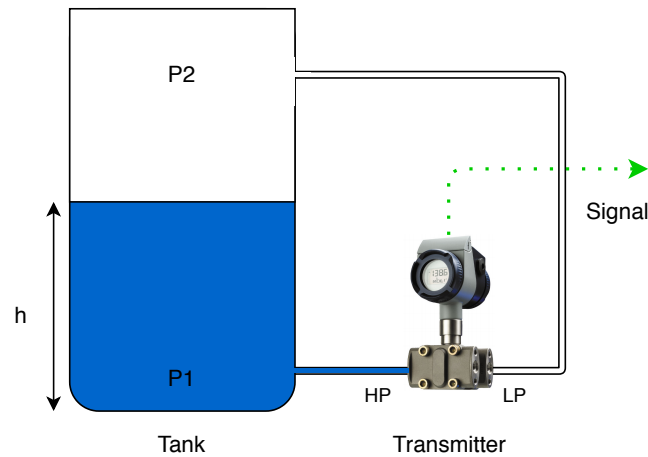


Figure 2.4: Differential pressure measurement for a closed tank. The transmitter has a diaphragm as pressure sensing element which deflects to one side by pressure difference. The deflection gets converted into an electrical signal.

$$\Delta P = \text{Pressure}(HP) - \text{Pressure}(LP)$$

$$\Delta P = P_1 - P_2$$

$$= \rho gh$$

where  $\rho$  is density of fluid and  $g$  is gravitational force. The transmitter calculates the level  $h$  from the above formula.

### Electromagnetic flowmeter

The operating principle is based on Faraday's law of electromagnetic induction. When electrically charged particles of water or any conductive fluid flows through a magnetic field generated by field coils, voltage is induced in the charged particles. This voltage, picked up by sensing electrodes, is directly proportional to the flow velocity of the fluid. The magnetic field, the direction of flow, and the induced voltage are all perpendicular to

each other. To cancel out interference due to electrochemical effects of the fluid or other external magnetic field, it is recommended to generate the magnetic field by a pulsed direct current with alternating polarity [Lipták, 2006].

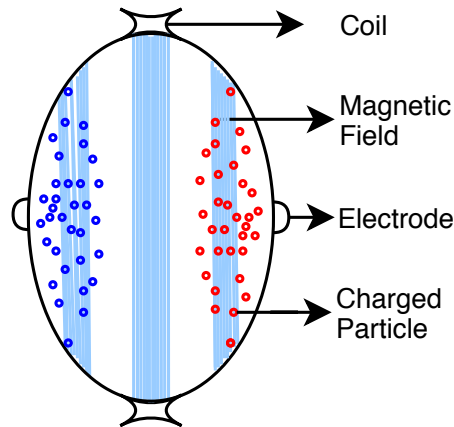


Figure 2.5: *Cross-sectional view of the tube. There is an accumulation of positively and negatively charged particles near the electrodes under the influence of a magnetic field.*

## 2.3 Automation

### 2.3.1 Hardware

The lab setup consists of different modules connected to a Central Control Unit. Each module is composed of a DAQ, a HMI and a Raspberry Pi as shown in figure (2.6).

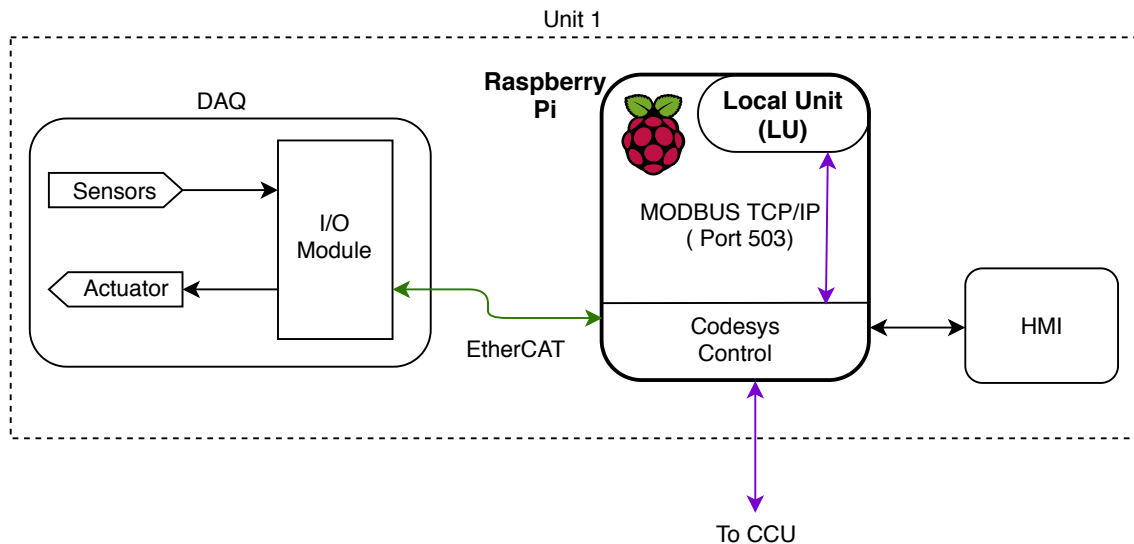


Figure 2.6: *Schematic of the different components in a laboratory module.*

#### 2.3.1.1 Data acquisition

Data acquisition (DAQ) is the process by which a physical phenomena like pressure or temperature is measured and transformed into electrical signals and later converted into a digital format for processing, analysis, and storage by a computer [Park et al., 2003]. In general, a DAQ is built by bringing together a variety of blocks from different manufacturers. The basic blocks of a data acquisition system is seen in the figure below.

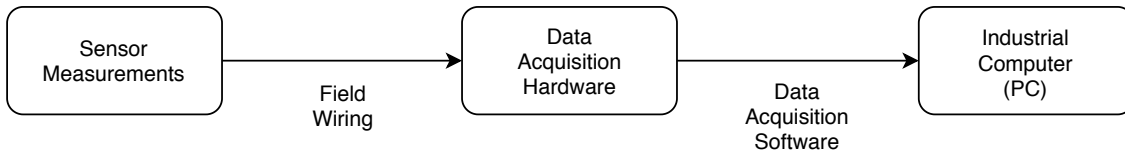


Figure 2.7: Block diagram of a PC-based data acquisition system

Field wiring is the physical connection from the sensors to the data acquisition hardware. Linearization is needed when sensors produce signals that are not linearly related to the physical measurement. Data acquisition hardware is the component that processes and converts the input analog signal into a digital format, using Analog to Digital Converters (ADC's). Data acquisition software is needed to merge the data acquisition hardware and PC together. The software runs on the PC under an operating system and turns the computer into a complete data acquisition, analysis and display system.

In the scenario where sensor measurement is affected by external noise, the data could get corrupted and hence signal conditioning is required. A signal conditioning unit usually contains a low pass filter that remove high frequency noise and/or an amplifier to amplify the filtered signal. The unit is placed before data acquisition hardware.

In table (2.1) it can be seen the different sensors and actuators in the pumping module as an example to show the different types of signals between the field and the I/O modules. All the I/O modules are connected to the Raspberry Pi by EtherCAT.

	I/O Module	I/O	Signal type
Pumps	Beckhoff EL2502	Digital output	24 V PWM
ON/OFF Valves	Beckhoff EL2008	Digital output	24 V
Temperature and pressure	Beckhoff EL3068	Analog input	0-10 V
Flow sensor	Beckhoff EL3048	Analog input	0-20 mA
Conductivity sensor	Beckhoff EL3048	Analog input	0-20 mA
Differential pressure	Beckhoff EL3048	Analog input	0-20 mA
Level sensor	Beckhoff EL3068	Analog input	0-10 V
Ball valves	Beckhoff EL4008	Analog output	0-10 V

Table 2.1: Actuators, sensors and its signal type.

In order to maximize the resolution of the sensor reading, it is desired that the maximum and minimum of the signal matches with the physical range of the sensor or actuator. For example, the differential pressure sensor readings will be constrained by the size of the tank, so it is desired that the minimum level matches with the minimum of the signal and analogously for the maximum level. The resultant signal will be then converted to a 16 bit integer with a value between 0 to 65535 in case of unsigned integer or between -32767 to 32767 for signed integers.

It is worth mentioning that some sensors and actuators have different signal range than the I/O module. For example, flow sensors in table (2.1) use the well-known 4-20 mA signal although the I/O module is prepared for a 0-20 mA signal. That will cause the minimum reading to be 4 mA. This issue has to be taken in account when converting the integer value to a real value which represents the physical magnitude. This will be explained further in section (2.3.2) .

### 2.3.1.2 Raspberry Pi

The Raspberry Pi is a full-blown desktop PC that is really cheap. It runs on Linux, a free operating system. The user could also choose from a wide range of programming languages to implement his/her projects. The Pi contains a processor (CPU), a graphics processing unit (GPU), and some memory.

The HMI is a tactile display connected to the Raspberry Pi with a ribbon cable. It shows a graphical interface with the relevant sensor data using a web browser. The Raspberry Pi will run Codesys Control that will allow to use the Raspberry Pi as a softPLC.

As a precaution to avoid overflowing in the two tanks (consumer and pumping stations), a simple level control is in place. When the level in the tank reaches a certain high limit, the in-feed valves are closed and similarly for a certain low limit, the out-feed valves are closed. This level control is implemented by the Raspberry Pi.

### 2.3.2 Software: CODESYS

Codesys is an automation development software that control engineers can program. It converts any PC or embedded device into an industrial controller.

Codesys supports five different programming languages: Instruction List (IL), Structured Text (ST), Ladder Diagrams (LD), Function Block Diagrams (FBD) and Sequential Function Chart (SFC) which allow to use a common software to work with different PLCs brands and automation components. Codesys consist in two major components:

- Codesys Development System: Allows to configure and program controller applications
- Codesys Control: Execution on the target device of the application code compiled by Codesys Development System

Once the controller application has been transfer to the Codesys Control in the target device, this can run autonomously. In the present project a Raspberry Pi has been used as target device. The controller application can be transfer to the Raspberry Pi via Secure Shell (SSH) protocol.

Figure (2.8) shows a network with a workstation running Codesys Development. This workstation is able to load the application code to the different target systems, in this case to the four Raspberry Pi which will be running Codesys Control. At the bottom are shown the different I/O devices which will interface with Codesys Control.

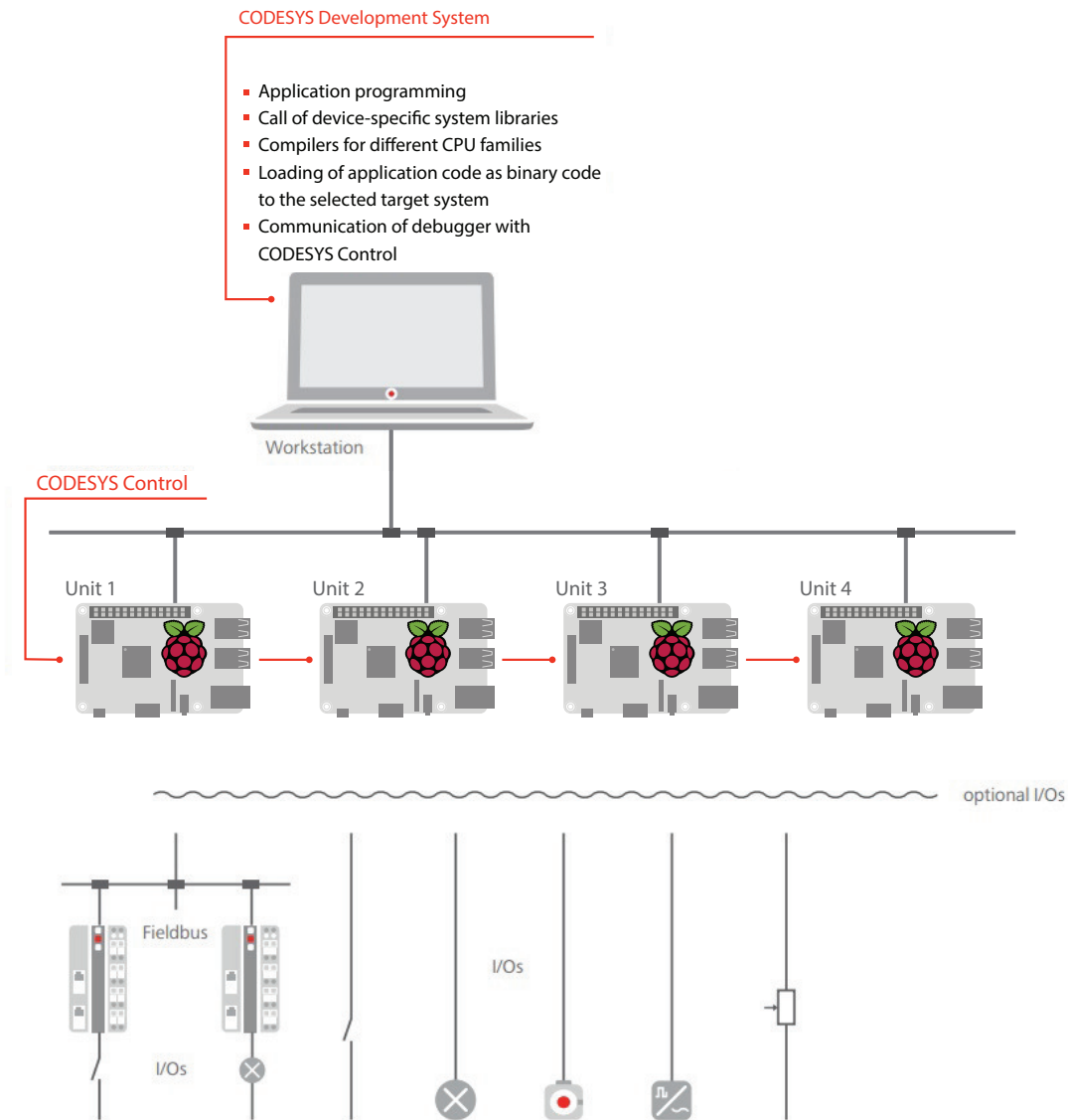


Figure 2.8: Network with a workstation running Codesys Development and four Raspberry Pi running Codesys Control. Source [CODESYS, 2019]

The Raspberry Pi will be running a Codesys Control code, previously loaded by Codesys Development via SSH protocol. Codesys Control will take care of the following tasks:

- Receive and send outputs and inputs from/to the DAQ via EtherCAT
- Correct sensors offset and linearize its output to get as much resolution as possible.
- Publish the system information to the localhost so it is accessible from a web browser.
- In case Remote Control is selected, it will run a Modbus slave to communicate with the CCU.
- In case Local Control is selected, it will run a Modbus slave to communicate with the LU.

Codesys Control will receive the integer value send by the DAQ and will convert this value to a real value with a more meaningful value. This is done by taking in account the range of the sensor. For example, consider a flow sensor that can give a minimum reading of 0

$L/min$  and a maximum of  $32 L/min$  which will correspond to  $4 mA$  and  $20 mA$  respectively. When converting the integer value send by the DAQ to  $L/min$  we will convert the integer value 6554 ( $4 mA$ ) to  $0 L/min$ , 65535 ( $20 mA$ ) to  $32 L/min$  and the values in between accordingly to the linear relationship.

From the HMI it is possible to switch from Local Controller to Remote Controller. In case Local Controller is selected, Codesys Control will communicate with the Local Unit (LU) running inside the Raspberry Pi. This LU consist of a Python code with some preset configurations which can be modified from the HMI.

In case Remote Controller is selected, Codesys Control will communicate with the Central Control Unit (CCU). The HMI will be no longer able to modify actuators values and it will only display information.

### 2.3.3 Communication protocol: Modbus TCP/IP

In order to send control inputs to actuators and receive sensor outputs a communication protocol has to be implemented. A communication protocol is a set of rules that allows reliable transmission of information. Some industrial communication protocols have been developed in order to ensure compatibility for the different hardware and software manufacturers.

MODBUS is an industrial standard communications protocol. It is simply a messaging service that runs on different physical layers. Two particular versions are: 1. Serial MODBUS, that use RS-485 / RS-232 as physical layer and 2. MODBUS TCP or MODBUS TCP/IP, that use Ethernet as physical layer. The latter version is the one used in the laboratory.

In the MODBUS protocol, data is exchanged in a master–slave relationship. Each slave has a unique address, which helps the master in identifying them while communicating. Some characteristics of the MODBUS protocol cannot be changed such as the frame format, frame sequences and handling of communications errors. The user is allowed to change the following: baud rate, parity check method, number of stop bits and transmission mode (ASCII or RTU).

Modbus TCP/IP uses Ethernet as physical layer, IP as network layer and TCP as transport layer. Figure (2.9) shows how a Modbus TCP/IP packet is constructed by a Modbus Application Protocol (MBAP) header and a PDU. The MBAP header is 7 bytes long and has the following fields:

- **Transaction Identifier:** Is used to associate the future response with the request.
- **Protocol Identifier:** Always 0 for Modbus.
- **Length:** Number of following bytes.
- **Unit Identifier:** Used to identify a server located on a non TCP/IP network.

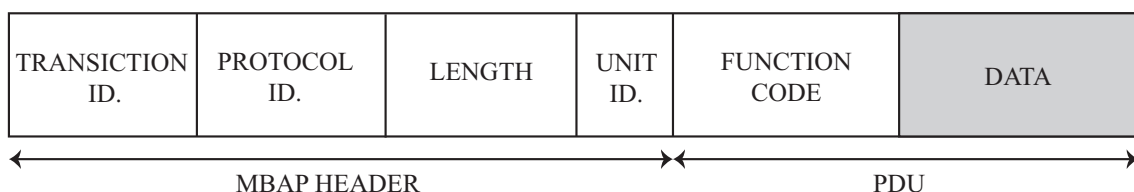


Figure 2.9: *Format of Modbus TCP/IP packet*

The function code contain one byte that tells the slave what kind of action to take. Table (2.2) shows the most important functions.

Code	Function
01 (01H)	Read Coil Status
02 (02H)	Read Discrete Inputs
03 (03H)	Read Holding Registers
04 (04H)	Read Input Registers
05 (05H)	Write Single Coil
06 (06H)	Write Single Holding Registers
15 (0FH)	Write Multiple Registers
16 (10H)	Write Multiple Holding Registers

Table 2.2: *Standard function codes used on Modbus*

	Data Type	Master Access	Comments
Discrete Input	Boolean	Read Only	Provided by an I/O system
Coils	Boolean	Read/Write	Alterable by an application program
Holding Registers	16 bit word	Read/Write	Alterable by an application program
Input Registers	16 bit word	Read Only	Provided by an I/O system

Table 2.3: *Modbus data format*

As in the present project any boolean sensors/actuators are used, the functions used in the project are:

- **Read Input Registers (04H):** Input registers are used for the value of the analog inputs from the field (read only). This function allows to read the content of analog input registers.
- **Write Single Holding Register (06H):** Holding registers are used for the value of analog outputs to the field (Read/write). This function allows to write the contents of an specific analog output holding register.
- **Write Multiple Holding Register (10H):** Write a block of contiguous registers.

The slave may provide additional information in the data field such as starting register, number of register to be read etc. When the slave responds, it uses the same function code to indicate an error-free response followed by the required data in the data field.

MODBUS still remains as a popular choice for data exchange in the industrial automation community because it is a simple protocol that requires little programming effort to setup and get it running. Some advantages are [MODBUS, 2019]:

- Minimum hardware is enough, development cost is less and development is easy for any operating system
- The Modbus protocol is open and there are no licensing fees
- Interoperability among devices from different manufacturers
- Easy to add devices to the network

In this chapter, deterministic (or white-box) models are developed to describe the dynamics of some key components of the sewer network. We model the buffer tank in the sewer network, flow in a gravity sewer pipe. We also show how the flow in a sewer pipe can be seen as a delay model.

The dynamics of the sewer system has to be understood if one desires to design a control system. Such understanding of the complex dynamic behavior is formulated as dynamic models. In this project, we do not intend to develop a very detailed description of the involved processes but rather intend on developing simple models that suits the purpose of prediction and control.

## 3.1 Tank volume

Critical situations arise when the inlet flow to the wastewater plant exceeds its treating capacity. In those situations, some untreated wastewater has to be discharged to the receiving waters. The idea of building storage tanks to hold back excessive wastewater until the treatment plant is ready to handle them has been extensively used before.

A simplified mathematical model, using continuity equation, is developed to analyze a buffer tank storing wastewater. The continuity equation is an expression of the principle of conservation of mass. For a control volume with a single inlet and a single outlet, the mass balance equation would be:

$$\frac{dM(t)}{dt} = m_{in}(t) - m_{out}(t) \quad (3.1)$$

where  $M$  is the total mass ( $kg$ ),  $m_{in}$ ,  $m_{out}$  are mass inflow and outflow rates. Rewriting the same equation with volumetric flow rates (with  $\rho$  as sewage density ( $\frac{Kg}{m^3}$ ) and taking into account the overflow  $Q_{over}$ :

$$\frac{\rho dV(t)}{dt} = \rho Q_{in}(t) - \rho Q_{out}(t) - \rho Q_{over}(t) \quad (3.2)$$

or

$$\frac{dV(t)}{dt} = Q_{in}(t) - Q_{out}(t) - Q_{over}(t) \quad (3.3)$$

where density  $\rho$  is cancelled out as it is very close to a constant in the relevant temperature range. The discrete-time or difference equation describing the same phenomena would be

$$V_{k+1} = V_k + T_s(Q_{in,k} - Q_{out,k} - Q_{over,k})$$

where  $V_k$  is the tank volume ( $m^3$ ) at instance  $k$  and  $T_s$  is sampling time.

The model is also later used for determining the appropriate tank size needed to optimally store and release wastewater into the sewer network down at the municipality of Fredericia. The potential benefit of adding a tank in the sewer system is to take care of the temporal variations in wastewater flow and the concentration of contaminants at the inlet of the treatment plant.

## 3.2 Flow in pipe

The transportation of water through a channel or a network of channels and pipes is governed by the conservation of mass and momentum equations. The Saint-Venant equations [de Saint-Venant A, 1871] describe one-dimensional unsteady open channel flow. Sewage flow in sewer mains can be considered as an open channel flow because the sewage is not subjected to any parallel shear stresses from the empty space above. The flow profile is similar to what we see in rivers.

The flow of water through a channel is a distributed process because the flow rate and level vary in time and space throughout the length of the channel. The general form of Saint-Venant equations is given by:

$$\frac{\partial A}{\partial t} + \frac{\partial Q}{\partial x} = 0 \quad (3.4)$$

$$\frac{1}{gA} \frac{\partial Q}{\partial t} + \frac{1}{gA} \frac{\partial}{\partial x} \left( \frac{Q^2}{A} \right) + \frac{\partial h}{\partial x} + S_f - S_b = 0 \quad (3.5)$$

where  $Q$  is sewage flow ( $m^3/s$ ),  $A$  is the wetted area or cross-sectional area of the sewage flow ( $m^2$ ),  $h$  is sewage level inside the sewer ( $m$ ),  $S_b$  is slope of sewer,  $S_f$  is friction coefficient,  $x$  is the spatial variable measured in the direction of the sewage flow ( $m$ ),  $t$  is time ( $s$ ) and  $g$  is acceleration due to gravity ( $m/s^2$ ). Equation (3.4) is about the mass conservation and equation (3.5) is about momentum. Rewriting (3.5) as:

$$\frac{1}{A} \frac{\partial Q}{\partial t} + \frac{1}{A} \frac{\partial}{\partial x} \left( \frac{Q^2}{A} \right) + g \frac{\partial h}{\partial x} - g(S_b - S_f) = 0 \quad (3.6)$$

The above 5 terms describe the following physical quantities [Te et al., 1988]: 1 - Local acceleration, 2 - Convective acceleration, 3 - Pressure force, 4 - Gravity force and 5 - Friction force. Terms 1 and 2 are together known as Inertia.

Some assumptions taken while deriving the Saint-Venant equations are:

- The flow is one-dimensional
- The longitudinal axis of the channel is approximated as a straight line
- The fluid is incompressible and of constant density throughout the flow
- Only hydrostatic pressure exists

## Manning's equation

This empirical equation [Manning et al., 1890], is commonly used to analyze uniform steady state flow in open channels. The channel shape can be circular, rectangular, triangular,

etc. It is hence used in studies of sewer systems with large diameter circular pipes. Flow velocity is given by:

$$v = \frac{K_n}{n} R^{2/3} S_f^{1/2} \quad (3.7)$$

where  $v$  is sewage velocity ( $m/s$ ),  $K_n$  is a constant whose value depends on the measurement units used in above equation,  $n$  is the Gauckler–Manning coefficient, which depends on sewer characteristics such as the flow resistance, roughness and curves in the network. The variable  $R$  is the hydraulic radius ( $m$ ), ratio of cross-sectional area of the sewage flow and the wetted perimeter.  $S_f$  is friction coefficient. Volumetric flow is nothing but

$$Q = v \cdot A \quad (3.8)$$

$$Q = \frac{K_n}{n} A R^{2/3} S_f^{1/2}$$

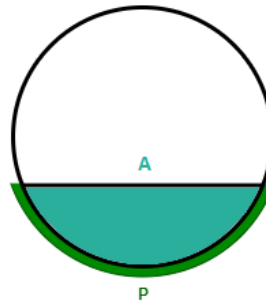


Figure 3.1: *Cross-sectional view of flow in a circular pipe*

### 3.2.1 Modeling of sewer system in Fredericia

For real-time control of sewer networks, we need a simplified version of Saint-Venant equations. Even though equations (3.4) and (3.5) captures a high level of detail of the system's dynamic behaviour, using them often leads to increased complexity and high computational cost [Crossley, 1999].

Type of Conduit	Manning's roughness coefficient		
	Minimum	Normal	Maximum
Steel (lockbar and welded)	0.010	0.012	0.014
Cast Iron (coated)	0.010	0.013	0.014
Cement (neat surface)	0.010	0.011	0.013
Concrete (finished)	0.011	0.012	0.014
Brick (lined with cement mortar)	0.012	0.015	0.017
Polyvinyl Chloride (smooth inner walls)	0.009	0.010	0.011

Table 3.1: Some examples to compare different manning's roughness coefficients [Chow, 1959].

One approximation of Saint-Venant equations is neglecting the first two terms of momentum equation (3.5) because in most practical cases they are very small compared to the third term [Wanka and Königer, 1984].

$$\frac{\partial h}{\partial x} = S_b - S_f \quad (3.9)$$

Now, using equations (3.7) and (3.9), the flow velocity can be written as

$$\begin{aligned} v &= \frac{K_n}{n} R_h^{2/3} \sqrt{S_b - \frac{\partial h}{\partial x}} \\ Q &= \frac{K_n}{n} A R_h^{2/3} \sqrt{S_b - \frac{\partial h}{\partial x}} \end{aligned} \quad (3.10)$$

Then equations (3.4) and (3.10) can form the basis for a hydrodynamically modelled sewer.

### Model with delay

The transport of fluids such as water could also be seen as a wave propagation. Since there is a net mass transfer involved, the waves are translatory. To understand the wave phenomena in gravity and pressure driven fluid mass flows, kinematic wave or dynamic wave analysis is important. When the inertial and pressure forces are not significant in momentum equation (3.5), kinematic waves govern the flow. Dynamic waves govern flow when these forces are important. In a kinematic wave, the flow does not accelerate considerably as the gravity and friction forces balance out each other.

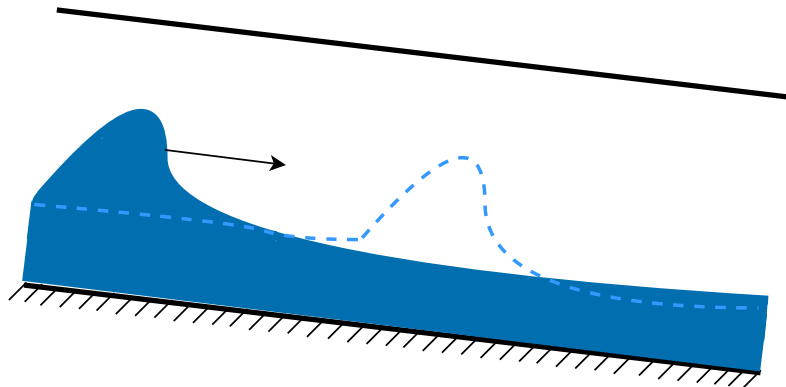


Figure 3.2: *Motion of a wave. The propagation of small fluctuation in flow is shown.*

In equation (3.5), disregarding the first three terms, the remaining two terms can be replaced by a flow expression for a fully filled pipe, equation (3.20) and an expression which gives the flow for a partially filled pipe (relative to flow for a fully filled pipe), equation (3.22). The wetted area (derivation shown in appendix (C.1)) can be expressed as

$$A = r^2 \cdot \arccos\left(\frac{r-h}{r}\right) - \sqrt{h(2r-h)}(r-h) \quad (3.11)$$

Inserting the approximate expressions of  $Q$  and  $A$  in the continuity equation (3.4):

$$\frac{\partial A}{\partial h} \frac{\partial h}{\partial t} + \frac{\partial Q}{\partial h} \frac{\partial h}{\partial x} = 0 \quad (3.12)$$

The two factors  $\frac{\partial Q}{\partial h}$  and  $\frac{\partial A}{\partial h}$  will be work dependent. But here, we use a linearized version of this equation and apply small fluctuations to flow  $Q$  and therefore water level  $h$ . The two factors are treated as constants (assuming the fluid does not gain kinetic energy and no work is done on the fluid) and the relationship between them is

$$c = \frac{\partial Q}{\partial A} = \frac{\frac{\partial Q}{\partial h}}{\frac{\partial A}{\partial h}} \quad (3.13)$$

and we get the equation

$$\frac{\partial Q}{\partial t} + c \frac{\partial Q}{\partial x} = 0 \quad (3.14)$$

This equation describe waves propagating with unchanged shape and speed  $c$ . It can be verified by assuming that the flow (or water level) in position  $x = 0$ ,  $Q(0, t)$  is known as a function of time  $t$ . The flow in an arbitrary position  $x$  will then be given by

$$Q(x, t) = Q(0, t - \frac{x}{c}) \quad (3.15)$$

Taking the partial derivatives with respect to  $t$  and  $x$

$$\frac{\partial Q}{\partial t} = \frac{\partial Q(0, t - \frac{x}{c})}{\partial(t - \frac{x}{c})} \frac{\partial(t - \frac{x}{c})}{\partial t} = \frac{\partial Q(0, t - \frac{x}{c})}{\partial(t - \frac{x}{c})} \quad (3.16)$$

$$\frac{\partial Q}{\partial x} = \frac{\partial Q(0, t - \frac{x}{c})}{\partial(t - \frac{x}{c})} \frac{\partial(t - \frac{x}{c})}{\partial x} = \frac{\partial Q(0, t - \frac{x}{c})}{\partial(t - \frac{x}{c})} \left( -\frac{1}{c} \right) \quad (3.17)$$

and inserting these two expressions into equation (3.14) results in

$$\frac{\partial Q(0, t - \frac{x}{c})}{\partial(t - \frac{x}{c})} + c \frac{\partial Q(0, t - \frac{x}{c})}{\partial(t - \frac{x}{c})} \left( -\frac{1}{c} \right) = 0 \quad (3.18)$$

which satisfies the equation for wave propagation. The kinematic wave model is described by the continuity equation and manning's formula for a uniform and steady flow. But by introducing small fluctuation in flow, we see that this fluctuation travels a distance  $x$  in time  $\frac{x}{c}$  without changing its shape. Hence, for a nonuniform flow, the transport of water can be seen as a delay model.

This approach of modeling the flow in a pipe as a delay leads to a simplified version of a sewer system model. The Saint-Venant equations are not used when describing flow. A simple model describing the proposed sewer system for Fredericia can be represented as [Morten Vesteraa et al., 2018]:

$$\begin{aligned} V(k+1) &= V(k) + T_s(Q_i(k) - U(k)) \\ Y(k+\tau) &= Q_h(k+\tau) + U(k) \end{aligned} \quad (3.19)$$

where  $V$  corresponds to the volume in the buffer tank ( $m^3$ ),  $Q_i$  describes the wastewater flow from the industries ( $\frac{m^3}{hr}$ ),  $Q_h$  describes the wastewater flow from the households ( $\frac{m^3}{hr}$ ),  $U$  is the input (controlled flow from buffer tank) in ( $\frac{m^3}{hr}$ ),  $\tau$  is the transport delay ( $hr$ ),

$Y$  is the overall measured flow at the WWTP inlet ( $\frac{m^3}{hr}$ ) and  $T_s$  is the sampling time.

$Q_h(k)$  describes the flow at present time, while  $Q_h(k + \tau)$  describes the flow after accounting for delay. The reason for using the delay is that, since there is a distance between the tank and the inlet to the WWTP, it takes some time for the wastewater to travel that distance. This means that when a pump input is given, it will only affect the overall inflow after the delay  $\tau$ .

### 3.2.2 Modeling of laboratory setup

Tank dynamics can be found from the differential pressure level sensor measurements. The output of the sensor after linearization is in *millimeters*. Using the known radius of the tank, this level is then converted into volume in *litres*.

Regarding overall flow measurement, in section (2.2) we saw that level measurements can be obtained from sensors placed along the length of gravity sewer pipe. The process of converting level measurements into flow measurements is shown below. From equations in (3.21), a equation for full flow (filled) pipe can be written as:

$$Q_f = \frac{K_n}{n} A_f R_f^{2/3} S_f^{1/2} \quad (3.20)$$

where  $Q_f$ ,  $A_f$  and  $R_f$  are flow, wetted area and hydraulic radius for a full flow pipe.

$$\begin{aligned} A_f &= \pi r^2 = \frac{\pi d^2}{4} \\ R_f &= \frac{A}{P} = \frac{\pi r^2}{2\pi r} = \frac{d}{4} \end{aligned} \quad (3.21)$$

When level of water in a pipe is known, the flow can be calculated with the empirical formula [Michelsen, 1976]:

$$Q = \left( 0.46 - 0.5 \cdot \cos\left(\pi \frac{h}{d}\right) + 0.04 \cdot \cos\left(2\pi \frac{h}{d}\right) \right) \cdot Q_f \quad (3.22)$$

where  $h$  is level and  $d$  is the pipe diameter.

Manning's equation describes flow in an open channel but can also be used for closed pipes with a free or exposed water surface. A comparison of level and flow is made between manning equation and SWMM (hydraulic water quality simulation model), shown in the appendix (C.2).

# Control 4

This chapter will first describe how the flow (at the WWTP inlet) is modeled. The model is used with a Kalman filter to make predictions of flow patterns. The importance of predicting flow disturbance is discussed in section (4.4) and subsequently, a disturbance model (flow from residential areas) is created. Then, we discuss about Model Predictive control (MPC), control objectives, development of performance function and constraints. This chapter is more about theory whereas the implementation and analysis is described in chapter (5).

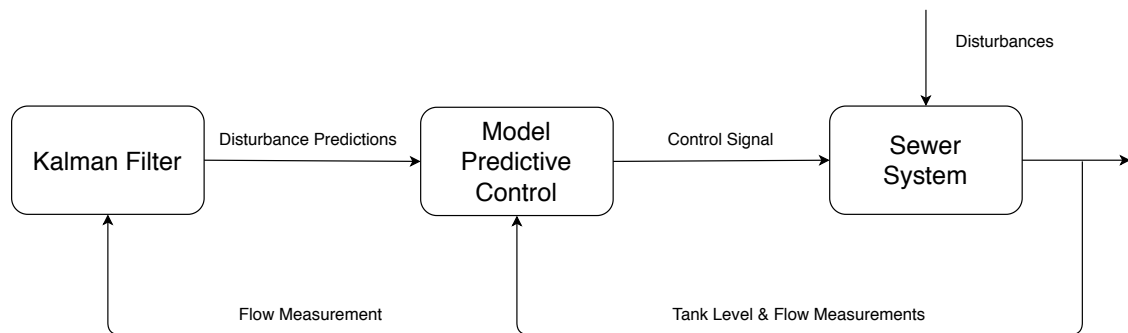


Figure 4.1: *Block diagram of the control system.*

## 4.1 Time-series analysis in the frequency domain

A time series is just consecutive data points separated by a unit time interval. From Fred-erica Spildevand og Energi A/S, we have flow measurements at the WWTP inlet for one month sampled at 5 *minutes*, seen in appendix (A.1). These flows are averaged out and the resulting average flow for a single day is selected and analyzed. This is done because we desire to find variations in flow with a period of one day.

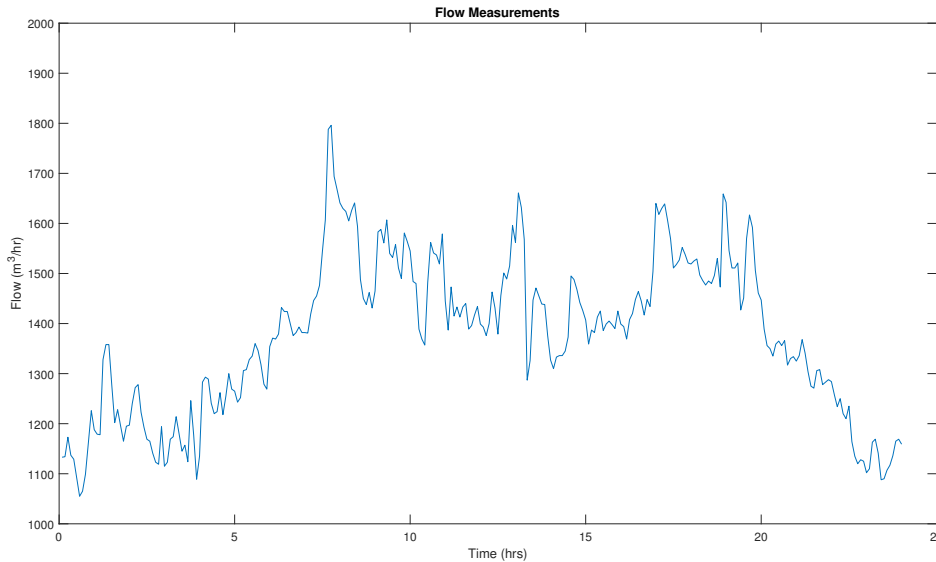


Figure 4.2: Average flow for one day entering the WWTP. Each measurement is taken at every 5 minutes. This roughly resembles the flow pattern seen in figure 1.5 in chapter (1).

Flow entering the WWTP is assumed to be periodic with time period of one day. Now we use fourier analysis to approximate this data with a weighted combination of sine and cosine terms whose frequencies are integral multiples of a fundamental frequency. This approximation is described by the fourier series.

$$y(t) = a_0 + \sum_{n=1}^N a_n \sin(n\omega t) + b_n \cos(n\omega t) \quad (4.1)$$

where  $y(t)$  is the flow data,  $a_0/a_n/b_n$  are the fourier coefficients,  $\omega$  is the fundamental frequency and  $N$  is the data length. The approximation in equation (4.1) is perfect for periodic signals as the value of  $N$  tends to infinity.

In order to convert our time series data into the form above, we first need to determine the frequency content of the data. The Discrete Fourier Transform (DFT) algorithm can be used to determine which all frequencies a complicated data is composed of. Then we describe this data as a sum of many individual frequency components thereby transforming a complicated signal/data into much simpler parts.

The equation for DFT and its inverse looks like:

$$Y(k) = \frac{1}{N} \sum_{n=0}^{N-1} y(n) e^{-i2\pi kn/N} \quad k = 0, 1, \dots, N-1 \quad (4.2)$$

$$y(n) = \sum_{k=0}^{N-1} Y(k) e^{i2\pi kn/N} \quad n = 0, 1, \dots, N-1$$

where  $Y(k)$  is the Fourier transform. After expanding the exponential term, we get

$$Y(k) = \sum_{n=0}^{N-1} y(n) \cos\left(\frac{2\pi kn}{N}\right) - i \sum_{n=0}^{N-1} y(n) \sin\left(\frac{2\pi kn}{N}\right) \quad (4.3)$$

From the above expression, its evident the algorithm calculates the correlation between the data  $y(n)$  and a cosine/sine of a certain frequency. To identify the dominant frequency components, we plot the power spectrum as seen in figure (4.3). The spectrum is symmetric about its middle ( $N/2$ ) and hence it is sufficient to display only the left half of the spectrum (up to the nyquist frequency at the centre).

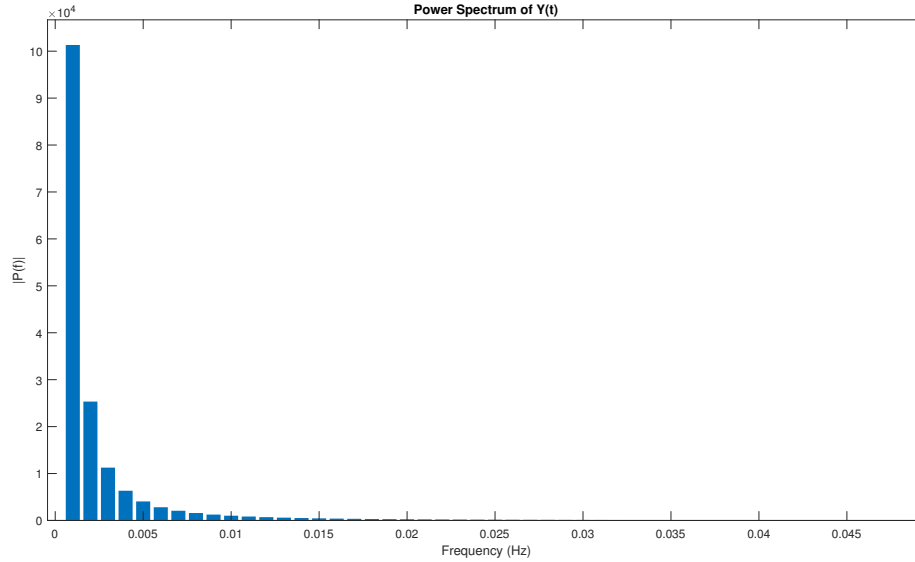


Figure 4.3: Bar plot of power spectrum which is the square of DFT's magnitude. At low frequencies, the magnitudes are large. A zoomed out version can be seen in appendix (B.1).

Here, to find those dominant frequencies, we look at instances at which the power spectrum of  $Y(k)$  is greater than a specified threshold. To convert these instances into actual frequencies ( $Hz$ ), we use the following formula:

$$f = \frac{k \cdot f_s}{N} \quad k = 0, 1, \dots, N/2 \quad (4.4)$$

where  $k$  can be any value between 0 and  $N/2$ ,  $f_s$  is the sampling frequency and  $N$  is the number of samples in our data.

## 4.2 State-space model

Alternatively writing a continuous time sinusoidal in amplitude phase form as

$$y(t) = a_0 + a \cdot \cos(\omega t + \phi) \quad (4.5)$$

where  $a_0$  is the mean or zero frequency term,  $a$  is the amplitude,  $\omega$  is the frequency and  $\phi$  is the phase difference.

We can define an autonomous state space model (SSM)

$$\dot{x} = Ax + Bu \quad (4.6)$$

$$y = Cx + Du \quad (4.7)$$

whose state vector, system matrix, input and output matrix are

$$x(t) = \begin{bmatrix} a_0 \\ a \cdot \cos(\omega t + \phi) \\ a \cdot \sin(\omega t + \phi) \end{bmatrix} \quad (4.8)$$

and

$$A = \begin{bmatrix} 0 & 0 & 0 \\ 0 & 0 & -\omega \\ 0 & \omega & 0 \end{bmatrix} \quad B = [0] \quad C = [1 \quad 1 \quad 0] \quad D = [0] \quad (4.9)$$

$y(\omega)$  is the fourier transform of  $y(t)$ . Real part and imaginary part of the fourier transform coefficients are used in  $C$ . The above SSM contains just a single frequency. When we have multiple frequencies, the sinusoidal signal and SSM would look like

$$y(t) = a_0 + \sum_{n=1}^N a_n \cdot \cos(n\omega t + \phi_n)$$

$$x(t) = \begin{bmatrix} a_0 \\ a_1 \cdot \cos(\omega_1 t + \phi_1) \\ a_1 \cdot \sin(\omega_1 t + \phi_1) \\ a_2 \cdot \cos(\omega_2 t + \phi_2) \\ a_2 \cdot \sin(\omega_2 t + \phi_2) \\ \cdot \\ \cdot \\ \cdot \\ \cdot \\ a_k \cdot \cos(\omega_k t + \phi_k) \\ a_k \cdot \sin(\omega_k t + \phi_k) \end{bmatrix}$$

$$A = \begin{bmatrix} 0 & 0 & 0 & 0 \\ 0 & A_1 & 0 & \dots \\ 0 & 0 & A_2 & \dots \\ \cdot & \cdot & \cdot & A_k \end{bmatrix} \quad \text{where} \quad A_i = \begin{bmatrix} 0 & -\omega_i \\ \omega_i & 0 \end{bmatrix} \quad i = 1, 2 \dots k$$

$$C = [1 \quad 1 \quad 0 \quad 1 \quad 0 \quad \dots \quad 1 \quad 0]$$

The discrete-time equivalent of  $A$  in equation (4.9), with sampling time  $\tau$  is

$$\Phi(\tau) = e^{A\tau}$$

and

$$\Phi(\tau) = \begin{bmatrix} 1 & 0 & 0 \\ 0 & \cos(\omega\tau) & -\sin(\omega\tau) \\ 0 & \sin(\omega\tau) & \cos(\omega\tau) \end{bmatrix} \quad (4.10)$$

Now we perform these steps:

1. Load the flow data
2. Calculate the discrete fourier transform
3. Set a threshold ' $h$ ' for the power spectrum  $|P(f)|$
4. Identify frequencies ' $f$ ' for which  $|P(f)| > 'h'$
5. Build the state space model
6. Simulate the model to compare with flow data

In the figure below, three threshold values of the power spectrum was chosen and the consequent models were simulated and compared.

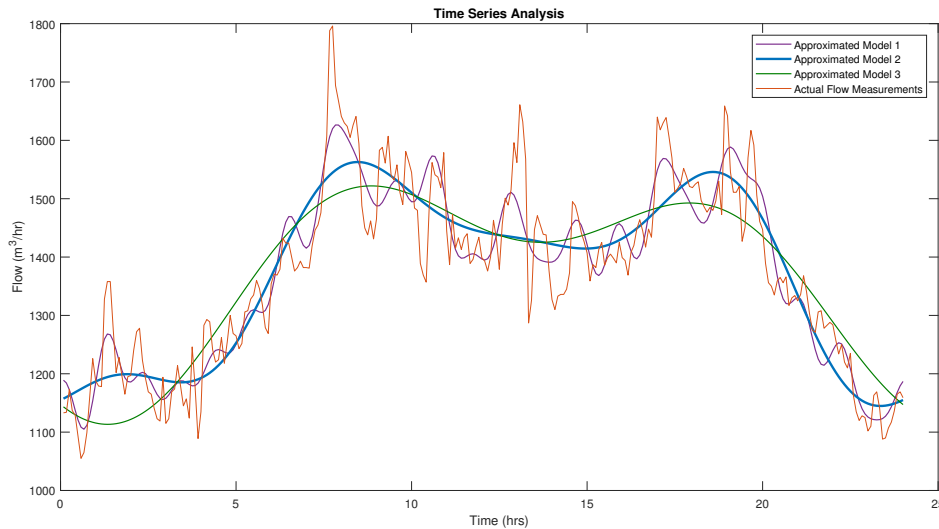


Figure 4.4: *Different model approximations of the original flow data. The thresholds set for the model 1, 2 and 3 are respectively 2500, 900 and 400. The purple curve considered 10 frequencies in the model. The blue curve considered only 5 frequencies in the model. The latter model is used in the subsequent section.*

### 4.3 Kalman filter

The Kalman filter has been used for data prediction tasks and other purposes for the last 50 years or so [Kalman, 1960]. Using state space method to build the Kalman filter also simplifies the implementation of the filter in the discrete domain.

The discrete state space model is written as

$$\begin{aligned}x_{k+1} &= \Phi x_k + w_k \\ y_k &= H x_k + v_k\end{aligned}$$

where  $x_k$  is the state vector of the process at time  $k$ ,  $\Phi$  is the state transition matrix of the process from the state at  $k$  to the state at  $k + 1$ ,  $w_k$  is the associated process noise with covariance  $Q$ ,  $y_k$  is the actual measurement of  $x$  at time  $k$ ,  $H$  is the output matrix;  $v_k$  is the measurement noise with covariance  $R$ . Both  $w_k$  and  $v_k$  are assumed to be a white gaussian noise processes.

Error term  $e_k$  is the difference between the estimate  $\hat{x}_k$  and  $x_k$  itself. The Kalman filter tries to minimize the mean squared error. To get to that, we must first describe the error covariance matrix  $P_k$  at time  $k$ :

$$P_k = E[e_k e_k^T] = E[(x_k - \hat{x}_k)(x_k - \hat{x}_k)^T]$$

The trace of this matrix is the sum of the mean squared errors. Therefore the mean squared error can be minimized by minimizing the trace of  $P_k$ .

The two important steps of the Kalman filter are the prediction step and measurement update step with Kalman gain  $K$ .

Measurement update Step:

$$\begin{aligned} K_k &= (P_k H^T)(H P_k H^T + R)^{-1} \\ \hat{x}_k &= \hat{x}_k + K_k(y_k - H \hat{x}_k) \\ P_k &= (I - K_k H)P_k \end{aligned}$$

Prediction Step:

$$\begin{aligned} \hat{x}_{k+1} &= \Phi x_k \\ P_{k+1} &= \Phi P_k \Phi^T + Q \end{aligned}$$

The state space model used in this section has considered 5 different frequencies and the dimensions are as follows:

$$x_k = [ ]_{11 \times 1} \quad \Phi = [ ]_{11 \times 11} \quad H = [ ]_{1 \times 11}$$

The Kalman filter algorithm was tested for different scenarios and the estimation results are plotted. The estimate is compared against the actual flow measurements.

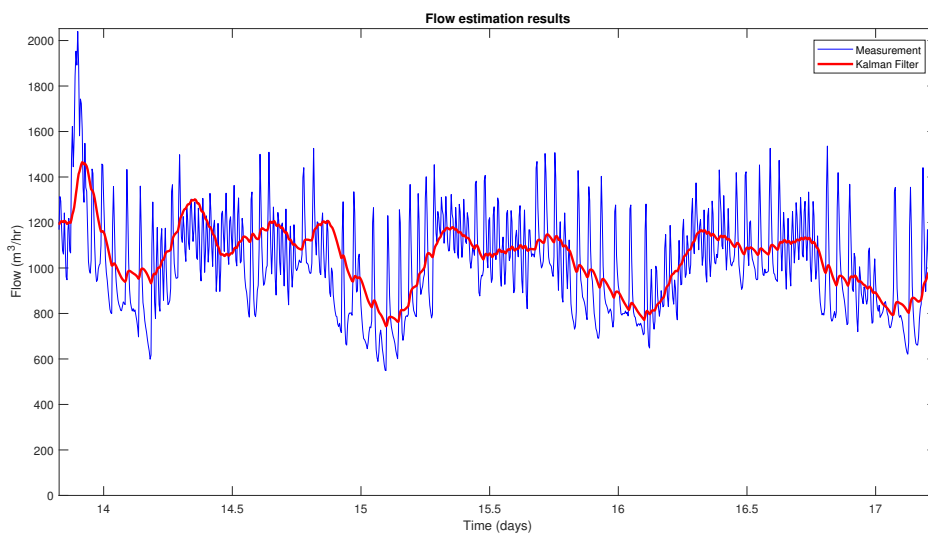


Figure 4.5: The Kalman filter estimation for the days 14 to 17. The process noise ( $Q$ ) and measurement noise ( $R$ ) had a variance of 0.01 and 25 respectively.

The above figure shows the result when Kalman filter is used for 1-step prediction. It is however only useful when we can make predictions of flow pattern much ahead in time. The Kalman filter can be used for n-step prediction as well. To illustrate such predictions, we first choose the days when it is not raining. Then we discard some of the measurement readings. Whenever there are no measurements available, the Kalman filter algorithm just performs the prediction step for flow without the updation step. Some results are shown below for different prediction horizons.

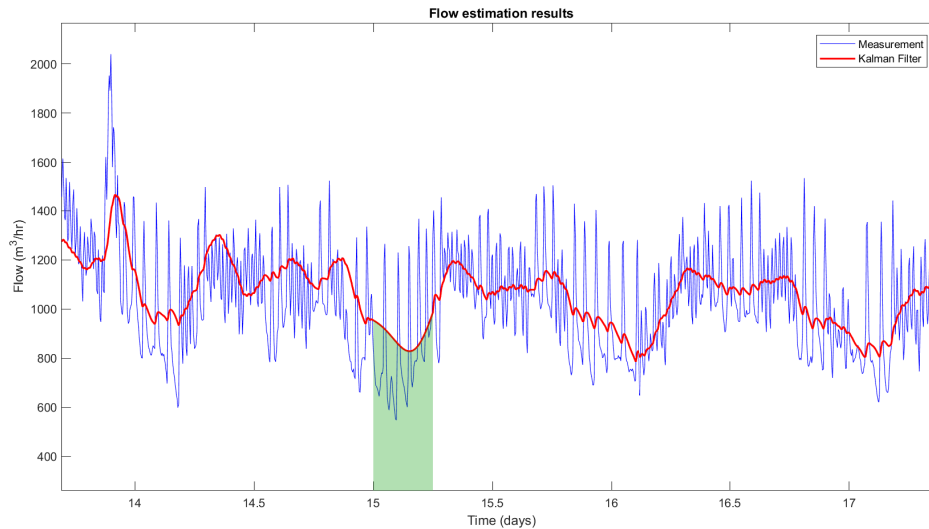


Figure 4.6: *The Kalman filter estimation for the first 6 hours of day 15. No new measurements were taken in this period. The process noise ( $Q$ ) and measurement noise ( $R$ ) had a variance of 0.01 and 25 respectively.*

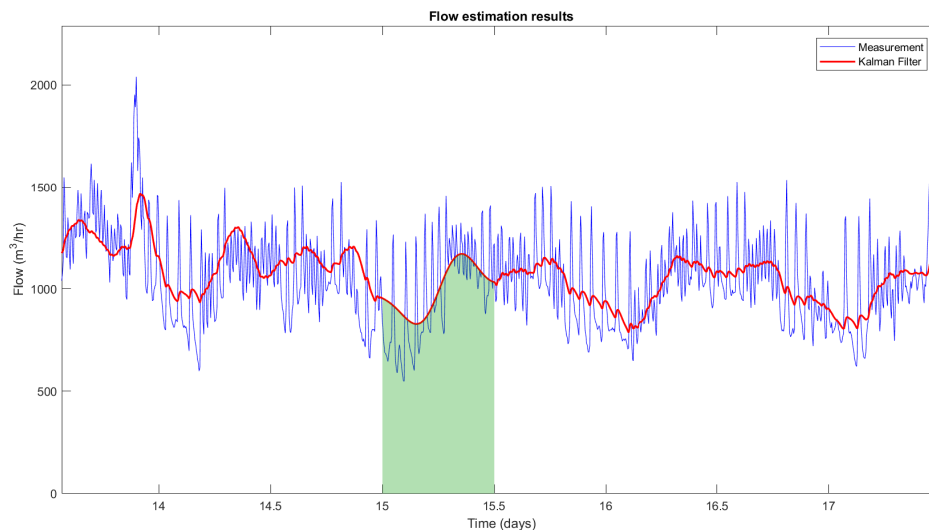


Figure 4.7: *The Kalman filter estimation for the first 12 hours of day 15. No new measurements were taken in this period. The process noise ( $Q$ ) and measurement noise ( $R$ ) had a variance of 0.01 and 25 respectively.*

Ideally, we would need to make predictions for a 24 hour period since the controller optimization window (prediction horizon) is one day.

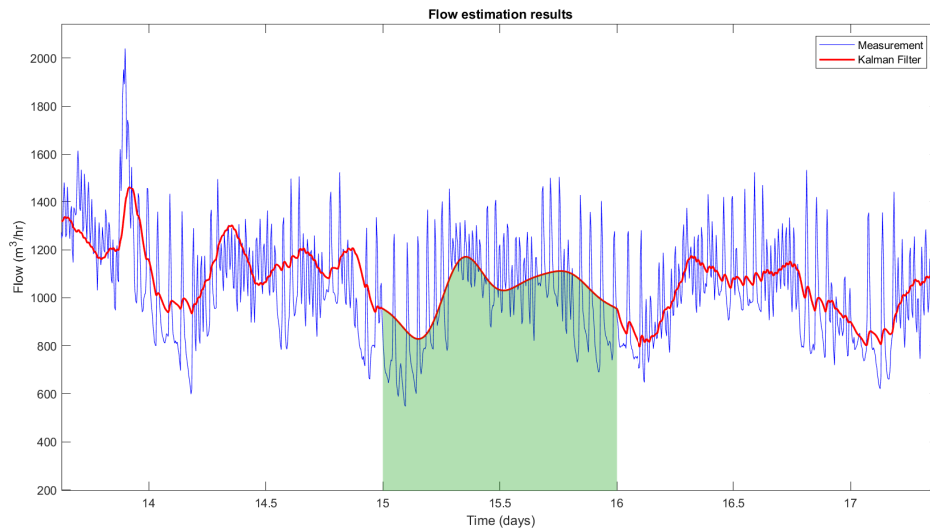


Figure 4.8: The Kalman filter estimation for day 15. No new measurements were taken in this period. The process noise ( $Q$ ) and measurement noise ( $R$ ) had a variance of 0.01 and 25 respectively.

## 4.4 Delay in the sewer network

So far, we have predicted the flow that would enter the WWTP. The flow changes in value for a 24 hour window. To even out this flow, it is necessary to predict wastewater flow from the residential areas. Having information about this flow disturbance would make it easier for the controller to release wastewater from the buffer tank accordingly to end up with a smooth flow at WWTP inlet. The controller also has to account for the delay in wastewater transport from the buffer tank to treatment plant, figure (2.1).

To calculate the flow from residential areas, we need to subtract the industrial wastewater flow from the WWTP inlet flow keeping the delay in mind. This delay can be measured by noting the time it enters the sewer pipe and the time it leaves the sewer pipe and comes into WWTP. In a real sewer network, this is not possible to measure but for the laboratory setup with transparent sewer pipe it is easy to do so. The other way to find out transport delay of wastewater in a real sewer network would be to calculate it by performing cross correlation analysis.

### 4.4.1 In Fredericia

From the results seen in section 4.3, it is clear that finding a flow model close enough to the actual flow measured in a day can be really helpful. The kalman filter was able to use this model and make good predictions of flow.

Now, we move on to find a model for flow disturbances from the residential areas. Wastewater at the WWTP inlet is a mix of wastewater from industries and houses. To find real flow measurements leaving the houses, it is mandatory to know the exact delay in the sewer line. Subtracting the industrial flow from the flow measured at WWTP inlet after taking care of transport delay can give us the disturbance flow.

Figure (4.9) shows how wastewater enters the treatment plant in Fredericia. Referring to the same figure, we have information of flow leaving the heavy industries and the flow at

the WWTP inlet. If we have knowledge of flow leaving the pumping station, it is possible to calculate the delay in the thick blue line using cross correlation analysis.

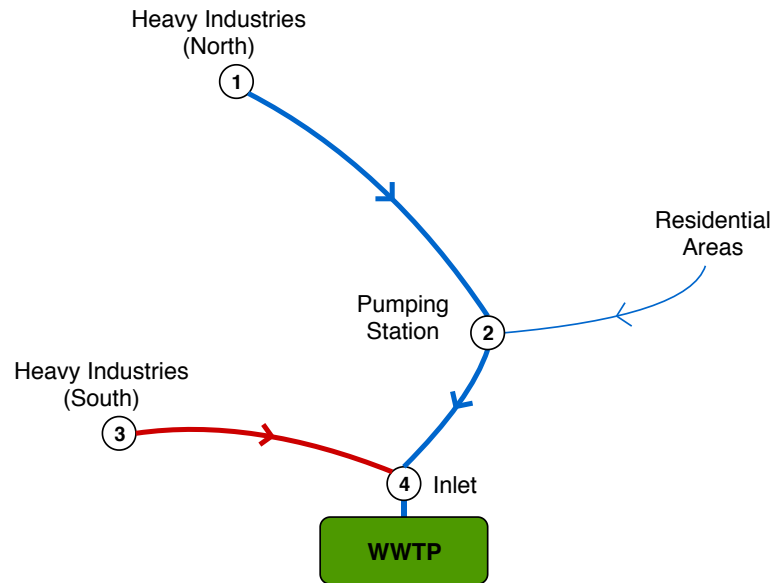


Figure 4.9: *Simple illustration of wastewater transport and collection in the city of Fredericia.*

With this tiny problem present, we can not obtain the exact flow measurements from the households. So instead, we created a flow pattern that resembles the actual flow data (which can be seen in appendix (A.3)). The magnitude and periodic behaviour is very much similar to actual flow data.

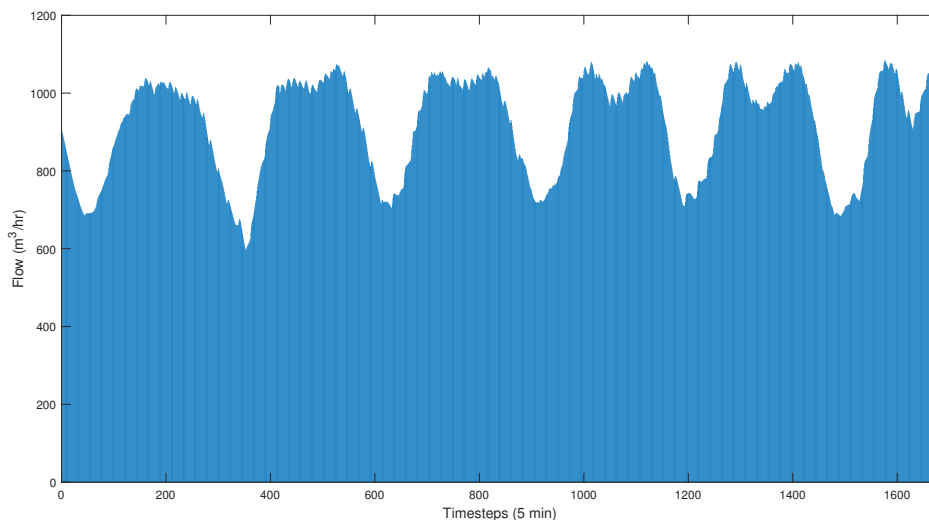


Figure 4.10: *Bar plot of wastewater flow from residential areas for a period of 5 days.*

Therefore, with this flow profile, we take the average flow for a day and repeat the same steps mentioned in section (4.1) to obtain a model using fourier analysis. For the rest of the project work, this model is used for the prediction of household wastewater flow.

## 4.4.2 Cross correlation analysis in laboratory

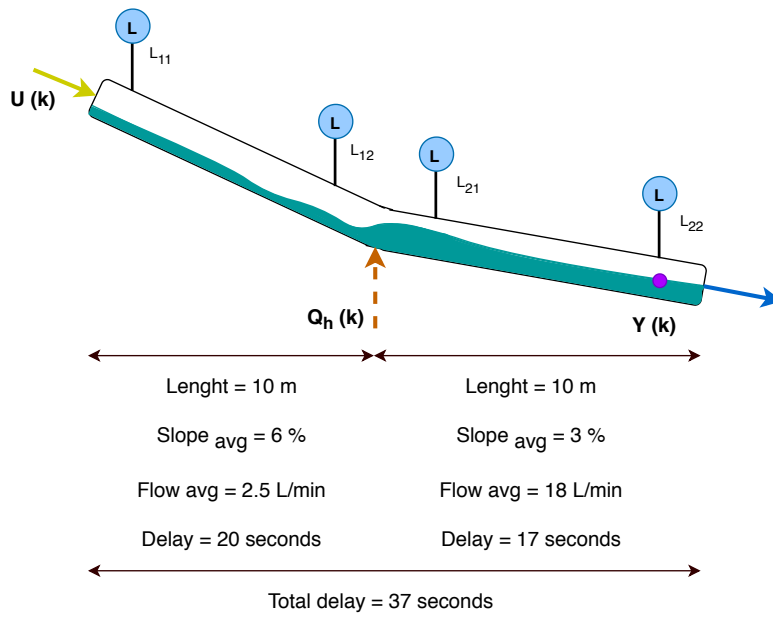


Figure 4.11: Layout of the sewer pipe with its flow inlets and level sensors. This was chosen in order to minimize the backwards flow of water from households in the middle section. The delays were measured separately using a timer.

For the laboratory setup, apart from measuring delays with a timer, we also calculated the delay from the middle to bottom section of sewer pipe using cross correlation. Data used to do this analysis is shown in appendix (B.4). The theory of correlation is explained below.

Cross correlation is a technique to find out the degree to which two time series are similar with each other. Consider two time series  $x(i)$  and  $y(i)$  where  $i = 1, 2, \dots, N$ . The cross correlation  $r$  at delay  $d$  is expressed as:

$$r = \frac{\sum_i \left( (x(i) - \mu_x) * (y(i) - \mu_y) \right)}{\sqrt{\sum_i (x(i) - \mu_x)^2} \sqrt{\sum_i (y(i) - \mu_y)^2}} \quad (4.11)$$

Where  $\mu_x$  and  $\mu_y$  are the means of the corresponding time series. The above equation is computed for all delays  $d = 0, 1, 2, \dots, N - 1$  and results in a cross correlation series of length  $2 * N$ . The denominator in the equation is used to normalize the correlation coefficients such that  $-1 \leq r(d) \leq 1$ , the bounds  $(-1$  and  $1)$  indicates maximum correlation and 0 indicates no correlation.

While evaluating the cross correlation, there is small issue to consider for the indexes  $i - d < 1$  and  $i - d > N$ . The common approach (as done in Matlab) is assigning zero to these points. The second method is assuming one series is circular and the indexes exceeding the dimension ( $N$ ) are wrapped back within range, for example  $x(N + 10) = x(10)$ . With this method, its not possible to compute the normalized cross-correlation of the two time series (of different lengths) as Matlab does not support it.

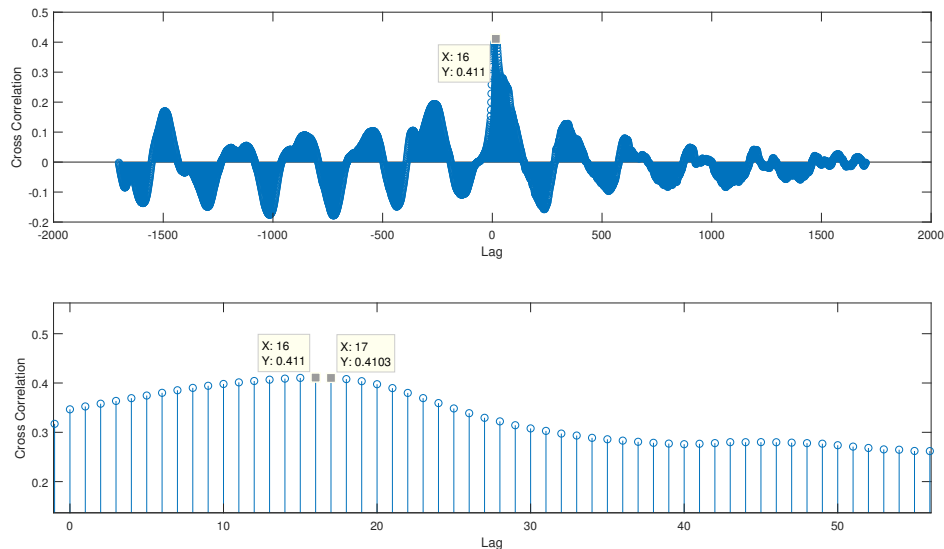


Figure 4.12: *Delay analysis for the bottom half of the sewer pipe. Cross correlation done between the flow entering in the middle and the flow at the end of the sewer pipe. The matlab command 'xcorr' was used. Data used to do this analysis is shown in appendix (B.4).*

As seen from the figure, the two flow data have highest correlation at 16 *seconds* and 17 *seconds*. Hence, we can confirm that the measured delay of 17 *seconds* is accurate. This analysis is merely done to defend the delay value used in our system model.

## 4.5 Model predictive control

Monitoring and control of any complex system like a sewer network is not easy and straightforward. Such a challenging system requires a control method that can reduce the burden of complexity and make real-time control possible. The controller should also be capable of handling multiple inputs and outputs because a sewer network will indeed have many sensors and actuators for measurement and control. The controller should also compensate for the effects of undesirable dynamics such as delays and dead times, consider physical constraints and nonlinear behaviours [Ocampo-Martinez, 2010].

Hence, in the field of wastewater system control, one of the well suited method is the use of Model Predictive Control (MPC), also referred to as Receding Horizon Control. The basic idea of MPC, [Maciejowski, 2002], is:

- Computation of a control sequence that minimizes a cost (objective) function
- The use of a model to predict the process output over a horizon of fixed length
- The application of the first control signal from the computed sequence and moving the horizon one timestep forward

## 4.6 System to control

In chapter (2), we described the laboratory system built to carry out the experiments. However, we used the system, shown in figure (4.14) to run our tests. The reasons for this decision were to use make use of more accurate and reliable flowmeters. These flow

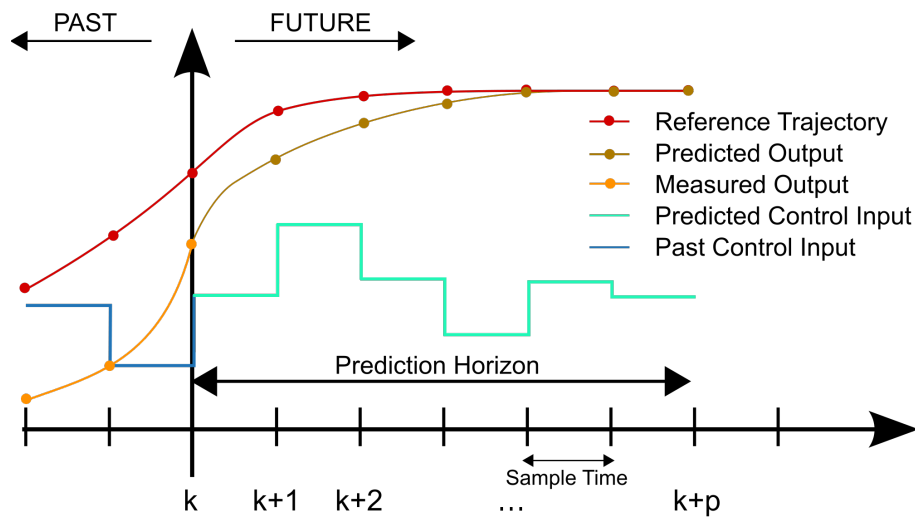


Figure 4.13: Overview of how MPC works. To reach a set point, the controller calculates a sequence of optimal control inputs ( $U$ ) that minimizes a certain cost function. With this sequence of control inputs ( $U$ ), the output of the system ( $Y$ ) is predicted over some prediction horizon. Then, the first value of ( $U$ ) is given to the system, and this procedure is repeated for each time step. [de Oliveira Kothare and Morari, 2000]

measurements are needed for the local PI/PID controllers ensuring good performance of the valve and pumps. This setup also brings us closer in replicating a sewer network because of using pressurized pipes in pipe station. Both gravity and pressure sewer lines make up the construction of a real sewer network. For simplification of the model, we only consider flow in gravity sewer pipes.

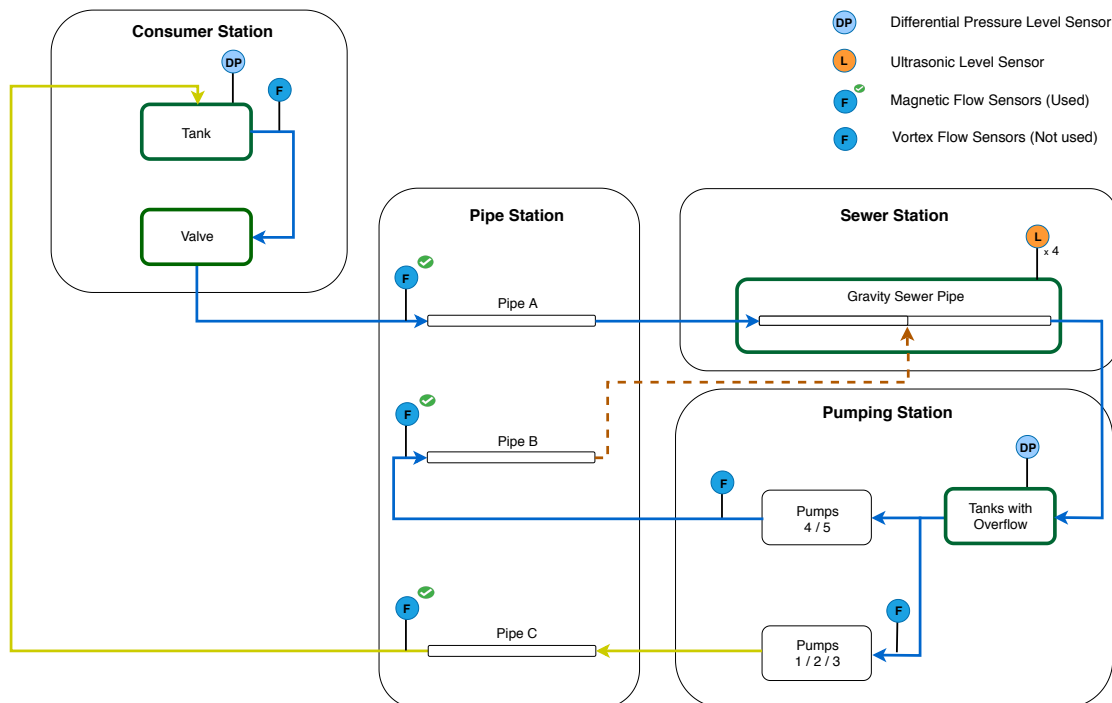


Figure 4.14: This is the final configuration used for the study. The minimum flow measurement is now 0.5 L/min when using flowmeters from Endress+Hauser in pipe station. The tubes in pipe station have a small diameter and results in a full tube flow.

Now, while describing the system in detail, we also relate it to the real-life scenario of the sewer network at Fredericia in parallel. Looking at figures (4.11) and (4.14) will help with the explanation.

The project idea is to use a large buffer tank (in consumer station) to hold back water. This replicates a tank holding industrial wastewater from heavy industries in the north of Fredericia. We send a periodic flow of water to the middle of sewer pipe to simulate disturbances of wastewater from household areas. From the mentioned tank, we send a controlled flow to the top of sewer pipe (in pumping station) in moments when the flow from the household is low. Right now in Fredericia, there is no tank readily available. This study will help in proving the feasibility of building such a tank. The industrial wastewater directly enters the sewer network and household wastewater has multiple entries to the gravity sewer network.

The tank in consumer station is equipped with a level sensor, so that change in volume of the tank can be calculated at any given time. Release of water from the tank is done through a valve, controlled by a local PID controller which constantly receives a reference from MPC.

#### 4.6.1 Control objective

While choosing the control objectives for this project, we wanted them realistic enough to be implemented in the near future. The challenges faced by the wastewater industry were presented in Chapter (1). With those in mind, we have three main control objectives:

- 1 Minimize flow variation at the WWTP inlet
- 2 Minimize variation of contaminants flowing into the WWTP
- 3 Minimize energy consumption

The group has decided to focus on the first objective, reducing variance in the wastewater flow into the WWTP. Now, in the lab, this translates to minimizing the flow variation at the bottom of sewer pipe. To be specific, we minimize the variance of  $Y$ . This can be done by adding water to the top of pipe from the buffer tank whose flow outlet is controlled by MPC.

#### 4.6.2 Model

As seen from the figure (4.11), the two flows (controlled industry water and household water) mix together and exit the sewer pipe from the bottom. This combined flow then pours down into overflow/weir in the pumping station. In reality, this would be the flow entering the WWTP.

With  $V$  corresponding to the volume in the buffer tank ( $L$ ),  $Q_i$  the wastewater flow from industries ( $L/min$ ),  $Q_h$  the predicted water flow from the households ( $L/min$ ),  $U$  being the input (valve flow) that is controlled ( $L/min$ ),  $\tau$  the transport delay of water in the pipe ( $s$ ),  $Y$  being the measured overall flow into the WWTP ( $L/min$ ) and  $T_s$  the sampling time, our sewer network can be defined as [Morten Vesteraa et al., 2018]:

$$\begin{aligned} V(k+1) &= V(k) + T_s(Q_i(k) - U(k)) \\ Y(k+\tau) &= Q_h(k+\tau) + U(k) \end{aligned} \tag{4.12}$$

There is a distance of 20 *meters* between the top and bottom of the sewer pipe and it takes some time (approximately 37 *seconds*) for the water to travel this distance, refer figure

(4.11). This is the reason for using delay term in our model. This also means that when a flow input is introduced at the top of sewer pipe, it will only affect the overall inflow after the delay of  $\tau$  seconds.

### 4.6.3 Performance function

To optimize the system using MPC, we develop a performance (cost) function. This function can be used to control the plant output (flow at the bottom of pipe) and minimize control action (flow input to at the top of pipe). The cost function is of the form:

$$\mathcal{J} = \sum_{k=1}^{H_p} \left( Q_h(k + \tau) + U(k) - \mu \right)^2 \quad (4.13)$$

subject to system dynamics and constraints

$$\begin{aligned} V(k + i + 1) &= V(k + i) + T_s(Q_i(k + i) - U(k + i)) \\ Y(k + i + \tau) &= Q_h(k + i + \tau) + U(k + i) \\ V_{min} &\leq V \leq V_{max} \\ U_{min} &\leq U \leq U_{max} \end{aligned} \quad (4.14)$$

Where  $\mathcal{J}$  is the cost function to be minimized,  $R$  and  $S$  are weighing parameters.  $H_p$  and  $H_u$  are the prediction and control horizon respectively, where the condition  $H_u \leq H_p$  should hold. Regarding the control/prediction horizon, we have kept  $H_u$  equal to  $H_p$ . By choosing this, we get better predictions at the cost of higher computation.

Now expanding the first term in equation 4.13 gives

$$\begin{aligned} \mathcal{J} &= \sum_{k=1}^{H_p} \left( Q_h(k + \tau) + U(k) - \sum_{i=1}^{H_p} \frac{(Q_h(i + \tau) + U(i))}{H_p} \right)^2 \\ &= \sum_{k=1}^{H_p} \left( Q_h^2(k + \tau) + U^2(k) + \left( \sum_{i=1}^{H_p} \frac{(Q_h(i + \tau) + U(i))}{H_p} \right)^2 + 2Q_h(k + \tau)U(k) \right. \\ &\quad \left. - 2Q_h(k + \tau) \sum_{i=1}^{H_p} \frac{(Q_h(i + \tau) + U(i))}{H_p} - 2U(k) \sum_{i=1}^{H_p} \frac{(Q_h(i + \tau) + U(i))}{H_p} \right) \end{aligned} \quad (4.15)$$

Without further expansion, it is evident that adding the above equation and the mean of  $Y(\geq 0)$  leads to an expression containing quadratic and linear terms in  $U$  and it is similar to the form

$$\mathcal{J} = U(k)^T \mathcal{H}U(k) + \mathcal{G}^T U(k) + constant \quad (4.16)$$

where all the linear terms of  $U$  are collectively shown as  $\mathcal{G}$ , quadratic terms are shown by  $\mathcal{H}$  and remaining terms are regarded as a constant. By doing this, we have reformulated the optimization problem with a quadratic performance function. As seen in figure (4.15), a quadratically constrained problem is a convex problem. With a performance function that is quadratic in the control variable  $U$  and constraints that are linear in  $U$ , standard optimization tools like CVX and YALMIP are readily available to solve such minimization problems.

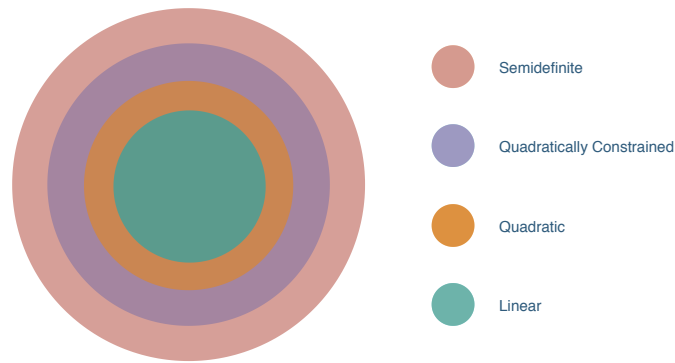


Figure 4.15: *Convex optimization problem set. Linear Programming is a subset of Quadratic Programming which is a part of Semidefinite Programming.*

#### 4.6.4 Constraints

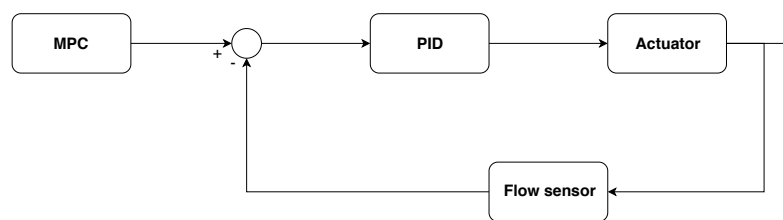


Figure 4.16: *Before moving onto constraints, the reader should take note that output from MPC is sent as setpoint to a local controller for valve and pumps.*

One mentioned benefit of MPC is its capability to consider constraints while calculating a control signal. These constraints can be given as inequalities and used in the optimization process. Some of the constraints are:

- **Actuator range** - which describes the limitations of the actuator. For instance, it could be the maximum flow leaving a pump outlet. An example what happens when you do not consider such actuator limitations is shown in the below figure. This can also be seen as a **constraint on the control input** ( $U$ ).

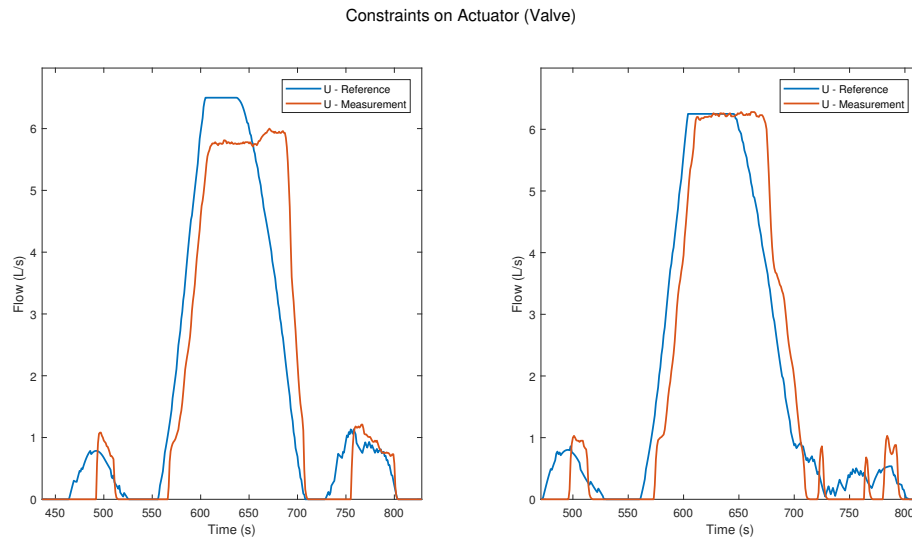


Figure 4.17: In subplot 1, when the MPC output exceeds the actuator limit, there is an overshoot in flow due to the buildup of error in PID. This slightly increases the variance of overall flow. In subplot 2, when suitable constraint is imposed on MPC output, we do not see this undesired overshoot.

- **Actuator slew rate** - which describe how fast the actuator can react. For instance, it could be how fast a valve can open. The valve would need time to overcome static friction (stiction) before opening to a required amount. Knowing this detail could very helpful while analyzing the controller performance.

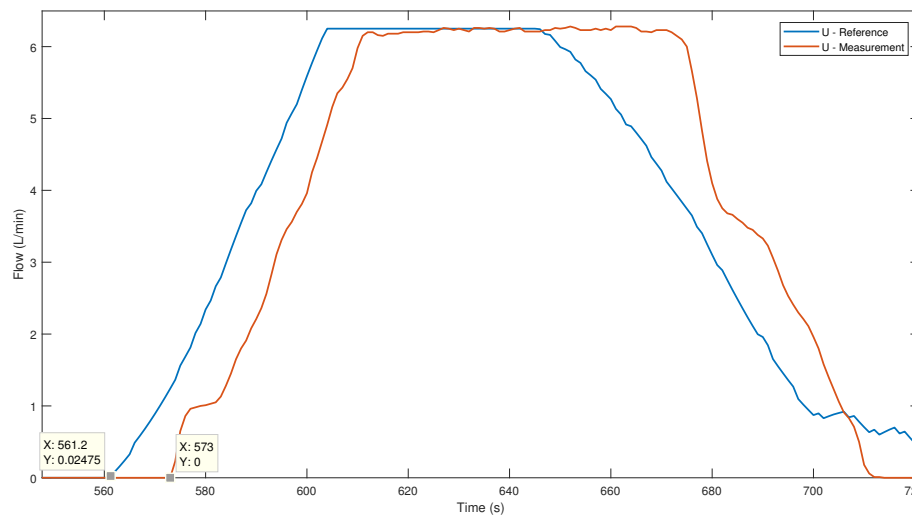


Figure 4.18: Reaction time for the valve. On average the valve takes 12 seconds to respond to the control signal.

- **Other physical constraints** - for instance it could be the maximum flow in a pipe or maximum storage in a tank.

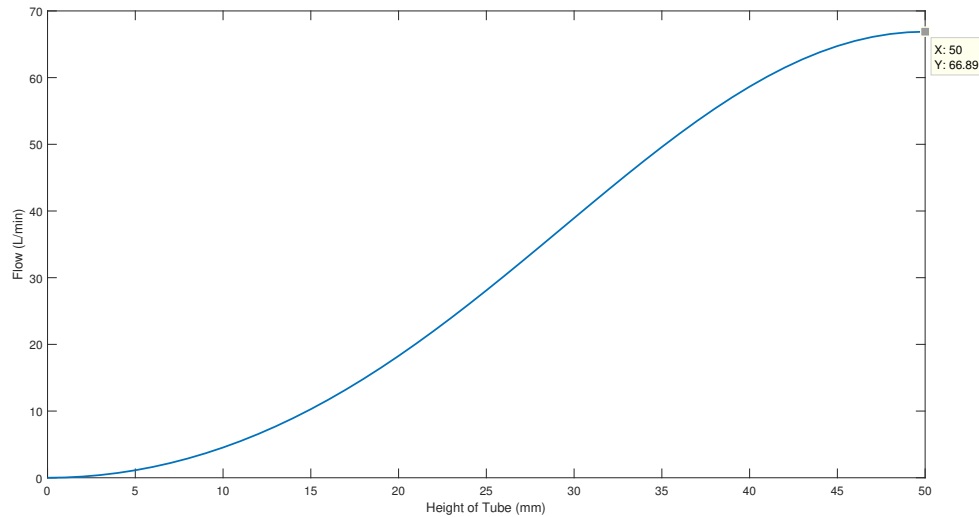


Figure 4.19: *Maximum flow that can possibly flow through the sewer pipe of diameter 50 millimeters. Flow calculated with manning equation.*

For the laboratory setup, two constraints were taken into account and reasons for focusing on these constraints are pointed out subsequently.

$$\begin{aligned} V_{min} &\leq V(k) \leq V_{max} \\ U_{min} &\leq U(k) \leq U_{max} \end{aligned} \quad (4.17)$$

- **Maximum volume  $V_{max}$  in the tank.** The physical tank can store only a certain amount of volume. The tank has a design capacity of 200 *litres*. Furthermore, the minimal volume  $V_{min}$  must always be bigger than or equal to zero as the volume cannot be negative.
- **Maximum input signal  $U_{max}$ .** As seen in figure (4.17), the maximum value of  $U$  should be limited to avoid an undesired overshoot in flow leaving the buffer tank. Again the minimum input signal  $U_{min}$  should result in a flow bigger than or equal to zero.

With regard to the first constraint, at a given time  $k$ ,  $V(k)$  is known as it is measured with a level sensor in the tank. With this measurement, future volumes of the tank can

be predicted as:

$$\begin{aligned}
V(k+1) &= V(k) + T_s(Q_i(k) - U(k)) \\
V(k+2) &= V(k+1) + T_s(Q_i(k+1) - U(k+1)) \\
&= V(k) + T_s(Q_i(k) - U(k)) + T_s(Q_i(k+1) - U(k+1)) \\
V(k+3) &= V(k+2) + T_s(Q_i(k+2) - U(k+2)) \\
&= V(k) + T_s(Q_i(k) - U(k)) + T_s(Q_i(k+1) - U(k+1)) + T_s(Q_i(k+2) - U(k+2)) \\
&= V(k) + T_s(Q_i(k) + Q_i(k+1) + Q_i(k+2) - (U(k) + U(k+1) + U(k+2))) \\
&\dots \\
&\dots \\
V(k+H_p) &= V(k) + T_s\left(\sum_{m=1}^{H_p-1} Q_i(m) - \sum_{m=1}^{H_p-1} U(m)\right)
\end{aligned} \tag{4.18}$$

## 4.7 Disturbances

For this system, the inlet to the buffer tank, denoted as  $Q_i$  is a disturbance. It is because wastewater released from the heavy industries in Fredericia can vary and be unpredictable at times. The water flow from residential areas  $Q_h$  is also seen as a disturbance. It has a periodic flow pattern which we used to build a model. We then use a Kalman filter that uses this model and takes in real-time flow measurements to give a predicted flow to MPC.

## 4.8 Summary



Figure 4.20: *The figure should help in summarizing this chapter.*

To interpret the figure, let's start with flow measurement block at the top. Real-time measurements are recorded for flow at the WWTP inlet (or the end of sewer pipe). Then the kalman filter takes in measurement to update its prediction of household flow (over a horizon of 1 day). This prediction is given to MPC which uses this prediction of flow disturbances and accordingly calculates the control signal. This control signal acts on a valve that releases water from the tank and thereby influencing the overall flow in the sewer pipe. Now, a new flow measurement is taken and the loop repeats for each iteration.



In this chapter the implementation of the controller on the laboratory version of sewer system is explained through a flowchart. The Model Predictive Controller is implemented in MATLAB/SIMULINK. Here we briefly explain how it is done.

## 5.0.1 YALMIP

In the field of control and systems theory, one of the most important tool is Semidefinite Programming (SDP). YALMIP, a free MATLAB toolbox, can be used to model and solve SDP's by interfacing external solvers. As Quadratic Programming (QP) falls within SDP, YALMIP was chosen for this project study purposes. In general, it is simple to develop an optimization problem in YALMIP. Another benefit is that YALMIP automatically detects the kind of problem defined by the user and selects a suitable solver [Löfberg, 2004].

The MPC problem is formulated in YALMIP to solve the optimization problem - minimizing a cost function over a finite horizon while satisfying user defined constraints. It is crucial for a real-time controller to be able to compute the output signal in less time than the time step. Given that our time step is 1 *second* and during this time other computational tasks must be done, it is extremely important that the YALMIP code is as efficient as possible. For this reason, the *optimizer* function has been used instead of *optimize*. The *optimizer* function allows to set up the optimization problem only once for each simulation so at each iteration only solving the optimization problem is needed.

## 5.0.2 SIMULINK

SIMULINK runs on the laboratory computer which is connected to the Local Area Network (LAN) via an ethernet cable. The physical system (stations/modules) are connected to LAN in the same way. We found satisfactorily performance of using SIMULINK for real-time simulation and testing.

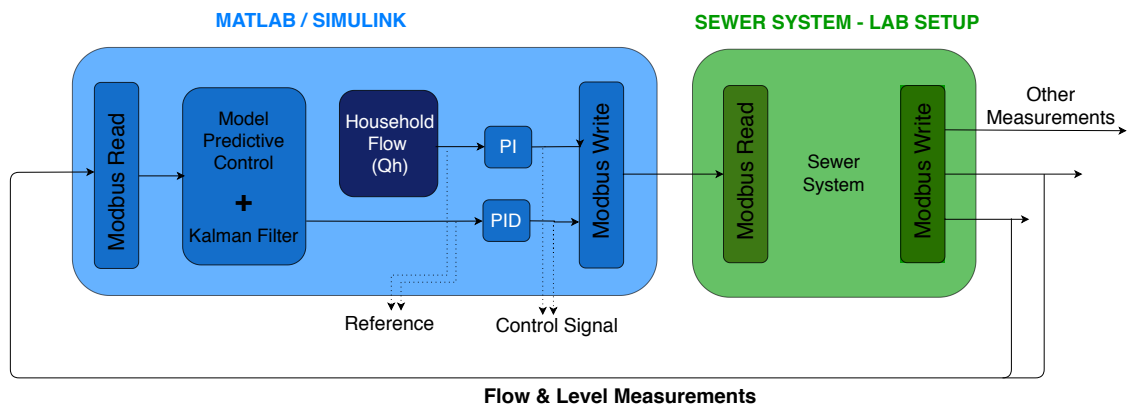


Figure 5.1: Software implementation. The control signal is sent to the input registers and measurements are read from the output registers.

The household flow ( $Q_h$ ) block is coloured different because it is the fundamental part of the experiment. There should be a constant supply of water to carry out an experiment. Flow as a timeseries is fed to a PI controller as reference and output of PI (control signal) is sent to the pumps.

As SIMULINK compiler is not compatible with object oriented code, YALMIP code has been placed inside a Interpreted Matlab Function. Modbus Read and Modbus Write have been placed in S-Functions, two for each lab module. The computational time has been verified to be lower than the time step, which allows real-time control.

## 5.1 Flowchart

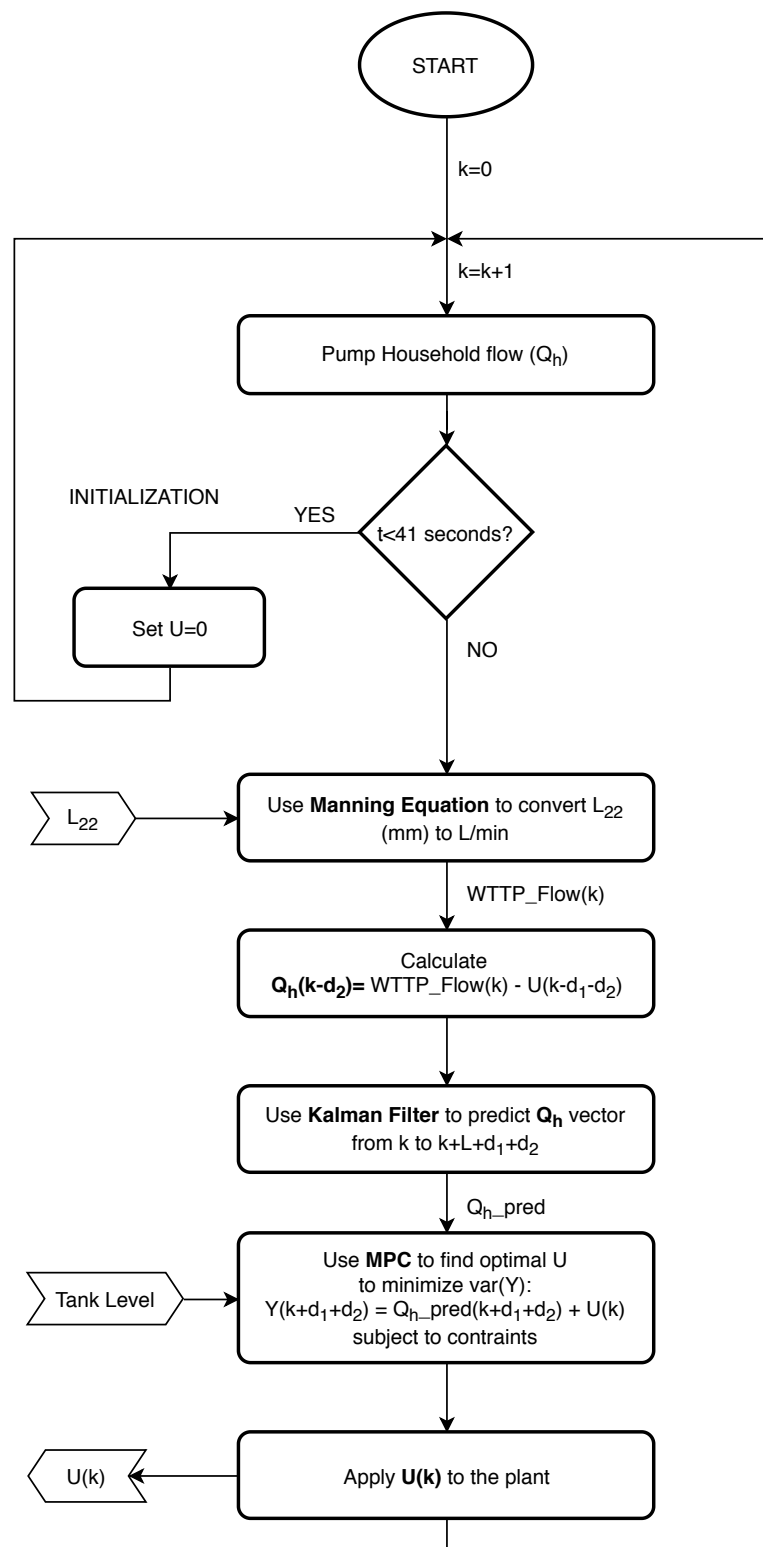


Figure 5.2: Flowchart

Figure (5.2) shows how an experiment is done. For the first 40 seconds there will be flow only coming from the households. The household flow  $Q_h$  is a defined timeseries from which the Fourier analysis has taken the model for the Kalman filter. This initialization

process is done in order to avoid the first measurements which may have overshoot and oscillations. Note that for the first  $d_2$  seconds (delay between the middle point to the end of the sewer pipe) there will be no flow where the level sensor ( $L_{22}$ ) is placed.

After the initialization we will use the measurements from level sensor  $L_{22}$  to compute what was the flow from the households  $d_2$  seconds ago. This is done using the Manning equation to convert the measurement in  $mm$  to  $L/min$  as described in Chapter (3), equation (3.22). We then subtract the flow from the consumer station  $U$  that was sent  $d_1 + d_2$  seconds ago (that is the delay between the top and the end of the sewer pipe).

Based on the last computed value and the previous ones, the Kalman Filter will predict the household flow from the current time step until  $L + d_1 + d_2$ .

Finally, the MPC will compute the the optimal  $U$  which minimizes the the variance of  $Y$  taking in account the current level of the industry tank and subject to the defined constraints.

# Tests and Results 6

---

In this chapter, different tests and their results will be discussed. Firstly, the simulation results are shown to prove that the control methodology works. The simulations have been done with real data from Fredericia. Later, laboratory tests are shown. The laboratory tests were carried with a scaled version of the real data.

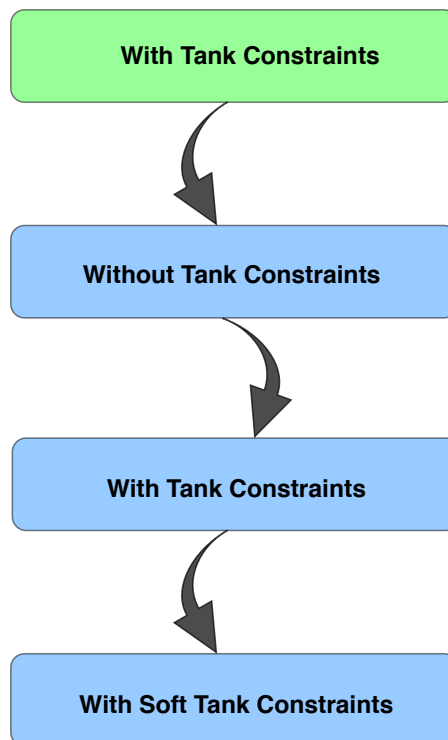


Figure 6.1: *Structure of this chapter. The green boxes are simulation results and blue boxes are experimental results from the lab.*

## 6.1 Simulation results

### System and performance function

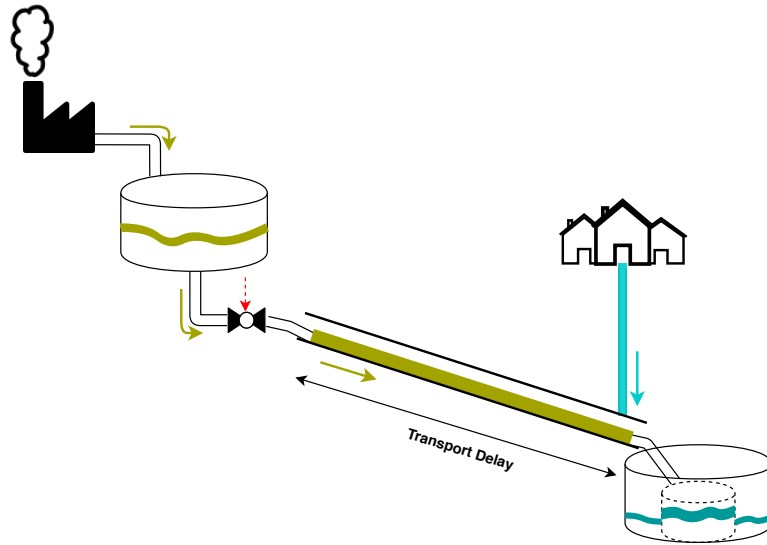


Figure 6.2: Here we assume all the household flow enters the sewer line at the end. There is a delay of 4 hours for the wastewater from buffer tank to reach the WWTP.

For the simulation studies, the performance function has been modified slightly.  $\mu$  is the mean flow of  $Y$ . The reason for adding an extra term can be understood by comparing figure (6.3) and figure (6.5). Figure (6.3) represents the controller performance for an objective function without mean.

$$\mathcal{J} = \sum_{k=1}^{H_p} \left( Q_h(k + \tau) + U(k) - \mu \right)_R^2 + \sum_{k=1}^{H_p} \left( \mu \right)_S \quad (6.1)$$

subject to system dynamics and constraints

$$\begin{aligned} V(k + i + 1) &= V(k + i) + T_s(Q_i(k + i) - U(k + i)) \\ Y(k + i + \tau) &= Q_h(k + i + \tau) + U(k + i) \\ V_{min} &\leq V \leq V_{max} \\ U_{min} &\leq U \leq U_{max} \end{aligned} \quad (6.2)$$

In this section, different simulations are shown to prove how the MPC is able to achieve the goal of minimizing the variance of the flow at the WWTP inlet.

For the next simulations, the Kalman Filter will be used to predict the household flow for the next 288 timesteps (1 day) at each iteration. This predicted flow will be fed to the MPC which must find an optimal controlled industrial flow that minimizes (6.1) constrained by equation (6.2).

The household flow, based on real measurements from the city of Fredericia was described in section (4.4) in chapter (4). This is used for the following simulation studies.

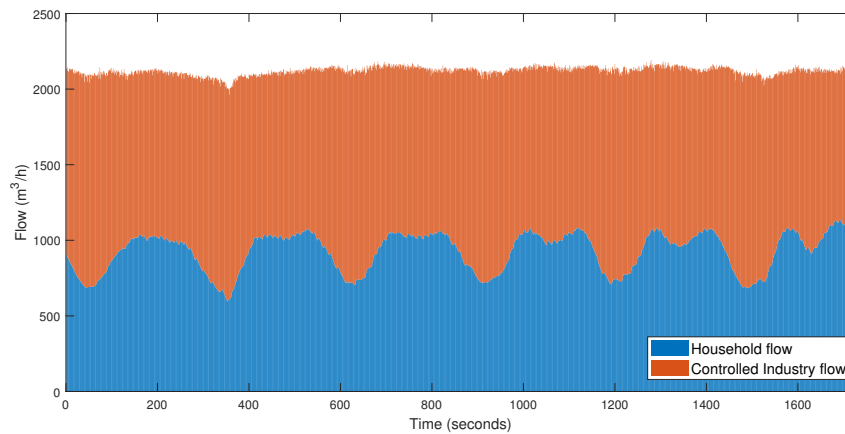


Figure 6.3: A six days simulation. The blue bars shows the household flow predicted by the Kalman Filter. Prediction window is 288 timesteps (or 1 day). The red bars shows the controlled industry flow computed by the MPC, these are summed on top of each other after shifting them 48 timesteps to visualize overall flow to the WWTP. No tank constraints and no mean in the performance function.

### 6.1.1 Simulation with tank constraint

Different tank sizes have been considered to show the performance of the controller. The tank will be fed by the uncontrolled industrial flow from which the MPC has knowledge for the next 288 timesteps ahead.

For the first simulation the tank volume has been set to  $5000 \text{ m}^3$  and the initial volume to full. Figure (6.4) shows what is the flow from the tank and the household at each timestep. Although the MPC computes the optimal industry flow for the next 288 timesteps, only the first one is used and plotted. Note that the controlled industrial flow takes 48 timesteps more than the household flow to reach the WWTP. If the industry flow is shifted 48 timesteps forward as in figure (6.5) the stacked flow will show the total flow at the inlet of the entry of the WWTP.

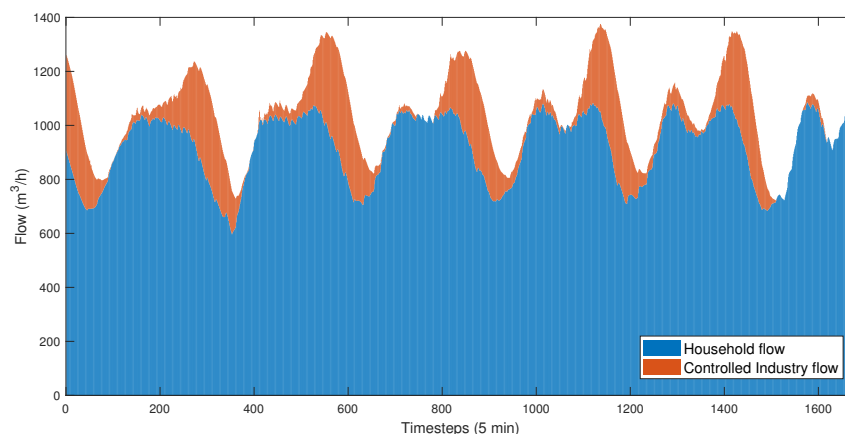


Figure 6.4: A six days simulation. The blue bars shows the household flow predicted by the Kalman Filter. Prediction window is 288 timesteps (or 1 day). The red bars shows the controlled industry flow computed by the MPC, these are summed on top of each other to visualize overall flow to the WWTP.

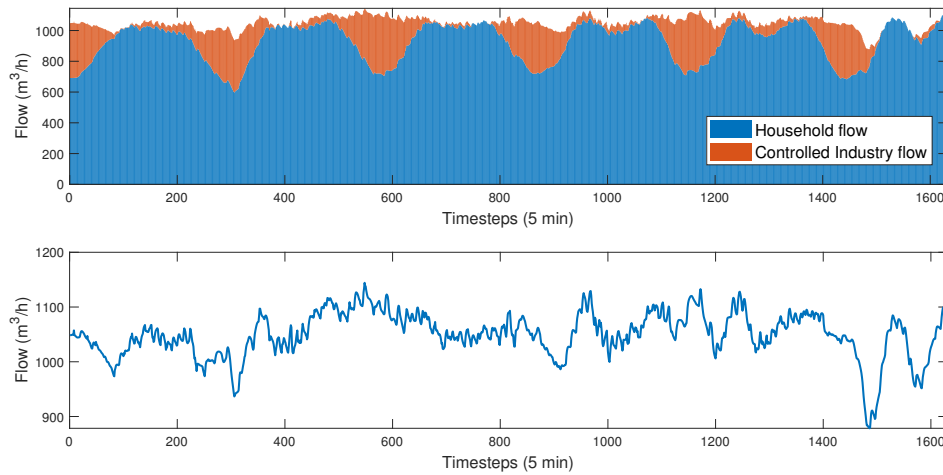


Figure 6.5: *The top plot shows shows the household flow shifted 48 timesteps. The bottom plot shows the overall inlet flow to the WWTP.*

As it can be seen in the bottom plot of figure (6.5), the MPC is able to reduce the variation of flow to a great extent.

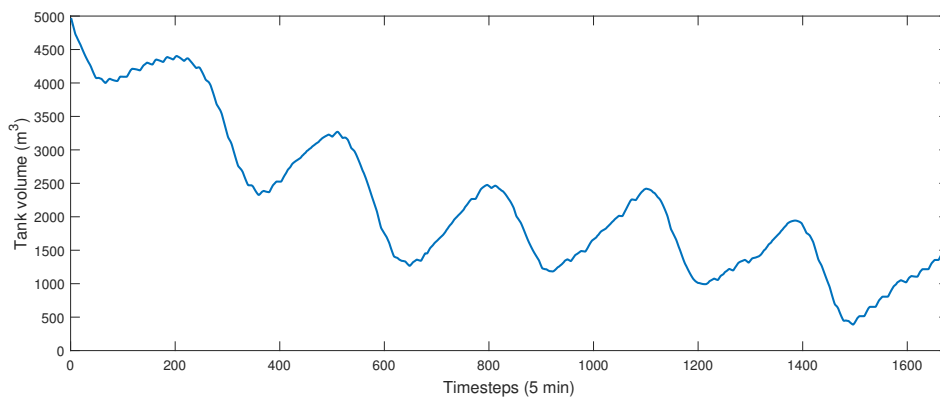


Figure 6.6: *Tank volume.*

If the tank volume is decreased to  $500 \text{ m}^3$  and the initial volume is set to zero the MPC will have less margin to not violate the constraints, hence the performance will decrease.

As shown in figure (6.8) and figure (6.9), industrial water has to be released when the household flow is at its peak, increasing the variance, to avoid overflow of the tank. The remaining water in the tank is not enough to fill up the valleys of the household flow.

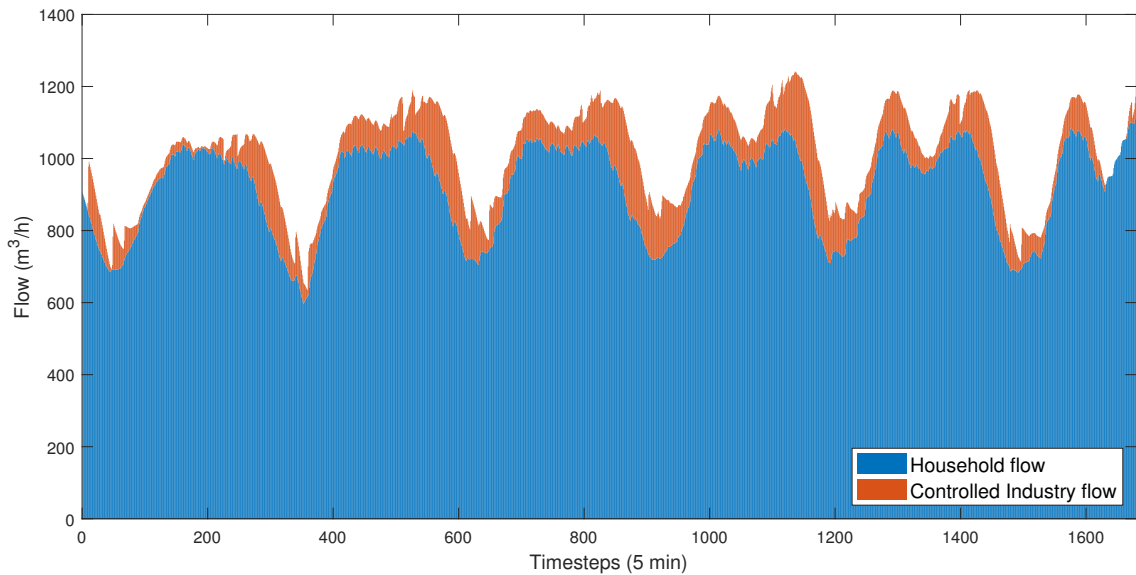


Figure 6.7: A six days simulation. The blue bars shows the household flow predicted by the Kalman Filter. Prediction window is 288 timesteps (or 1 day). The red bars shows the controlled industry flow computed by the MPC, these are summed on top of each other to visualize overall flow to the WWTP.

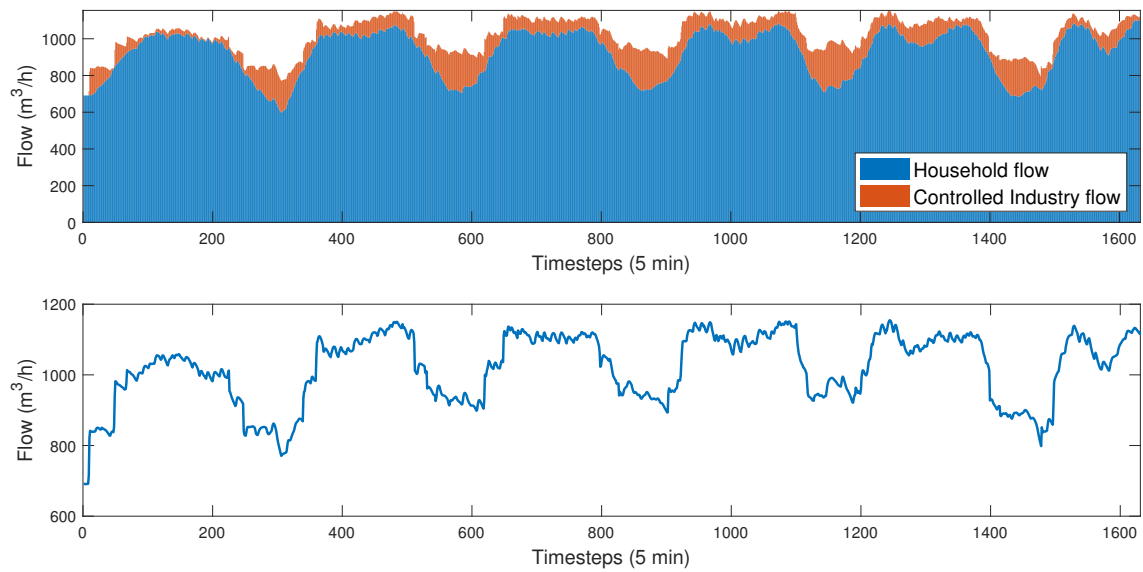


Figure 6.8: The top plot shows shows the household flow now shifted 48 timesteps. The bottom plot shows the overall wastewater flow into the WWTP. The results are not as good as figure (6.5) when there is a constraint on tank size.

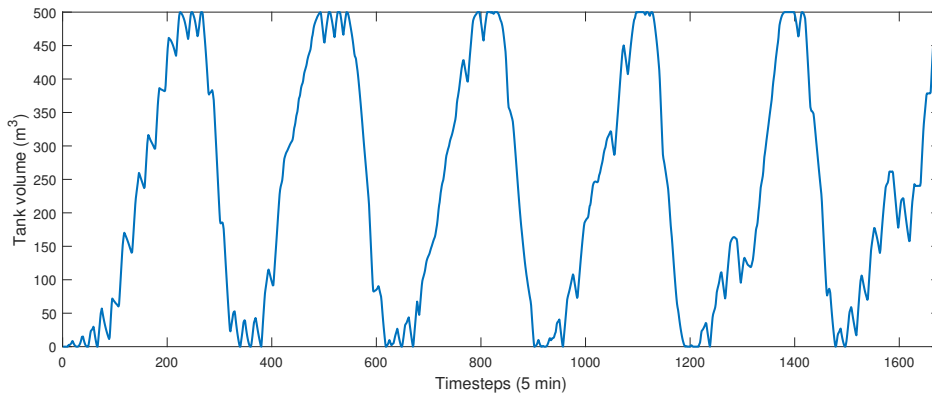


Figure 6.9: *Change in tank volume. When the upper limit is reached, the tank is forced to release wastewater into the sewer. This still results in a varying flow at the WWTP inlet.*

## 6.2 Experimental results

In order to prove the results obtained in the simulations, the same tests will be done in the lab. A scaled version of the flows is needed in order to execute the tests. The scaled flow has to be of a reasonable magnitude so all the actuators and sensors work on its operating range. The main constraint is that the outlet of the pressurized tank is only able to deliver up to  $6.5 \text{ L/min}$  with the current configuration. Consequently, the difference between the peaks and valleys of the household flow has to be below the mentioned limit.

Flows have to be also scaled in time so multiple test can be performed in one day. If the scaled period is too short the error of the delays determination will play a big role. As the total delay was found to be approximately  $37 \text{ seconds}$ , the period has to be much higher so an inaccuracy of a few seconds do not have a big impact in the performance. The decision was to scale a day of the real measurements to  $4 \text{ minutes}$  and  $48 \text{ seconds}$  so a complete test of a week will take around  $29 \text{ minutes}$ .

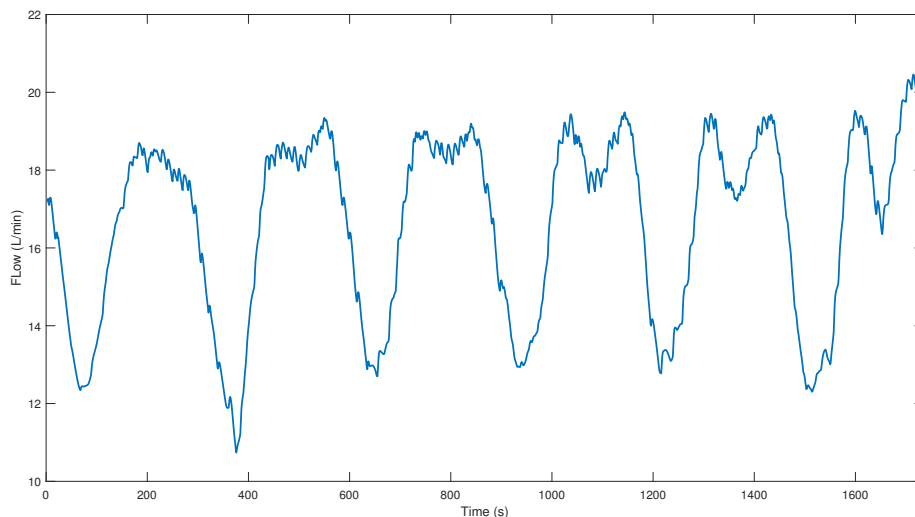


Figure 6.10: *Scaled household flow used for the laboratory study.*

### 6.2.1 Pump control

A set of pumps (pumps 4/5 in pumping station) will be used to deliver the household flow to the middle point in the sewer pipe. The household flow is a predefined timeseries. In order to follow the reference, a local PI controller has been designed.

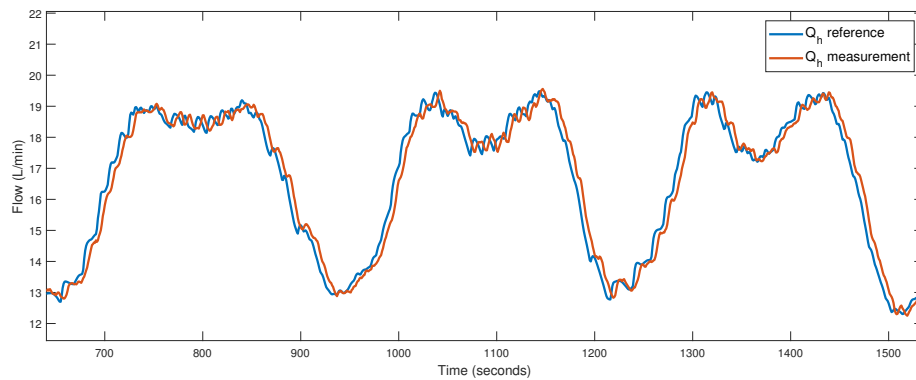


Figure 6.11: *Reference and delivered flow by the pumps*

### 6.2.2 Valve control

In figure (6.12), flow characteristic of the installed control valve, a curve mapping the percentage of flow versus the given valve opening is shown. This is how the valve operates in the real process, low gain for smaller opening (%) and high gain for larger opening (%). This was determined by measuring flow rates for different valve opening (%) spanning the operating range of the controller output and under steady-state conditions.

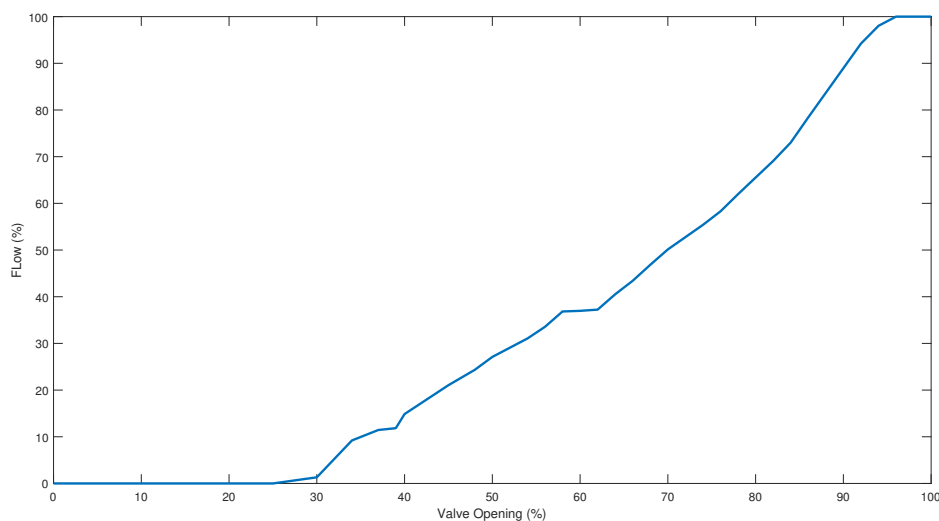


Figure 6.12: *Nonlinear flow characteristic curve of the control valve (Type - Ball Valve)*

This flow characteristic has a direct influence of the process gain. So, ideally, the characteristic should be linear to have a constant process gain. If the curve's slope varies a lot, the control loop performance can be considerably affected. Now instead of replacing the valve, one could easily change the valve characteristic by modifying the controller

output signal. This is done with a linearizer, a curve  $f(x)$  placed between the controller and the valve [Lipták, 2006].

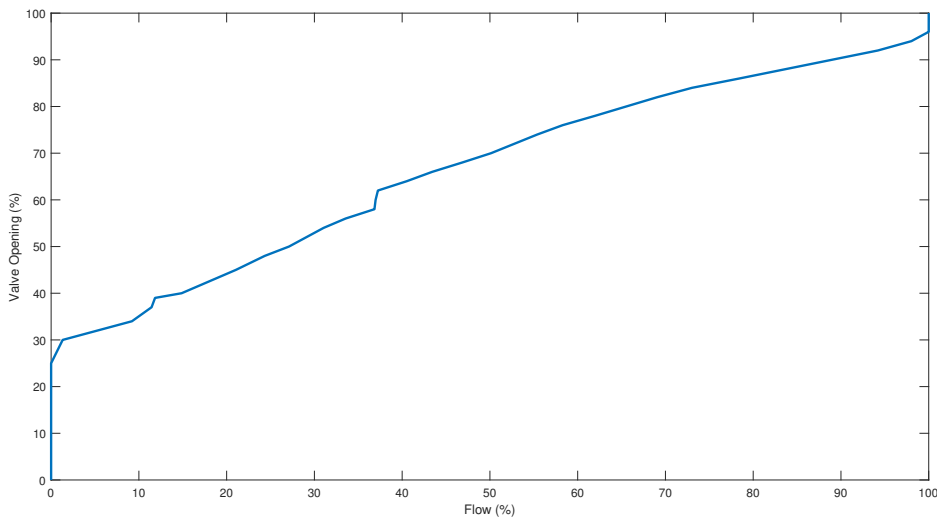


Figure 6.13: *Design of the linearizer is configured to be the inverse of the flow curve*

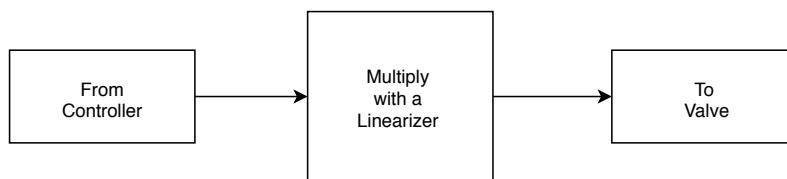


Figure 6.14: *Linearizing a nonlinear valve characteristic*

Later, the accuracy of the linearizer was tested to check whether the opening (%) and flow measurement are approximately at the same percentage of full scale for the entire operating range of the valve.

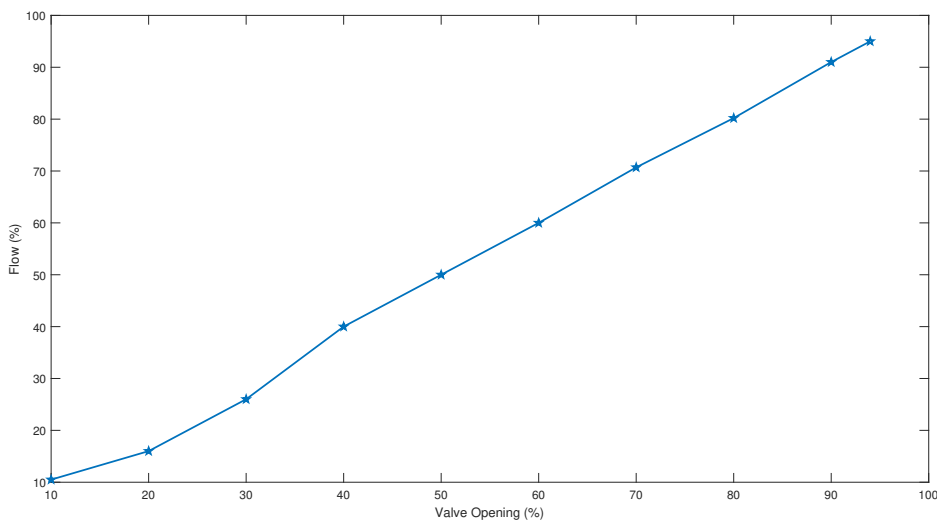


Figure 6.15: *Linearized flow characteristic of the valve*

Figure (6.16) shows the performance of the valve control after implementing the linearizer. It can be seen that the react time of the valves, around 8 *seconds*, is slower than the pumps. This difference in reaction time introduces a delay that should be taken in account in the MPC. Note also that for reference flows below 0.5 *L/min* the valve will be closed. This is done on account that the flow sensor is not able to get accurate readings for such a low flows. For a 0 *L/min* reference flow, the flow sensor may indicate that the flow is 0 *L/min* when the real flow could be slightly below 0.5 *L/min*.

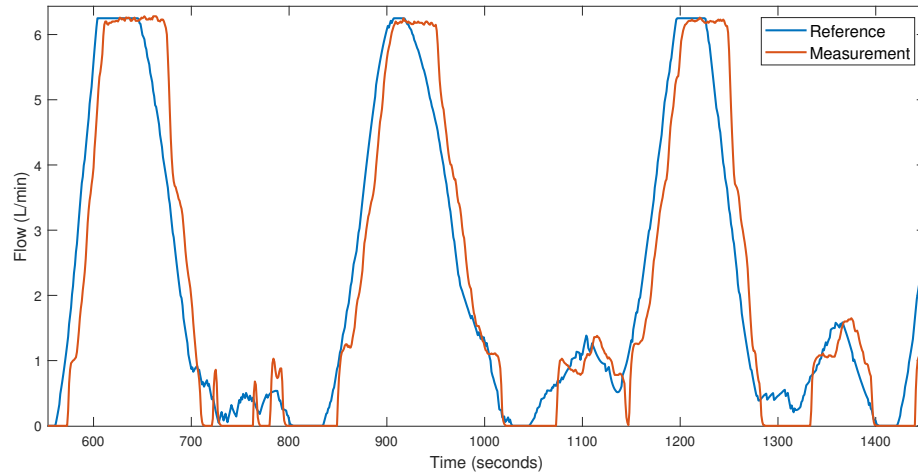


Figure 6.16: *In blue, the reference signal to the local controller. In red, the flow measured after the controlled valve.*

### 6.2.3 Manning equation

As it is desired to know the flow at the outlet of the sewer pipe but no flow sensor is placed there, it is needed to convert the readings from the level sensor to flow. This will be done using the Manning equation previously explained in chapter (3).

A test was done to check the accuracy of using a level sensor to estimate the flow. For the test, only household flow was delivered to the sewer pipe.

Figure (6.17) shows the raw readings of the level sensor. The next step is to apply the Manning equation to these raw readings to convert it to flow.

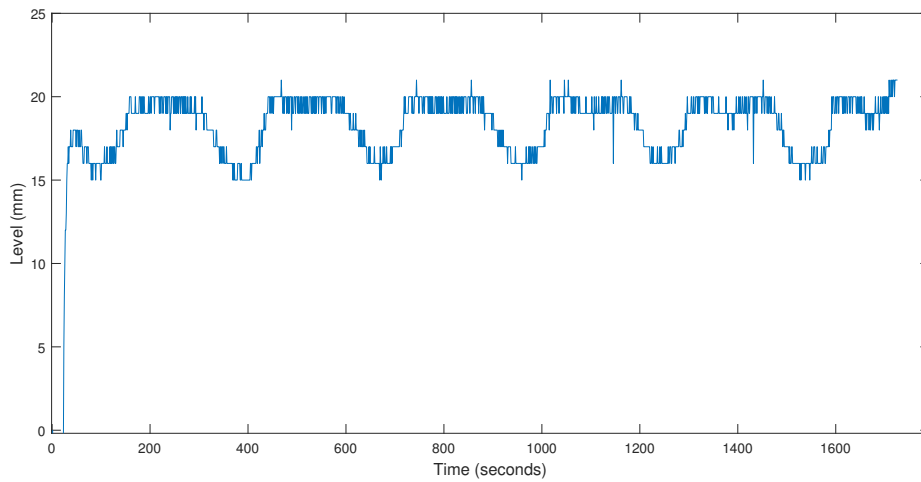


Figure 6.17: *Level of water in mm at the outlet of the sewer pipe*

Figure (6.18) shows the conversion result of applying the Manning equation.

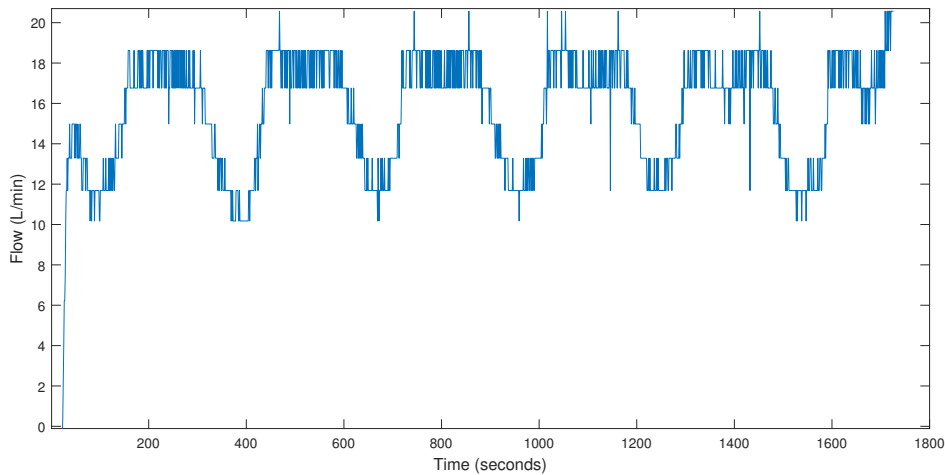


Figure 6.18: *Estimated flow at the outlet of the sewer pipe.*

To check if the conversion is good enough, the previous data was made smooth by applying a moving average filter and then compared with the household flow. The comparison can be seen in figure (6.19). With both of them being close to each other, the use of manning equation for flow estimation should not be a problem.

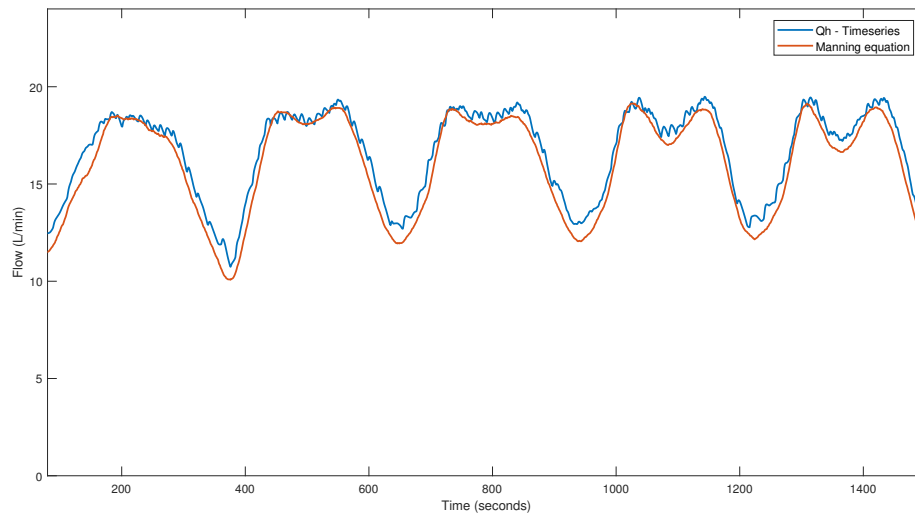


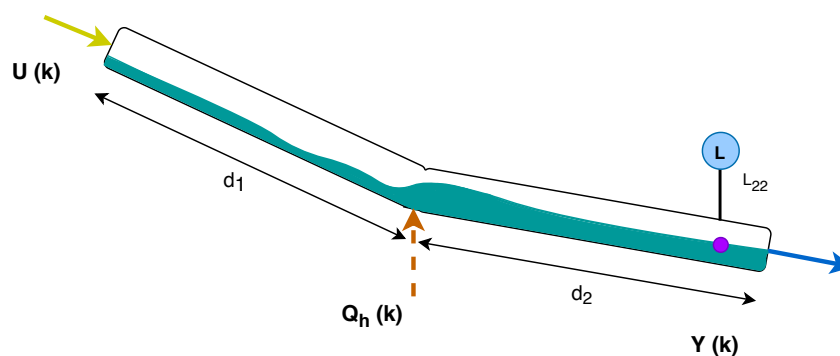
Figure 6.19: Comparison between the household flow fed to the sewer pipe (blue) and the estimation of the flow from applying the Manning equation to the level sensor readings (red).

#### 6.2.4 Kalman filter

To achieve a good performance, the MPC should have knowledge of the household flow for the entire control horizon. As the exact household flow is unknown and may vary from day to day, a Kalman filter was implemented in order to predict it.

To obtain the actual measurement of  $Q_h$  at time  $k$ , denoted as  $y_k$ , we need to subtract the industry flow  $U$  from the total flow at the outlet of the sewer pipe ( $Y(k)$ ) which will be estimated using the Manning equation. If we subtract from the total flow at the current timestep the inlet flow at the top of the sewer  $k - d_1 - d_2$  time steps before, we will obtain what the inlet household flow at the middle point of the sewer pipe  $k - d_2$  steps earlier in time. If it is confusing, the below figure will surely help.

$$y_k = Q_h(k - d_2) = Y(k) - U(k - d_1 - d_2) \quad (6.3)$$



$U(k)$  takes  $d_1 + d_2$  seconds to influence  $Y$      $Q_h(k)$  takes  $d_2$  seconds to influence  $Y$

Figure 6.20: Gravity sewer tube with transport delays.

The value obtained will be fed to the Kalman filter at the measurement update step. Then, it will predict  $Q_h$  flow for the next  $L + d_1 + d_2$  time steps. Note that the controller can not act on the first  $d_1 + d_2$  time steps so only the predictions from  $d_1 + d_2$  to  $L + d_1 + d_2$  are taken in account in the MPC.

Figure (6.21) shows a prediction of the Kalman filter at time step  $k=800$ . Based on the measurements (black), the Kalman filter predicts the future values from the time step  $k+1$  until  $k + L + d_1 + d_2$  (red). The dashed blue line shows the predictions that will be fed to the MPC, from  $k + d_1 + d_2$  until  $k + L + d_1 + d_2$ . To check if the Kalman filter is reliable, the measurements obtained afterwards are also plotted (green).

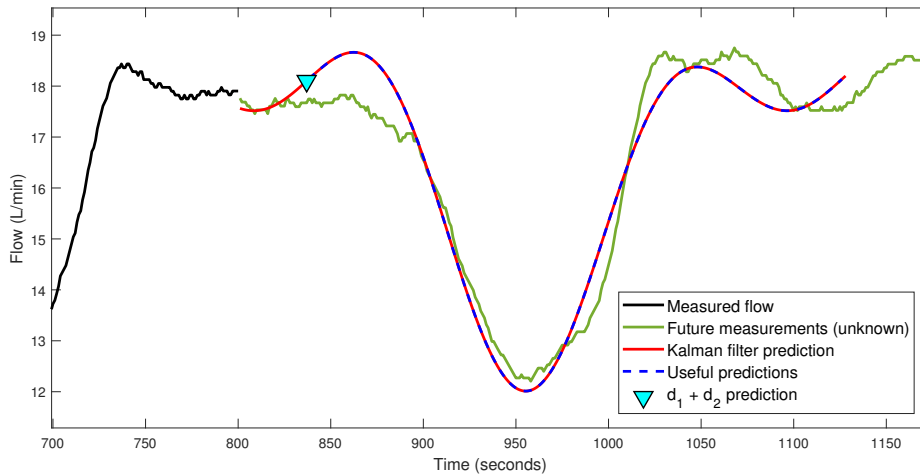


Figure 6.21: In black the measured flow until time step  $k=800$ , in green the future measurements unknown at that time step. The red line shows the  $L + d_1 + d_2$  predictions of the future flows. The dashed blue lines represent which of the predictions are useful for the MPC.  $Q=0.005$  and  $R=4$ .

Figure (6.22) shows all the measured flow at the outlet of the sewer pipe and all the  $k + d_1 + d_2$  predictions of the Kalman Filter. If the prediction is shifted  $d_1 + d_2$  timesteps forward, both lines should follow the same trend as shown in figure (6.23).

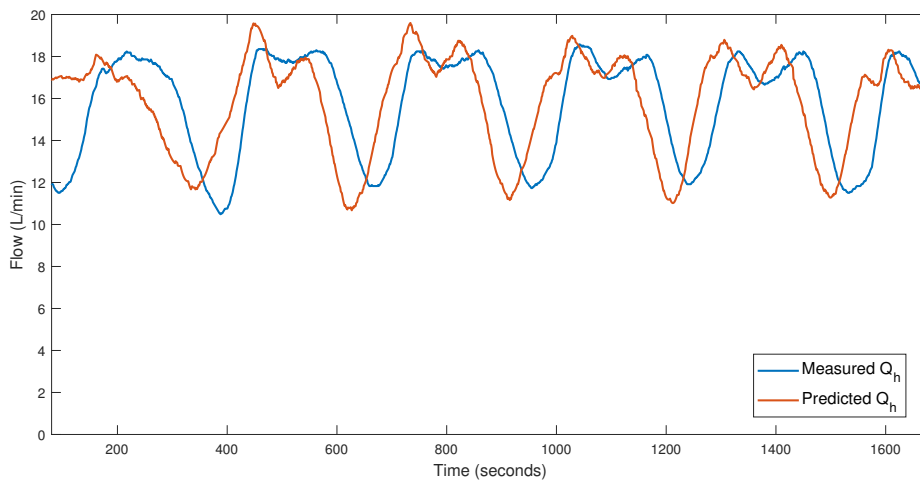


Figure 6.22: A  $d_1 + d_2$  step prediction and a comparison of the measured  $Q_h$  flow with the predicted  $Q_h$  flow.

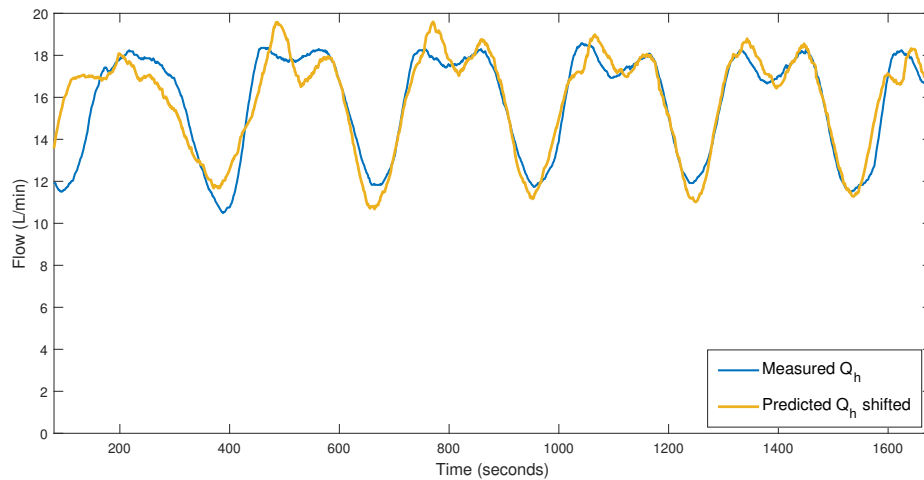


Figure 6.23: Comparison of the measured and the predicted  $Q_h$  flow with the latter being shifted  $d_1 + d_2$  timesteps.

## 6.2.5 Model predictive control

### 6.2.5.1 Without tank constraint

For the first test of the MPC, the tank volume constraint was omitted. Figure (6.24) shows the optimal  $U$  computed by the MPC that minimizes the variance of flow  $Y$  at  $k = 1000$ . The blue line are the values from  $k + d_1 + d_2$  to  $k + d_1 + d_2 + L$  of the Kalman filter predictions, and the red line are the optimal  $U$  from  $k$  to  $k + L$ . Only the first value  $U(k)$  will be used.

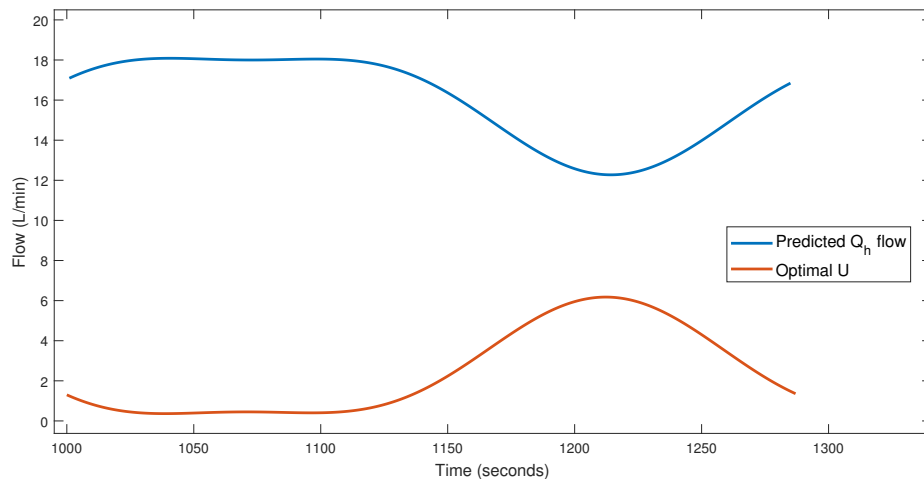


Figure 6.24: Optimal flow that minimizes the performance function at time step  $k=1000$

Figure (6.25) shows all the  $U(k)$  computed during a test. In red is also plotted the first useful value of the predicted household flow at each time step,  $Q_h(k + d_1 + d_2)$ .

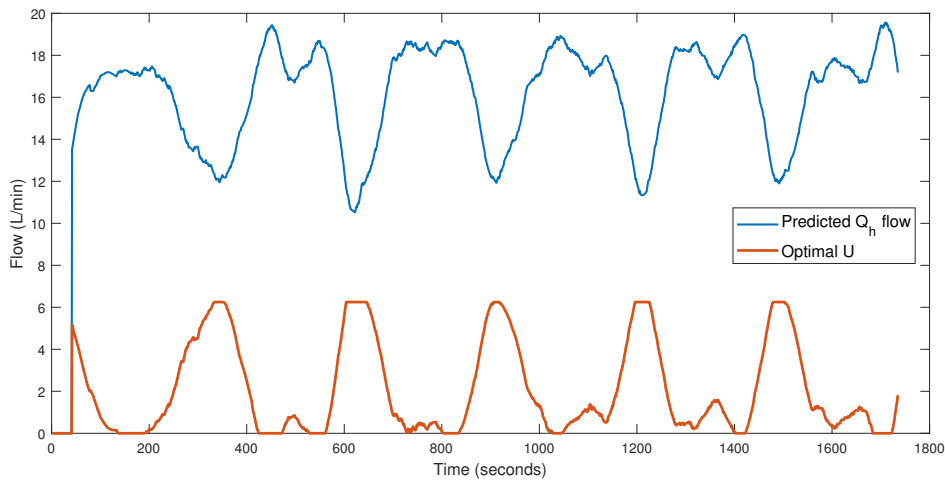


Figure 6.25: *Predicted household flow and optimal  $U$*

The resultant total flow  $Y$  of applying the computed optimal flow  $U$  are shown in figure (6.26). It can be seen that the variation of flow has been reduced significantly.

	Variance	Variance (after smoothing)
Without controller	8.240	7.070
With controller	1.660	0.988

Table 6.1: *Flow results before and after implementation of the controller. The variance is calculated over a period of 5 days or 1440 seconds. A moving average filter was used to smooth the data for a window size of 25 seconds.*

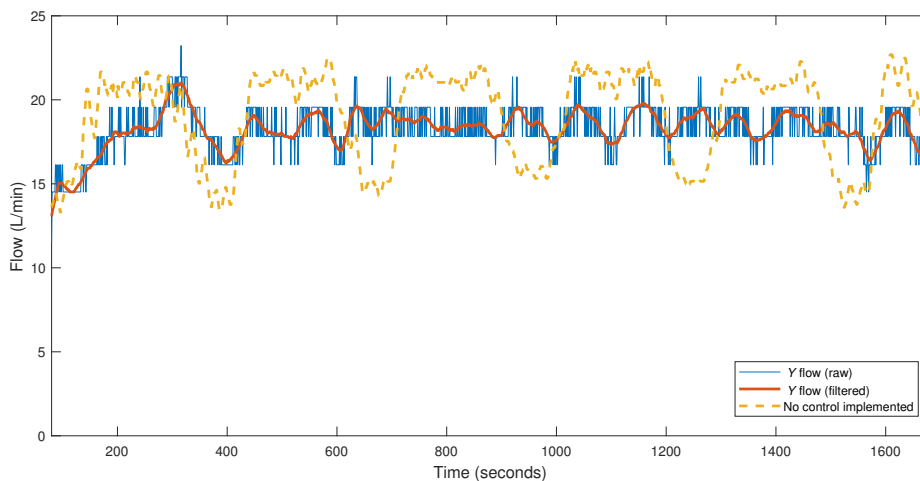


Figure 6.26: *Total flow estimated by the level sensor  $L_{22}$*

### 6.2.5.2 With tank constraint

As illustrated in figure (2.1), chapter (2), wastewater leaving the industry gets collected in a tank. From now on, the tests include the addition of water into the tank in consumer station. When MPC computes an optimal input while satisfying constraints on the tank volume, it also has to deal with the input flow to the tank. We send a prediction of this industrial inflow to MPC. The prediction horizon is 288 *seconds*. The industrial inflow used for the experiments is shown below. It is a scaled version of actual industrial flow data from Fredericia.

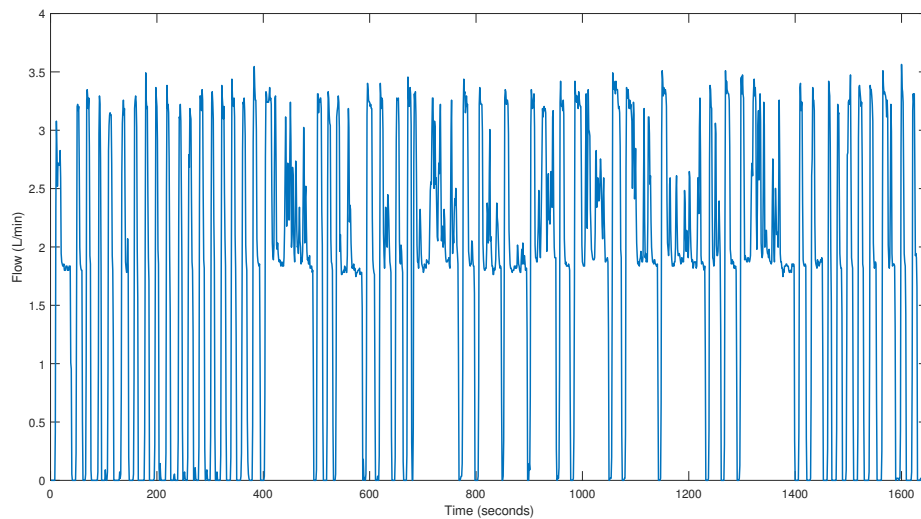


Figure 6.27: *Water entering the buffer tank. This flow is seen as disturbance from heavy industry.*

For the following tests, the tank constraints have been implemented. It is desired to keep the volume of the tank between certain bounds. For the first test, the maximum volume was set to 160 *L* and the minimum to 120 *L*.

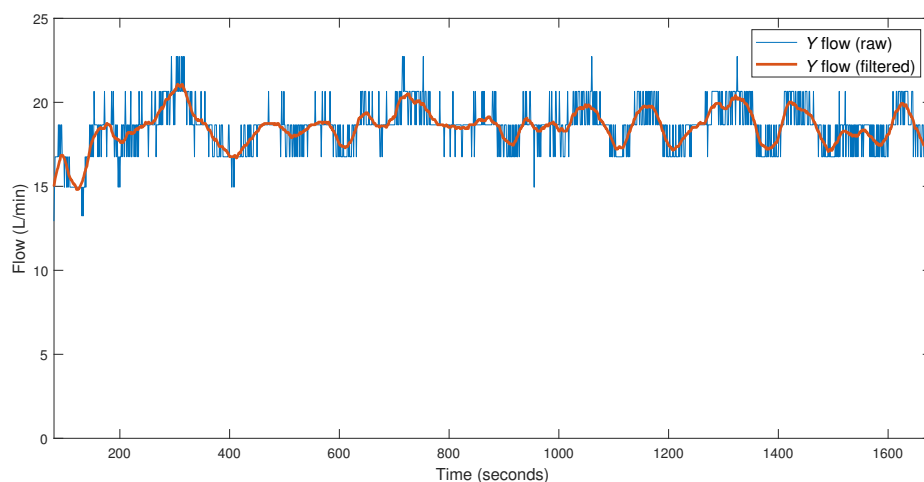


Figure 6.28: *Total flow  $Y$  estimated by the level sensor  $L_{22}$*

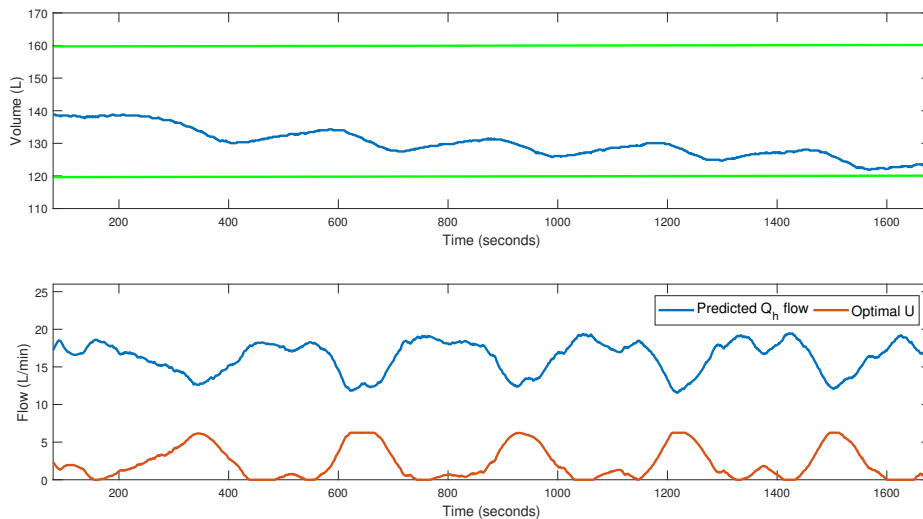


Figure 6.29: *Top: Tank volume for constraints (shown in green)  $V_{max} = 160$   $V_{min} = 120$ . Bottom: Predicted household flow and optimal  $U$ .*

It can be seen in figure (6.28) that the constraint does not have a significant impact in the performance. In figure (6.29), one quick observation shows you the volume of water in the tank keeps reducing. This is because the net outlet flow of water is more than the net inlet flow.

With the next test, we introduce tighter constraints. The volume of the tank was reduced further to 20 L by setting the maximum volume to 150 L and the minimum to 130 L. The intention of this test is to make the situation close to reality and challenge the controller more. In the real world, there could easily be instances when the buffer tank is close to getting full. The performance of the controller in such a case is compared to other results later.

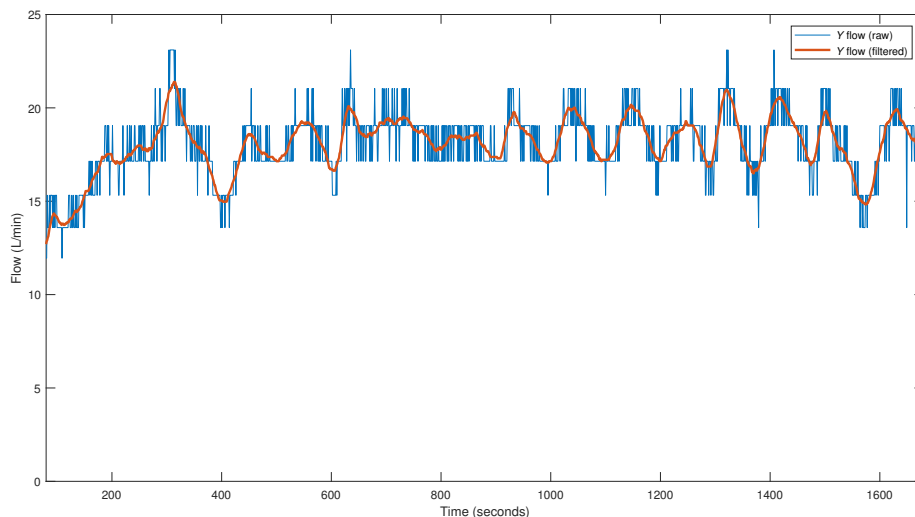


Figure 6.30: *Total flow estimated by the level sensor  $L_{22}$*

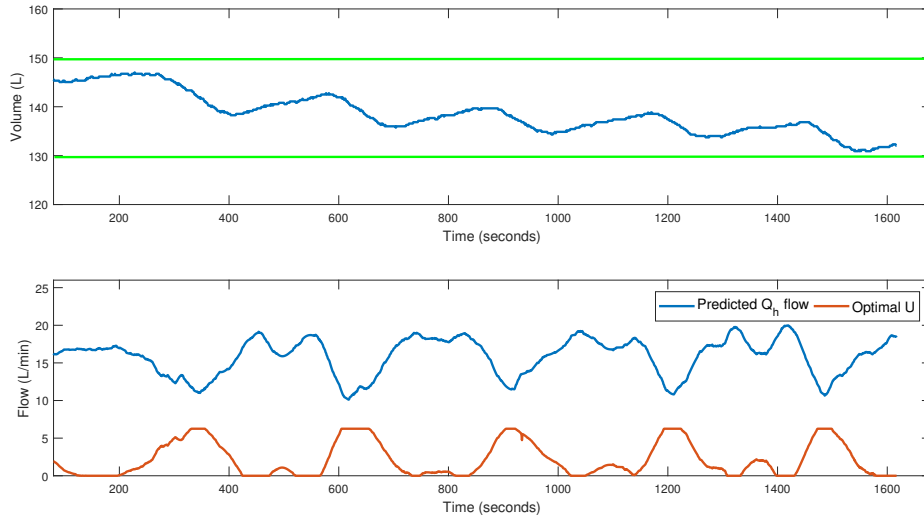


Figure 6.31: *Top: Tank volume for constraints (shown in green)  $V_{max} = 150$   $V_{min} = 130$ . Bottom: Predicted household flow and optimal  $U$ .*

Although the controller is able to keep the volume of the tank between the constraints, the performance of minimizing the flow variance is not as good as the previous test results, figures (6.26) and (6.28), especially for the last 400 time steps.

### 6.2.5.3 Soft tank constraint

To prevent the optimizer in YALMIP to stop working when no feasible solution can be found, the tank constraints have been 'softened'. This allows to cross the boundaries occasionally if it is necessary. To implement the soft constraints, the optimization problem was modified to [Maciejowski, 2002]:

$$\mathcal{J} = \sum_{k=1}^{H_p} \left( Q_h(k + \tau) + U(k) - \mu \right)^2 + \rho \epsilon \quad (6.4)$$

subject to

$$\begin{aligned} V_{min} - \epsilon &\leq V \leq V_{max} + \epsilon \\ 0 &\leq \epsilon \end{aligned} \quad (6.5)$$

where  $\epsilon$  is a so called slack variable and  $\rho$  a non-negative parameter. By choosing  $\rho$  to be large enough gives the same solution as the 'hard' constrained problem if a feasible solution can be found.

We performed a test to check this modified algorithm (6.4), (6.5) in work while having some unexpected disturbances acting on the system. The results are shown below.

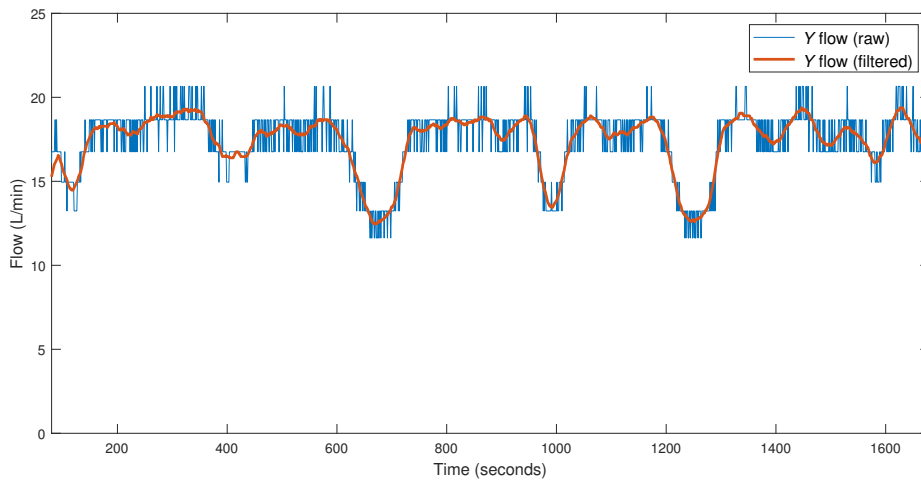


Figure 6.32: Total flow estimated by the level sensor  $L_{22}$

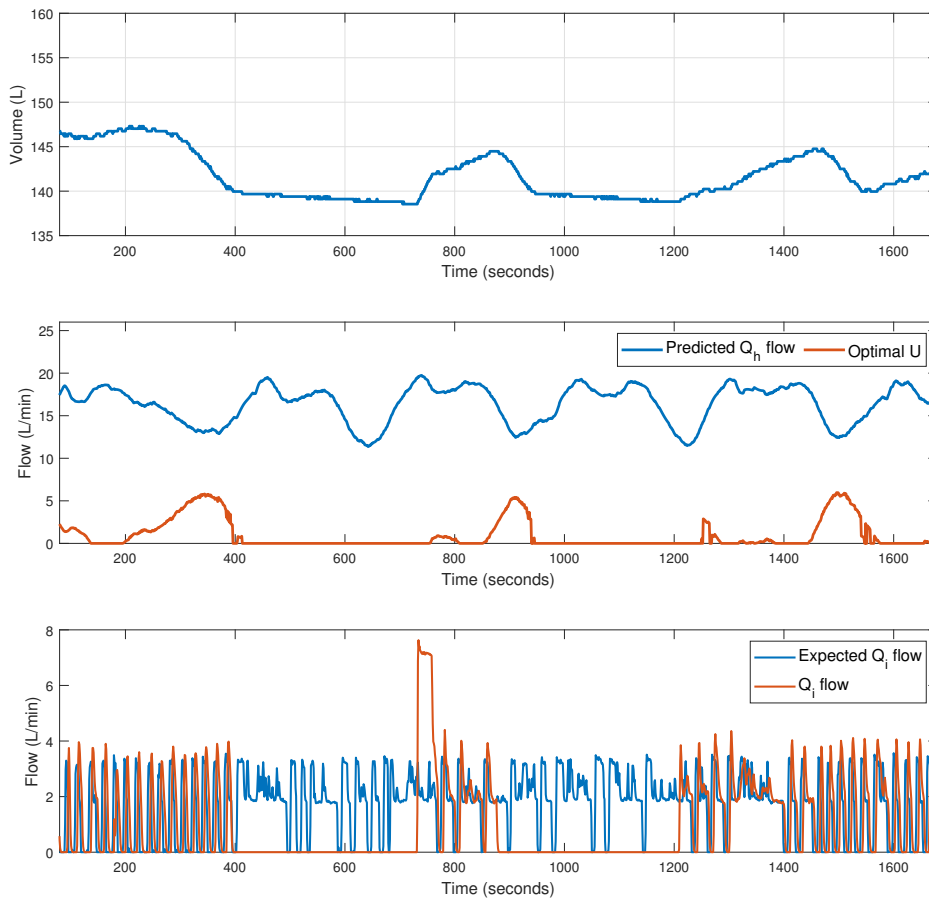


Figure 6.33: Top: Tank volume for constraints  $V_{max} = 160L$   $V_{min} = 140L$ . Middle: Predicted household flow and optimal  $U$ . Bottom: Expected  $Q_i$  and actual  $Q_i$  after applying disturbances

For the present test,  $\rho$  was set to 3. In order to force the violation of constraints, disturbances have been added to the inflow to the industry tank as shown in the bottom plot of figure (6.33). At time step  $k = 400$  and  $k = 950$  the MPC is expecting some inflow but  $Q_i$  was set to zero flow. As a result, no feasible solution can be found leading to a violation of the tank constraint.

As anticipated, the controller continued to work despite violating the constraints on the tank. It is in a way an improvement over the standard algorithm (6.1), (6.2). Hence, we have also designed and tested an on-line control strategy that dealt with the problem of infeasibility.



# Discussion 7

---

This chapter will lay out some issues identified with the project setup and discuss the results.

## Laboratory setup

- Pumps 1/2/3 has to make sure the tank in pumping station does not overflow. When it does not pump water out as expected, the tank overflows. This tank represents a WWTP so in theory we exceed the treating capacity of the plant. A solution is to lower the height of the three pumps so that there is continuous circulation of water between stations.

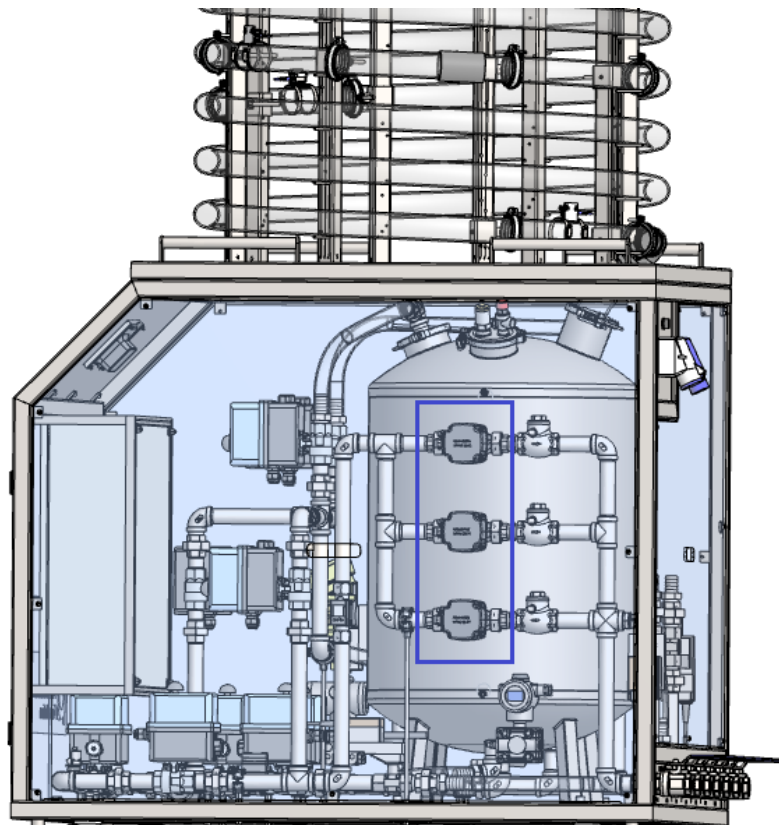


Figure 7.1: A good and detailed 3D model of the pumping station created by Poul Due Jensen Foundation, Grundfos. A blue box is put around the pumps.

- Another function of pumps 1/2/3 in pumping station is to pump water as seen in figure (4.14) to include flow disturbances from an industry. If the pumps do not perform as required, it results in less volume in the consumer tank. With this change, our MPC's decision also gets affected.

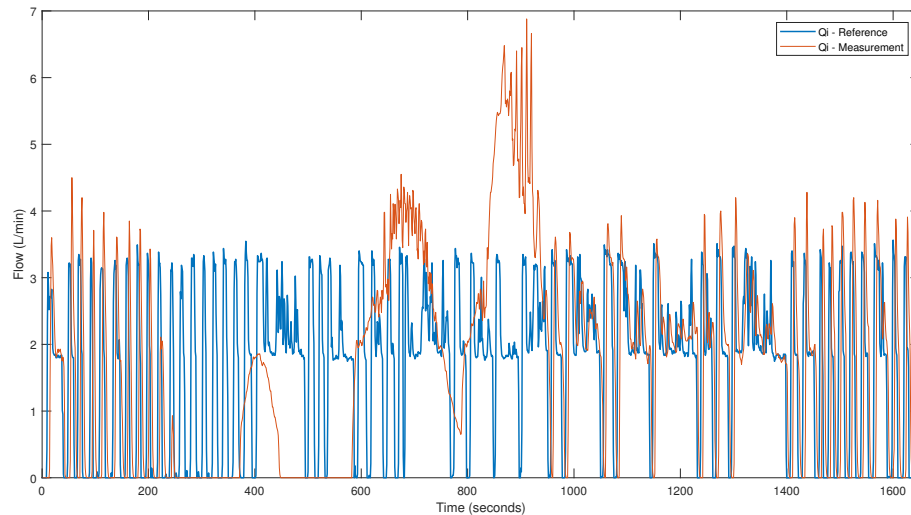


Figure 7.2: *Water entering the buffer tank. This flow is seen as disturbance from heavy industry. In this case, the pumps are not able to send water as desired.*

- If required, the transport delay from the top to bottom of sewer pipe can be increased by lowering the slope (placing the tube on top of each other) and increasing the length of the pipe.
- Air pockets in the tubes can be a big problem for the pumps and flow sensors to work efficiently. The user has to be careful in avoiding air flow into the tubes. The first precaution would be to not drain the two tanks completely. As long as the level control is active, this should not be an issue.
- Ultrasonic level sensors in the gravity sewer tube is used to measure water level and this reading is converted into flow. For this study, the output of the level sensor was taken up to 2 decimals. Taking 3 or more decimals for higher resolution could have perhaps helped with better flow measurement.
- Measurements from the level sensors were also different each day for the same flow. This is due to a slight change in position of the sensors. Due to this, every day, we had to tune the parameters in our Manning equation to get the correct flow values.
- The valve used for controlling flow from the buffer tank had to overcome a big stiction during operation. This inhibits the ability of valve to track the reference signal very well.
- In order to implement online MPC, it is crucial to be real-time. With the current setup it is possible to get a sampling time of 500 *ms* and compute the control signal each second. Mainly, the computed time is taken by YALMIP (around 500 *ms/iteration*) and Modbus read/write (around 20 *ms/sampling* and station). Setting the control horizon of the MPC to be larger could cause YALMIP not being able to compute the control signal on time.

## Experimental results

- Looking at figure (6.23), we see the predictions of household flow is accurate enough. The weights in the Kalman filter was chosen to trust the model more. The values were ( $Q = 0.005$ ) and ( $R = 4$ ). The intention of not trusting the measurements so much was because the flow estimations were based on readings of a noisy sensor and then converted to flow using Manning equation (not a perfect conversion), leading to an accumulation of errors.
- From figure (6.26), the flow control performance was good for an unconstrained tank. The variations are less when compared to overall flow without a controller.
- With the introduction of tank constraints, the variations of flow is somewhat more as seen in figure (6.28). When the filled volume of the tank approaches the lower limit of the constraint, the output flow from the tank does not meet with required flow. This eventually does not minimize flow variations as expected.
- When the constraints on the tank volume became more stringent, the performance in minimizing the flow variance is not that good. The result is shown in figure (6.30).
- With soft constraints in place, we have a more realistic real-time controller. This makes sure the controller works at all times even when large disturbances act on the system, seen in figure (6.33). The tank volume goes below 140 L but the experiment keeps running with an abrupt stop.
- If the research in biotechnology leads to the development of microorganisms immune to environmental changes, focus on controlling the conditions at the WWTP inlet will no longer be necessary.



# Conclusion 8

---

The focus of this thesis was to predict flow disturbances and implement a Model Predictive Control algorithm on a laboratory setup replicating a wastewater collection and transport system. The objective was to have a control on flow variations at the inlet of a wastewater treatment plant. A problem statement was formulated accordingly:

*How can a laboratory setup that mimic a real sewer network be assembled so that we can later utilize MPC, along with disturbance predictions and a storage tank that results in stable working conditions for the wastewater treatment plant.*

Three different stations/modules was put together to get the desired system in the laboratory. A model was also developed for a typical flow disturbance seen everyday. Using a kalman filter, disturbance model and real-time flow measurements, a good prediction of disturbance was possible. Making use of the system model and disturbance prediction, we successfully implemented a working Model Predictive Controller. This controller handled constraints on the buffer tank volume and the input signal to the valve and was able to minimize the flow variations significantly.

To conclude, the group claims a real-time Model Predictive Control can be implemented on a complex system such as a sewer system.

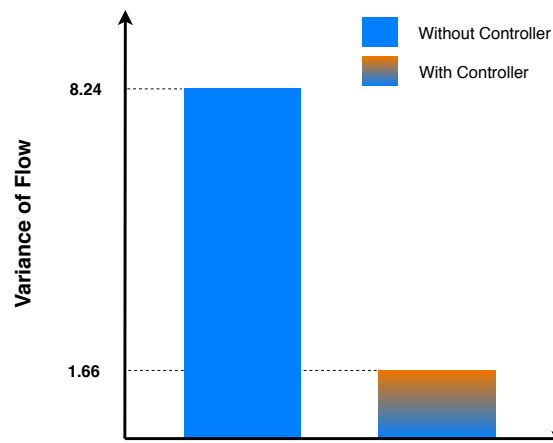


Figure 8.1: *Effectiveness of the controller in minimizing the flow variance*



# Future work 9

This chapter mentions some future work to do for continuation and/or improvement of this project.

## Temperature control

In this thesis, only flow control has been tested on the laboratory setup. As mentioned in chapter (2), temperature can be a proxy for contaminants. This section informs the reader about the configuration needed to implement temperature control together with flow control. A description of temperature sensor is also given.

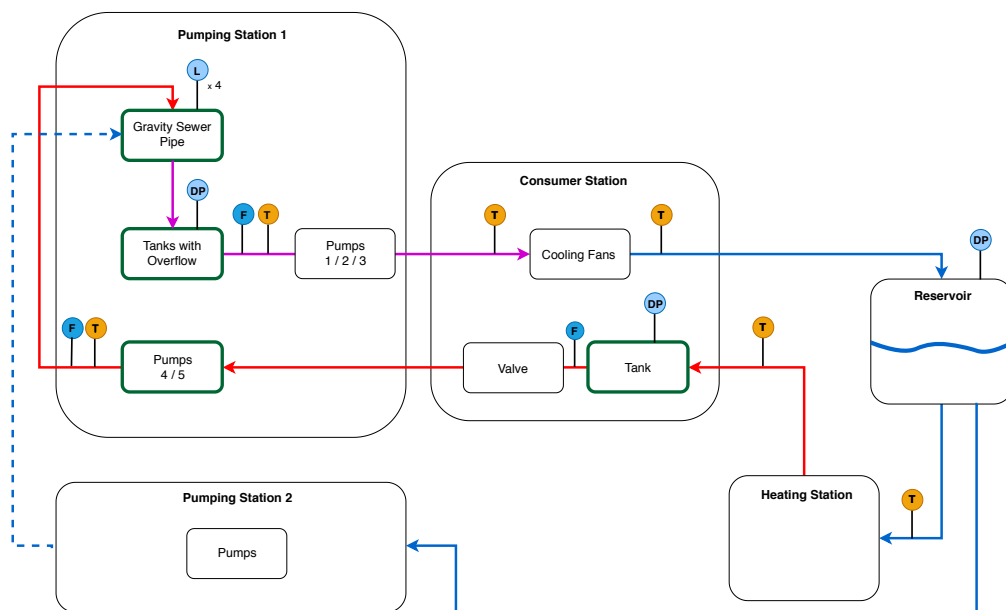


Figure 9.1: *Original configuration to replicate a sewer network. A second pumping station is expected to arrive shortly thus making this setup possible.*

Here, the green boxes indicate the essential components of a sewer network. The pumps 4/5 are the final control elements. Clear distinction has been made between hot water (*red*) and cold water line (*blue*). Temperature after mixing is shown with (*pink*).

The water from the reservoir is taken into the heating station and the hot water moves to the tank. From here, the hot water is pumped into the pipe sewer in a controlled manner. After flowing in the gravity sewer pipe, water moves to overflow tank. Then the water is led into the consumer station where cooling fans helps the water to cool down faster. Water is then stored and used again to continue this cyclic process. In the sewer line, cold

water is also pumped in to simulate the household wastewater flow. At the WWTP (tanks with overflow) inlet, temperature and flow readings of this mixed flow are taken and fed back to the controller.

### **Resistance temperature detector (RTD)**

The principle behind this method is that there is an increase in electrical resistance of the conductors with increasing temperature. The material may be platinum, copper or nickel. The most commonly used one is platinum (*PT100*) because of its excellent stability and repeatability. RTD's are very precise, accurate and reproducible. They are also highly sensitive to small changes in temperature [Lipták Béla G, 2003]. In the lab, these sensors are located near the pumps and the heating station. Additionally, a sensor is used to measure the temperature at the tank overflow after the mixing.

# Bibliography

---

- [Breasted, 1907] Breasted, J. H. (1907). *Ancient records of Egypt: historical documents from the earliest times to the Persian conquest*, volume 5. University of Chicago Press.
- [Cheremisinoff, 1997] Cheremisinoff, N. P. (1997). *Biotechnology for waste and wastewater treatment*. Elsevier.
- [Cheremisinoff, 2001] Cheremisinoff, N. P. (2001). *Handbook of water and wastewater treatment technologies*. Butterworth-Heinemann.
- [Chow, 1959] Chow, V. T. (1959). *Open-channel hydraulics*. caldwell.
- [CODESYS, 2019] CODESYS (2019). CODESYS Runtime. <https://www.codesys.com/products/codesys-runtime.html>.
- [Crossley, 1999] Crossley, A. J. (1999). *Accurate and efficient numerical solutions for the Saint Venant equations of open channel flow*. PhD thesis, University of Nottingham.
- [de Oliveira Kothare and Morari, 2000] de Oliveira Kothare, S. L. and Morari, M. (2000). Contractive model predictive control for constrained nonlinear systems. *IEEE Transactions on Automatic Control*, 45(6):1053–1071.
- [de Saint-Venant A, 1871] de Saint-Venant A, B. (1871). Théorie du mouvement non-permanent des eaux avec application aux crues des rivières et à l'introduction des marées dans leur lit. *comptes rendus acad sci paris* 73:148–154, 237–240.
- [Hodge, 2002] Hodge, A. T. (2002). *Roman aqueducts & water supply*. Bristol Classical Press.
- [Hvitved-Jacobsen et al., 2013] Hvitved-Jacobsen, T., Vollertsen, J., and Nielsen, A. H. (2013). *Sewer processes: microbial and chemical process engineering of sewer networks*. CRC press.
- [Jones, 1967] Jones, D. E. (1967). Urban hydrology-a redirection. *Civil Engineering*, 37(8):58.
- [Kalman, 1960] Kalman, R. E. (1960). A new approach to linear filtering and prediction problems. *Journal of basic Engineering*, 82(1):35–45.
- [Lazarova et al., 1999] Lazarova, V., Savoye, P., Janex, M., Blatchley Iii, E., and Pommepuy, M. (1999). Advanced wastewater disinfection technologies: state of the art and perspectives. *Water Science and Technology*, 40(4-5):203–213.
- [Leyva-Díaz et al., 2017] Leyva-Díaz, J., Martín-Pascual, J., and Poyatos, J. (2017). Moving bed biofilm reactor to treat wastewater. *International journal of environmental science and technology*, 14(4):881–910.
- [Lipták, 2006] Lipták, B. G. (2006). *Instrument Engineers' Handbook: Process Control and Optimization*. CRC Press.
- [Lipták Béla G, 2003] Lipták Béla G, Venczel, K. (2003). *Instrument Engineers' Handbook: Process Measurement and Analysis*. CRC Press.

- [Löfberg, 2004] Löfberg, J. (2004). Yalmip: A toolbox for modeling and optimization in matlab. In *Proceedings of the CACSD Conference*, volume 3. Taipei, Taiwan.
- [Lofrano and Brown, 2010] Lofrano, G. and Brown, J. (2010). Wastewater management through the ages: A history of mankind. *Science of the Total Environment*, 408(22):5254–5264.
- [Maciejowski, 2002] Maciejowski, J. M. (2002). *Predictive control: with constraints*. Pearson education.
- [Manning et al., 1890] Manning, R., Griffith, J. P., Pigot, T., and Vernon-Harcourt, L. F. (1890). *On the flow of water in open channels and pipes*.
- [Michelsen, 1976] Michelsen, H. (1976). *Ikke-stationær strømning i delvis fyldte kloakledninger: en dimensioneringsmetode og en analysemetode*. PhD thesis, Afdelingen for Jord-og Vandbygning, Den kgl. Veterinær-og Landbohøjskole.
- [MODBUS, 2019] MODBUS (2019). Why should I use Modbus TCP/IP? <http://www.modbus.org/faq.php>.
- [Morten Vesteraa et al., 2018] Morten Vesteraa et al., Llorenc Salleras Mestre, P. M. (2018). Model predictive control of a sewer system. *Control and Automation, Department of Electronics and IT, Aalborg University*.
- [National-Geographic, 2013] National-Geographic (2013). New Diseases, Toxins Harming Marine Life. <https://news.nationalgeographic.com/news/2012/04/130412-diseases-health-animals-science-environment-oceans/>.
- [Ocampo-Martinez, 2010] Ocampo-Martinez, C. (2010). *Model predictive control of wastewater systems*. Springer Science & Business Media.
- [Park et al., 2003] Park, J., John Park, A., and Mackay, S. (2003). *Practical data acquisition for instrumentation and control systems*. Newnes.
- [Schlütter, 1999] Schlütter, F. (1999). *Numerical modelling of sediment transport in combined sewer systems*. PhD thesis, The Hydraulics and Coastal Engineering Group, Dept. of Civil Engineering, Aalborg University.
- [Tandoi et al., 2017] Tandoi, V., Rossetti, S., and Wanner, J. (2017). *Activated sludge separation problems: theory, control measures, practical experiences*. IWA Publishing.
- [Te et al., 1988] Te, C. V., Maidment, D. R., and Mays, L. W. (1988). Applied hydrology. *Water Resources Handbook*.
- [Vymazal, 2010] Vymazal, J. (2010). Constructed wetlands for wastewater treatment. *Water*, 2(3):530–549.
- [Wanka and Königer, 1984] Wanka, K. and Königer, W. (1984). Unsteady flow simulation in complex drainage systems by hvm—hydrograph volume method. In *Channels and Channel Control Structures*, pages 607–621. Springer.
- [Webster, 1962] Webster, C. (1962). The sewers of mohenjo-daro. *Journal (Water Pollution Control Federation)*, pages 116–123.
- [Wolfe, 1999] Wolfe, P. (1999). History of wastewater. world of water 2000—the past, present and future. water world. *Water and Wastewater International Supplement to Penn Well Magazines, Tulsa, OH, USA*.

## A.1 Data from fredericia

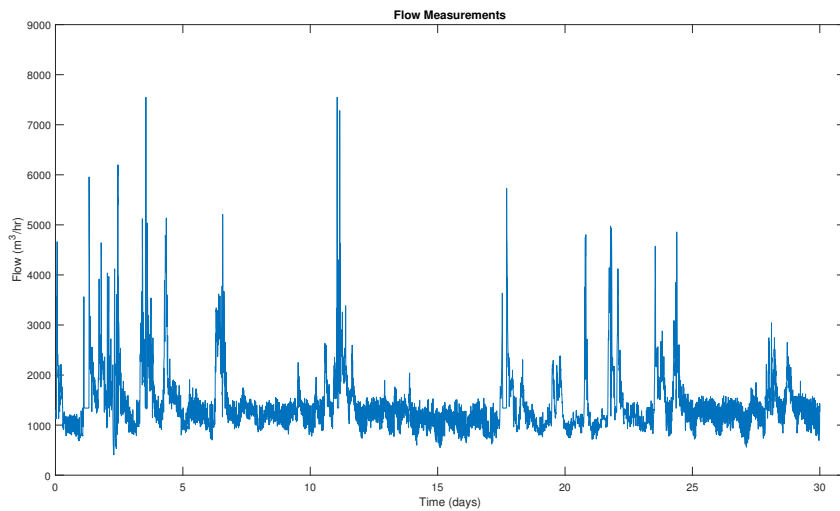


Figure A.1: *Flow measurements taken for a month at the inlet of wastewater treatment plant on October 2017. The huge spikes in flow are due to rain events. Here, each time step corresponds to 5 minutes.*

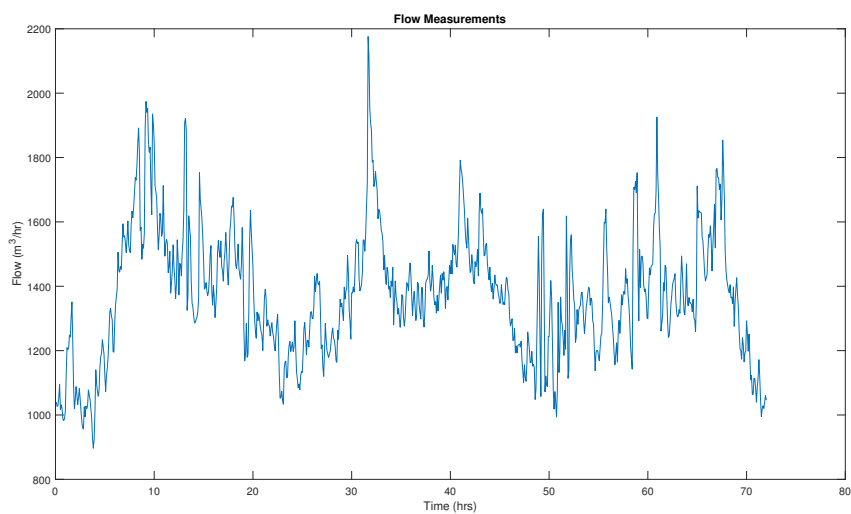


Figure A.2: *Average flow for 3 days entering the WWTP. Each measurement is taken at every 5 minutes. We can see that the flow profile roughly repeats each day (288 samples).*

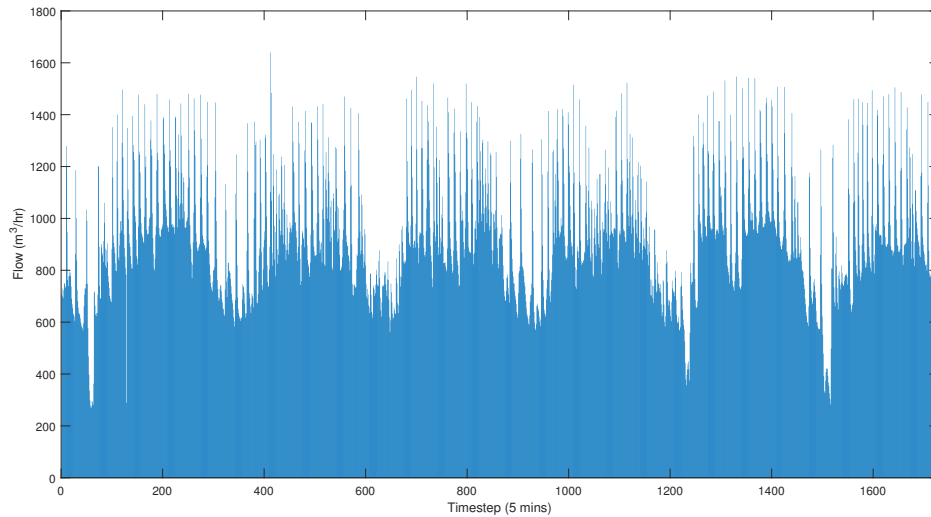


Figure A.3: *Flow measurements taken for 6 days at the inlet of wastewater treatment plant on Feb-Mar 2019. The spikes in flow are due to addition of industrial flows. Here, each time step corresponds to 5 minutes.*

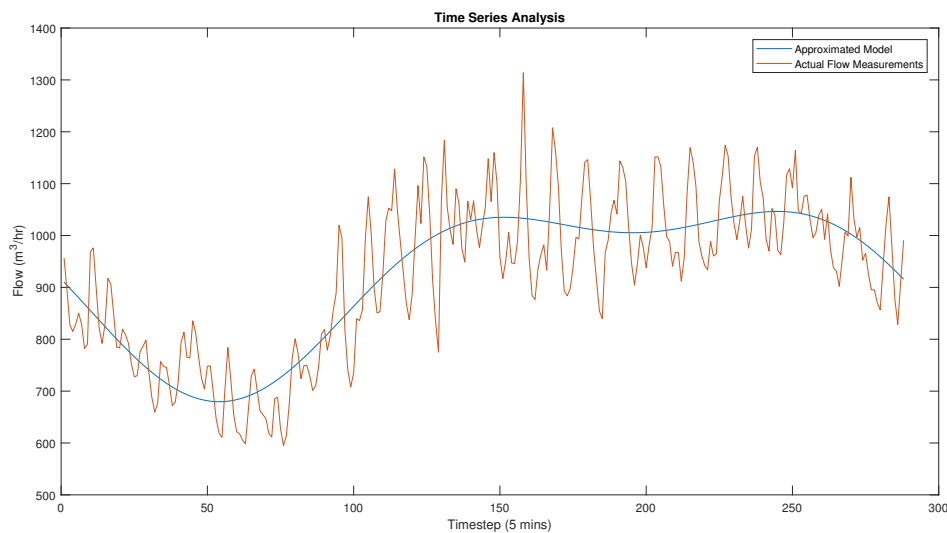


Figure A.4: *The orange curve is the average flow for a single day. If fourier analysis was done on this data, the model chosen would be the blue curve. The threshold set for the power spectrum is 1521 and the number of frequency components is 3.*

# Appendix B

## B.1 Other figures and simulation results

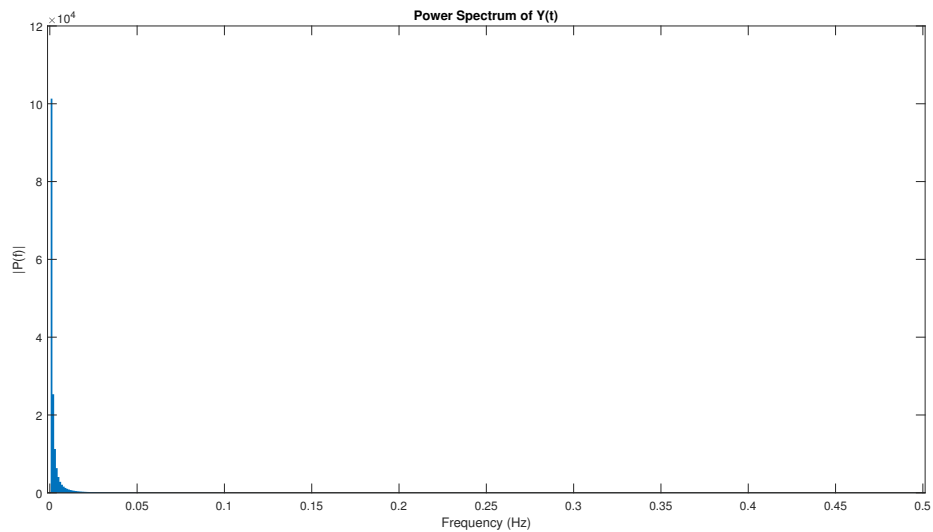


Figure B.1: *Bar plot of power spectrum. Zoomed out version of figure 4.3 in chapter (4). This figure is to simply show there are no other frequencies of interest.*

Referring to figure (4.9), to know more on the delay in the red line, cross-correlation was done on two flow data: 1. Flow from industry (south) and 2. Flow at WWTP inlet. The flow data and correlation results are shown in the next page.

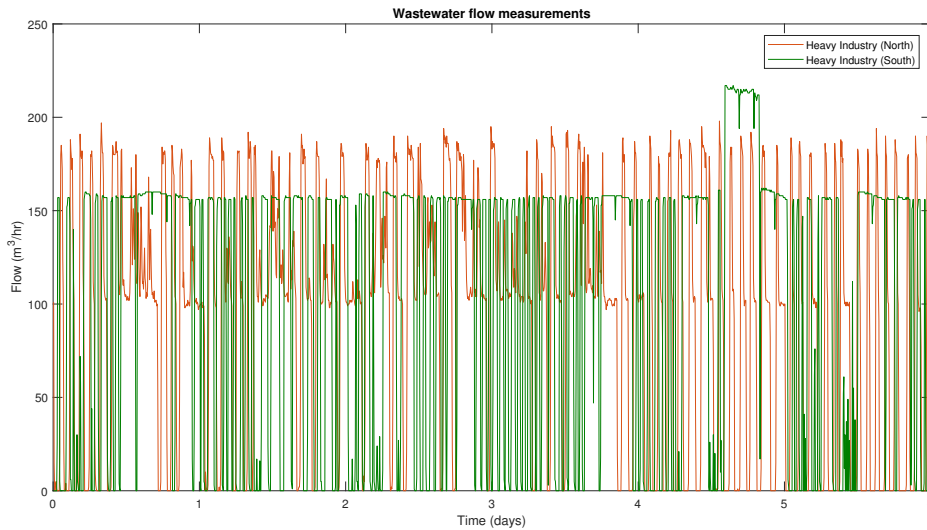


Figure B.2: Flow for 6 days measured at the industry outlet. Here, the flow measurements are recorded for every 5 minutes and we have 288 measurements in total for a one day.

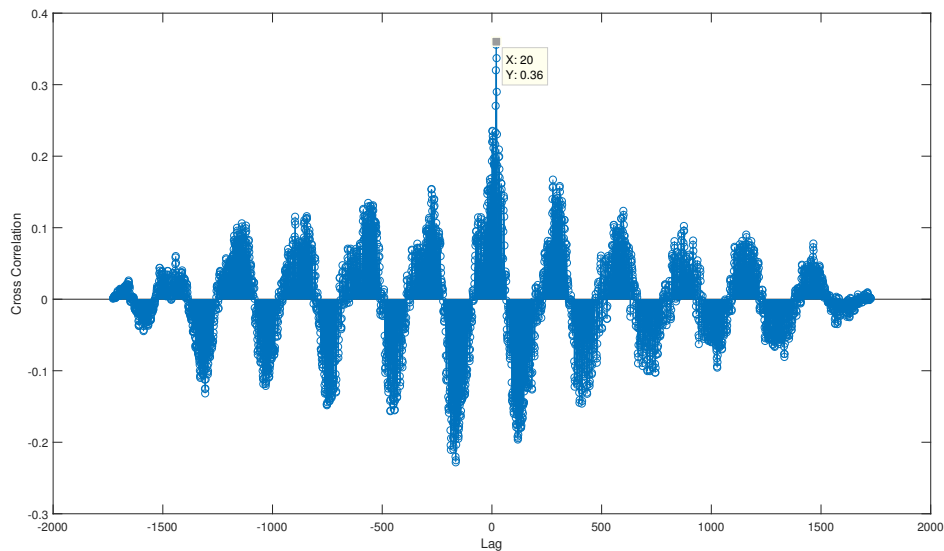


Figure B.3: Cross correlation analysis between the flow leaving heavy industry (south) and flow measured at WWTP inlet. The option 'coeff' was chosen for normalization..

At lag 20, the correlation value is the highest. Each lag unit corresponds to 5 minutes. Hence we say that the strongest correlation seen was for a delay of 100 minutes (1 hour and 40 minutes).

## Delay analysis for flow in laboratory setup

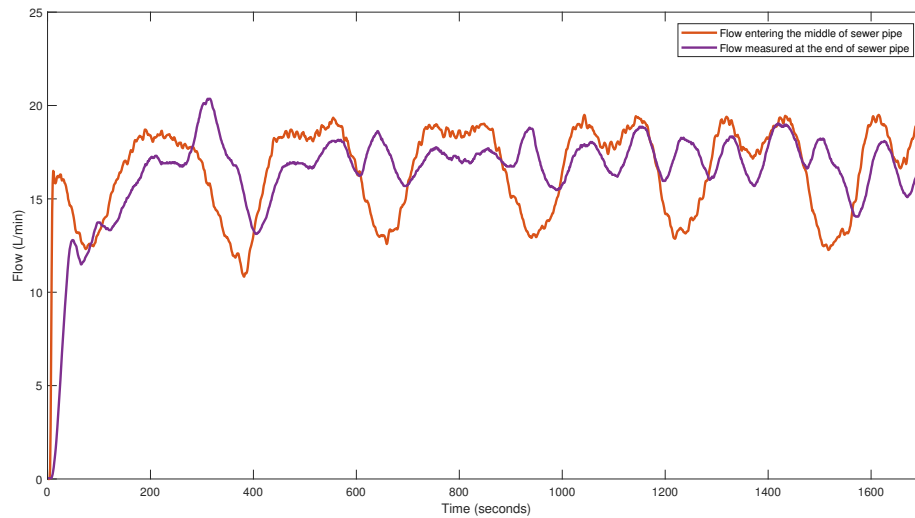


Figure B.4: *Flow profile used to calculate the delay in transporting water from the middle to end of sewer pipe. The result of cross correlation analysis is seen in figure (4.12) in chapter (4).*

## Performance of the pumps 1/2/3 (pumping station)

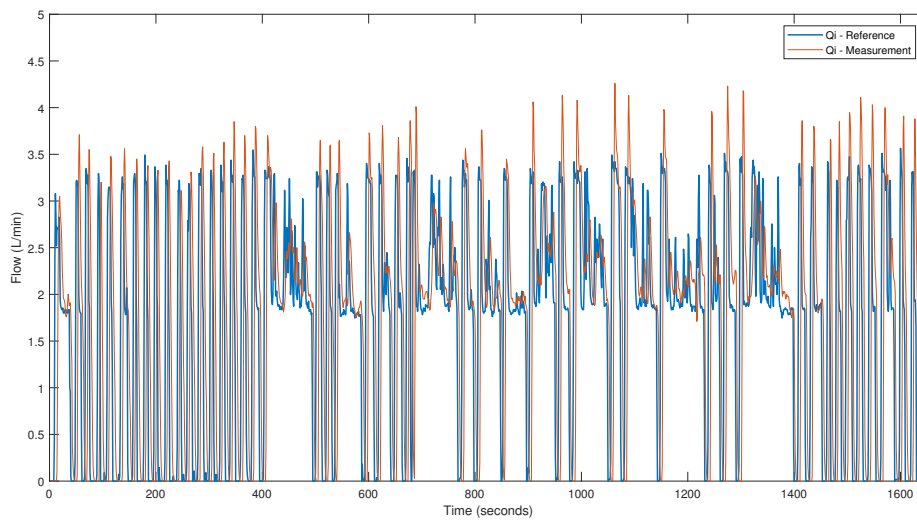


Figure B.5: *Water entering the buffer tank. This flow is seen as disturbance from heavy industry. In this case, the pumps are able to send water as required.*



## C.1 Wetted area calculation

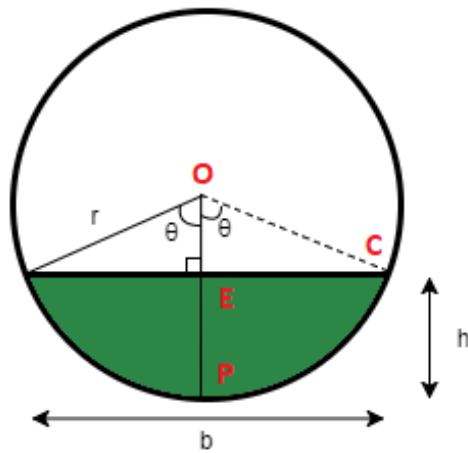


Figure C.1: Cross-sectional view of flow in a pipe. Angle  $\theta$  is in radians.

Area of the sector  $OPC$  is

$$\begin{aligned}
 &= \frac{\pi d^2}{4} \cdot \frac{\theta}{2\pi} \\
 &= \frac{\theta d^2}{8}
 \end{aligned} \tag{C.1}$$

Area of the region  $PEC$  is

$$\begin{aligned}
 &= \frac{\theta d^2}{8} - \frac{1}{2} \cdot (r \cos(\theta))(r \sin(\theta)) \\
 &= \frac{\theta d^2}{8} - \frac{d^2}{8} \cdot (\sin(\theta) \cos(\theta)) \\
 &= \frac{d^2}{8} \cdot \left( \theta - \frac{\sin(2\theta)}{2} \right)
 \end{aligned} \tag{C.2}$$

The wetted area  $A$  is twice the area of  $PEC$

$$= \frac{d^2}{4} \cdot \left( \theta - \frac{\sin(2\theta)}{2} \right)$$

Using Pythagoras theorem in triangle  $OEC$ , we have

$$b = 2\sqrt{h(2r - h)}$$

The angle can be denoted by

$$\theta = \cos^{-1}\left(\frac{r-h}{r}\right) = \operatorname{acos}\left(\frac{r-h}{r}\right)$$

Now the wetted area  $A$  can also be given as

$$\begin{aligned} &= \frac{d^2}{4} \cdot \operatorname{acos}\left(\frac{r-h}{r}\right) - \frac{d^2}{4} \cdot \left(\frac{\sin(2\theta)}{2}\right) \\ &= r^2 \cdot \operatorname{acos}\left(\frac{r-h}{r}\right) - r^2 \cdot \sin(\theta) \cdot \cos(\theta) \\ &= r^2 \cdot \operatorname{acos}\left(\frac{r-h}{r}\right) - r^2 \cdot \frac{b/2}{r} \cdot \frac{r-h}{r} \\ &= r^2 \cdot \operatorname{acos}\left(\frac{r-h}{r}\right) - \sqrt{h(2r-h)}(r-h) \end{aligned} \tag{C.3}$$

## Manning equation and SWMM

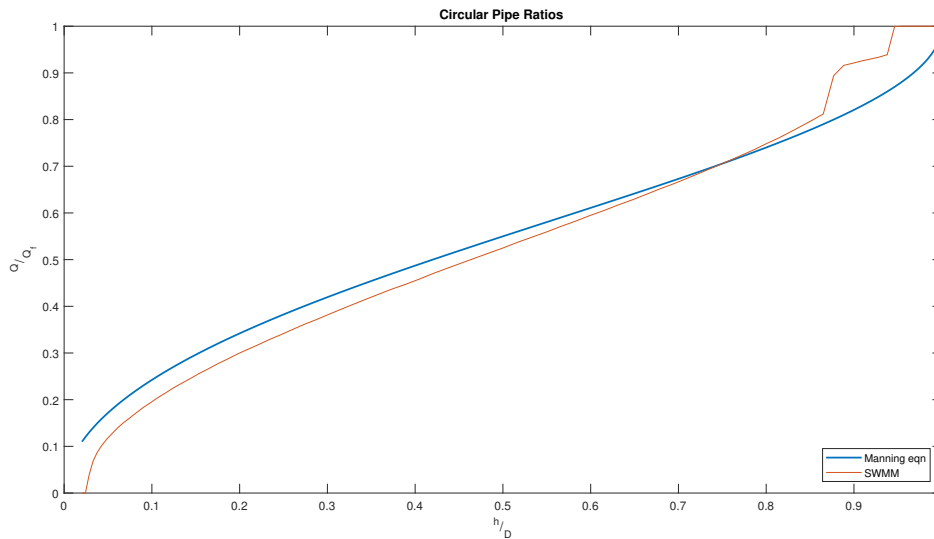


Figure C.2: A comparison of circular pipe ratios between manning equation and SWMM.

How this comparison was done:

- Define a level vector ( $H1$ ), [0.011 : 0.001 : 0.1]. Level gets incremented by 1 mm from 1.1 cm to 10 cm.
- Use manning equation, (3.22), to calculate flow ( $F$ ) for these levels
- In SWMM, create a conduit with same properties (friction coefficient, slope, roughness factor and diameter) used in manning equation
- Use ( $F$ ) and create a time series for flow to the inlet of the conduit
- Run the SWMM simulation and save the measured levels ( $H2$ )

## Pumping Station

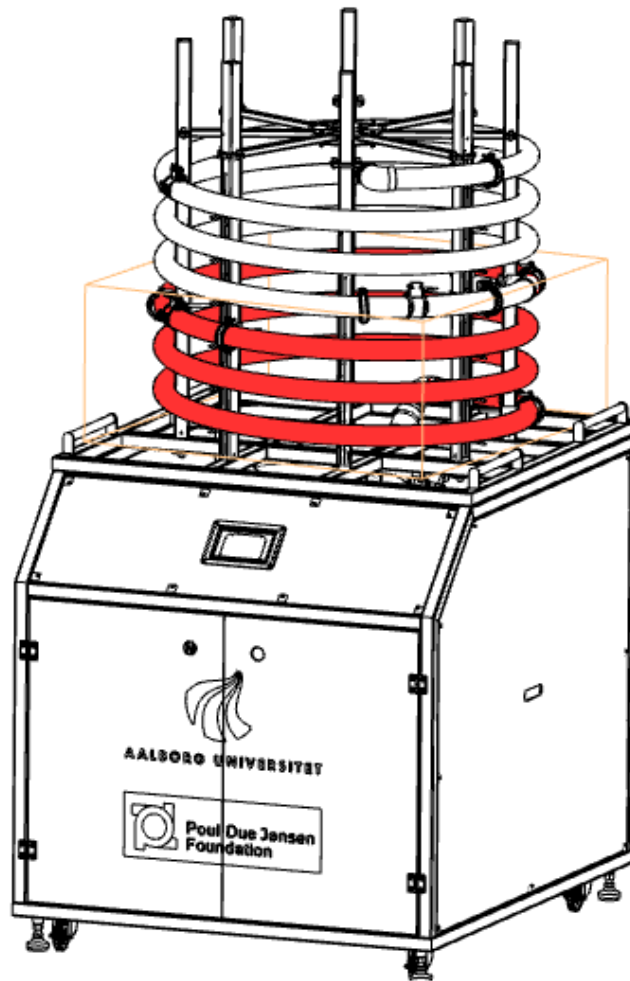


Figure C.3: 3D model of the pumping station created by Poul Due Jensen Foundation, Grundfos. The tube highlighted in red is the region of the sewer pipe in which water from household areas flow.